

**Role of the histone methyltransferase,
Mll2,
in embryogenesis and adult mouse**

Stefan Glaser

April 2005

Technische Universität Dresden

and

International Max-Planck Research School

Thesis abstract

Histone methyltransferases are key players in eukaryotic gene regulation. The goal of this thesis was to study the role of the histone methyltransferase Mll2 in developing embryos and adult mice. Targeting of mouse ES cells with a multipurpose allele and blastocyst injection had previously generated a mouse line allowing analysis of Mll2 function by knock-out and conditional mutagenesis using Cre/loxP. The first part of the thesis comprised the analysis of the Mll2^{-/-} phenotype, and included the cloning of a targeting construct to generate an ubiquitous, ligand-regulated Cre line. In the second part, we did conditional mutagenesis using the Rosa26-CreER(T2) line obtained from collaborators, and achieved complete knock-out of Mll2 in most tissues of embryos, neonates and adult mice.

Mll2 is essential during embryonic development, as mutant embryos were severely growth retarded, had significant increases in apoptosis, and failed in gestation between E 9.5 and E11. Conditional removal of Mll2 protein at gastrulation (E 6.5) produced a similar phenotype at E 11. In contrast, the absence of Mll2 function after E 11 did not result in obvious defects at E16 and indicates an essential role for Mll2 between E6 and E11. Indeed, we identified a loss of expression of 3 important developmental regulators in mutants of this developmental stage: Hoxb1, Mox1 and Six3 are candidate targets for Mll2 regulation that encode homeobox type transcription factors involved in specifying cellular identity. We observed correct establishment of their developmental expression patterns, which then decay in Mll2^{-/-} mutants at E9.5. These data concord with and extend current thoughts about the fly orthologue of Mll2, Trithorax, which suggest that it acts as an epigenetic lock in chromatin to maintain expression of certain transcription factors key to respective cellular identities, after their expression patterns have been established.

After birth, Mll2 is dispensable in most tissues, as conditional knock out in neonates and adult mice did not produce any pathological findings except infertility of mutant males and females. Histological analysis of testis revealed progressive loss of spermatogonia, associated with increases in apoptosis but without overt proliferation, meiotic or differentiation defects or loss of the supporting Sertoli cells. Consequently, in addition to its regulation of homeotic genes during development, Mll2 is required for the maintenance of various mitotic cell populations including ES cells, embryonal cells and germ cells.

*Dédié à 'Mamie' Michèle Paris
et à Anne Glaser*

Ce qu'il faut pour être heureux

*Il faut penser ; sans quoi l'homme devient,
Malgré son âme, un vrai cheval de somme.
Il faut aimer ; c'est ce qui nous soutient :
Sans rien aimer, il est triste d'être homme.*

*Il faut avoir douce société,
Des gens savants, instruits, sans suffisance,
Et de plaisirs grande variété
Sans quoi les jours sont plus longs qu'on ne pense.*

*Il faut avoir un ami, qu'en tout temps
Pour son bonheur, on écoute, on consulte,
Qui puisse rendre à notre âme en tumulte,
Les maux moins vifs et les plaisirs plus grands.*

*Il faut, le soir, un souper délectable,
Où l'on soit libre, où l'on goûte, à propos,
Les mets exquis, les bon vins, les bon mots
Et, sans être ivre, il faut sortir de table.*

*Il faut, la nuit, tenir entre deux draps
Le tendre objet que notre cœur adore,
Le caresser, s'endormir dans ses bras,
Et, le matin, recommencer encore.*

Voltaire

<u>THESIS ABSTRACT</u>	2
1. INTRODUCTION	8
1.1 Eukaryotic transcriptional control	8
1.1.1 Chromatin	8
1.1.2 Post-translational histone modifications	10
1.1.3 Histone acetyltransferases (HAT)	11
1.1.4 Histone deacetylases (HDAC)	12
1.1.5 Histone kinases	13
1.1.6 Histone methyltransferases (HMT)	13
1.1.7 Epigenetic regulation of cellular memory by the Polycomb and Trithorax group proteins	16
1.2 Manipulating the mouse genome	17
1.2.1 Mammalian multipurpose allele	17
1.2.2 Recombeneering the mouse genome with site-specific recombinases	18
1.2.3 The Mll2 multipurpose allele	19
1.2.4 Recombinogenic DNA engineering in E.coli	21
2. RESULTS	23
2.1 The Mll2 mouse line	23
2.1.1 Mapping of the mll2 gene.	23
2.1.2 Cloning of the mll2 targeting construct	23
2.1.3 Targeting of ES cells by homologous recombination	24
2.1.4 Strains, crosses and genotypes of mice	25
2.2 Constitutive mutagenesis of Mll2	30
2.2.1 Validation of the null/reporter allele on RNA level	30
2.2.2 Embryonic expression pattern of Mll2	32
2.2.3 Phenotype of Mll2 mutant embryos	33
2.2.4 Histological analysis of Mll2 mutant embryos	35
2.2.5 Molecular characterization of the Mll2 embryonic phenotype	36

2.3	Conditional mutagenesis of Mll2	41
2.3.1	Induction of the conditional Mll2 allele <i>in vitro</i>	41
2.3.2	Induction of the conditional Mll2 allele <i>in utero</i> and <i>in vivo</i>	42
2.3.3	Validation of the induced allele on <i>DNA</i> level	43
2.3.4	Validation of the induced allele on <i>RNA</i> level	45
2.3.5	Validation of the induced allele on <i>protein</i> level	49
2.3.6	Severe diarrhea in induced Rosa26-CreER(T2) mice	52
2.3.7	Phenotype of Mll2 mutant embryos	55
2.3.8	Phenotype of Mll2 mutant mice	57
2.3.9	Infertility of mutant females	59
2.3.10	Infertility of mutant males	64
2.3.11	Histological analysis of testis	69
2.3.12	Molecular characterization of the male infertility	71
2.4	Generation of an ubiquitous, inducible Cre mouse line	75
2.4.1	Cloning of the targeting construct Topoisomerase I-ER(T2)-Cre-ER(T2)	76
2.4.2	Cloning of genomic topoisomerase I sequence	78
2.4.3	Repair of a point mutation in the TopI-CreER(T2) targeting construct	83
2.4.4	Targeting of ES cells by homologous recombination	84
3.	DISCUSSION	86
3.1	The Mll2 multipurpose allele	86
3.2	The Rosa26-CreER(T2) allele	88
3.3	The Mll2 gene	92
4.	METHODS	97
4.1	DNA methods	97
4.1.1	Restriction enzyme digestion	97
4.1.2	Ligation	97
4.1.3	Transformation of chemical competent E.coli cells	97
4.1.4	Preparation of chemical competent E. coli cells	98
4.1.5	Mini preparation of plasmid DNA	98
4.1.6	Maxi preparation of plasmid DNA	99
4.1.7	Maxi preparation of BAC DNA	100
4.1.8	DNA precipitation	100
4.1.9	Phenol-Chloroform extraction	100
4.1.10	Agarose gel electrophoresis	100

4.1.11	Polymerase Chain Reaction (PCR)	101
4.1.12	PCR product purification	102
4.1.13	Cloning of PCR products and DNA fragments	102
4.1.14	DNA extraction from ES cells	103
4.1.15	DNA extractions from mouse tails	103
4.1.16	Southern analysis	104
4.1.17	ET cloning	106
4.2	RNA methods	109
4.2.1	Diethylpyrocarbonate (DEPC) – treated water	109
4.2.2	Total RNA extraction from cells	109
4.2.3	Total RNA extraction from tissue	109
4.2.4	Northern blotting	110
4.2.5	Reverse Transcription of RNA (cDNA synthesis)	111
4.2.6	Quantitative RT-PCR with SYBR green	112
4.2.7	DIG labeling of RNA probe (cRNA synthesis)	112
4.2.8	Whole mount <i>in situ</i> hybridization on mouse embryo	113
4.3	Protein methods	117
4.3.1	Crude protein extracts	117
4.3.2	Nuclear extracts	117
4.3.3	Polyacrylamide gel electrophoresis (PAGE)	118
4.3.4	Coomassie staining of protein gels	118
4.3.5	Western analysis	119
4.4	Cell culture	120
4.4.1	Preparing Mouse Embryonic Fibroblast cells (MEFs, feeders)	120
4.4.2	Expanding MEF cells	120
4.4.3	Freezing MEF cells	120
4.4.4	Culturing mouse ES cells	121
4.4.5	Harvesting ES cells	121
4.4.6	Freezing ES cells	122
4.4.7	Preplating	122
4.4.8	Electroporation	122
4.4.9	Transformation	123
4.4.10	Apoptosis assay	124
4.5.	Histology	126
4.5.1	Perfusion of mouse	126
4.5.2	Paraffin sections of testis	126
4.5.3	Paraffin sections of embryos	127

4.5.4	Immunohistochemistry on paraffin sections	127
4.5.5	TUNEL staining on paraffin sections	128
4.5.6	Cryosection	129
4.5.7	Immunohistochemistry on cryosection	129
4.5.8	Whole mount LacZ staining of embryos	129
4.5.9	Whole mount Fast-red staining of primordial germ cells (PGC)	130
4.6.	Transgenic mice	131
4.6.1	Genotyping	131
4.6.2	Tamoxifen gavage of mouse	131
5.	MATERIAL	132
5.1	Chemicals	132
5.2	Solutions	133
5.3	Buffer	134
5.4	Other reagents	134
5.4.1	Enzymes, marker and nucleotides	134
5.4.2	Kits	134
5.4.3	Antibodies	135
6.	REFERENCES	136
	ACKNOWLEDGEMENTS	144

1. Introduction

1.1 Eukaryotic transcriptional control

Amongst the most fascinating phenomena that science is exploring is the emergence of life on our planet. All life that is known to exist on earth today, although quite diverse in appearance, seems to be of the same form – one based on 2-deoxyribose nucleic acid (DNA) genomes and protein enzymes. DNA, which can be described as an informational macromolecule, is composed of two helical chains each coiled around the same axis (Watson et al., 1953). Following the elucidation that genes correspond to specific segments on the DNA and further progress in understanding transcriptional control in prokaryotes, public attention has turned to understanding transcription in eukaryotes: How are so many genes transcribed in a cell-type specific, developmentally regulated manner? A part of the answer has been found in a mode of regulation that involves **chromatin**.

1.1.1 Chromatin

The DNA of eukaryotic cells is organized and condensed by its association with small, basic histone proteins. This package of DNA and protein is termed chromatin, a structure that solves the problem of fitting 2 meters of DNA strands into the nucleus. In addition, chromatin provides a dynamic platform for all DNA-mediated processes within the nucleus.

The basic redundant unit of chromatin is the nucleosome core particle, typically an octamer composed of the four core histones H2A, H2B, H3 and H4, with 147 bp of DNA wrapped nearly twice around the histone core (Luger et al., 1997). Each nucleosome is separated by 10 – 60 bp of “linker” DNA. This repetitive arrangement establishes a chromatin fiber of ~ 10 nm diameter, which is believed to be folded into more condensed, ~30 nm thick fibers that are stabilized by binding of the linker histone H1 to each nucleosome core. Such 30 nm fibers are then further condensed to form 100

– 400 nm thick interphase fibers or the highest packaging density, found in metaphase chromosomes.

Each core histone is composed of a structured globular domain and an unstructured N-terminal tail. The conserved globular domain mediates histone-histone interactions within the octamer and organizes the two wraps of DNA. The aminoterminal 20-35 residue tail is rich in basic amino acids and is believed to protrude from the surface of the nucleosome; histone H2A is unique in having an additional 37 amino acid carboxy-terminal domain. These histone “tails” do not contribute significantly to the structure of nucleosomes, but probably influence the folding of nucleosomes into higher order structures. Indeed, *in vitro* removal of the histone tails results in nucleosomal arrays that cannot condense past the 10 nm fiber.

Coiling of DNA around the nucleosome is now recognized as a cornerstone of transcriptional control (Kornberg et al., 1999; Struhl et al., 1999). Nucleosomes can repress transcription by occluding sites of protein binding to DNA, thereby interfering with the interaction of DNA binding proteins i.e. activator and repressor proteins, polymerases, transcription factors and DNA-modifying enzymes. Moreover, chains of nucleosomes can become further condensed, and this higher-order coiling can represses transcription of entire chromosomal domains. The interaction of nucleosomes with additional chromosomal proteins in condensed *heterochromatin* can repress gene expression in a hereditary manner, while a more open, transcriptionally active state is found in *euchromatin*. There are at least three principal ways by which the nucleosomes contribute to the dynamics of chromatin. First, the composition of nucleosomes can be modulated by replacing the major histone proteins with specialized variants (Santisteban et al., 2000; Smith et al., 2002; Ahmad et al., 2002). Second, ATP-dependent chromatin-remodeling complexes can change the position of nucleosomes, which is believed to “loosen” nucleosome arrangement and allow DNA-binding proteins to gain access to their target (Martens et al., 2003). Finally, the histones are subject to a rich variety of posttranslational, covalent modifications.

1.1.2 Post-translational histone modifications

Separate lines of work on chromatin structure and gene activator proteins recently intersected to reveal a fundamental mechanism of eukaryotic gene regulation. Proteins previously identified as modulators of transcription were discovered to possess catalytic activities directed at histones. Identified histone modifications include lysine acetylation, lysine and arginine methylations, serine and threonine phosphorylations, lysine ubiquitylation and sumoylation, as well as ribosylation. These modifications could theoretically affect chromatin function through two distinct mechanisms. First, nearly all modifications alter the electrostatic charge of the histone. Consequently, this could affect the interactions between nucleosomes themselves and nucleosomes and DNA, thereby influencing the folding dynamics of nucleosomal arrays. Although it was observed that hyperacetylation by 6 to 12 acetates per histone does disrupt the folding dynamics of nucleosomal arrays *in vitro*, there is no further evidence for this model. In contrast, there is much evidence for a second model, where histone modifications can create binding surfaces for protein recognition and thus recruit specific functional complexes. Indeed, examples of such epitopal binding have been identified in the case of the bromodomain, which can recognize acetylated lysine, and the chromodomain, which can recognize methylated lysine (Dhalluin et al., 1999; Jacobs et al., 2002). The discovery of these specific interactions led to the “histone code” hypothesis, which posits that specific histone modifications recruit particular transacting factors to accomplish specific functions (Jenuwein and Allis, 2001). Recent studies have supported this view and shown that specific combinations of histone modifications often dictate a particular biological outcome. Methylation of H3 K9, H3 K27, and of H4 K20 and absence of H3 and H4 acetylation is often found in transcriptionally repressed regions of the genome (i.e. pericentric heterochromatin). Conversely, trimethylation of H3 K4, phosphorylation of H3 S10, and acetylation of H3 K14 and H4 K8 are often found in transcriptionally active euchromatin. Further, histone modifications not only affect transcriptional control, but also play fundamental roles in DNA repair, during the cell cycle, and in establishment of pericentric heterochromatin. In the case of DNA repair, the DNA damage checkpoint kinase ATM (yeast Mec1p) is recruited to a DNA double strand break where it phosphorylates histone H2A in yeast or H2AX in mammals. Particular patterns of histone modifications also correlate with global

chromatin dynamics during the cell cycle. Diacetylation of histone H4 at K4 and K12 is associated with histone deposition at S phase, while phosphorylation of histone H2A (at S1 and T119) and H3 (at T3, S10 and S28) are often found in condensed mitotic chromatin. Finally, the establishment of chromatin structure surrounding mammalian and fission yeast centromeres involves histone methylation and the RNA interference (RNAi) machinery (Schramke et al., 2003). The low transcription of double-stranded, noncoding RNAs from repetitive elements (retrotransposons) clustered in pericentric heterochromatin provides substrates processed by the RNAi machinery. The resulting 21-23 nucleotide RNAs associate with several chromatin components, target Ctr4 methylation at H3 K9 to pericentric regions, which subsequently recruits Swi6 (HP1) and leads to heterochromatin formation.

The identification of histone modifying enzymes and their respective target sites has made remarkable progress recently, and led to the definition of **histone acetyltransferase (HAT)**, **histone deacetylases (HDAC)**, **histone methyltransferase (HMT)** and **histone kinase** families.

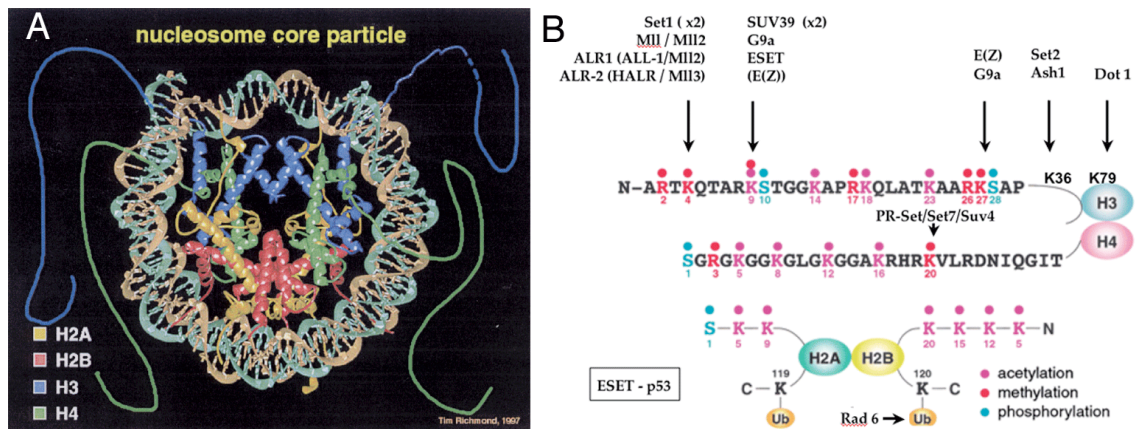


Fig.1 (A) Structure of the nucleosome (B) Histone methyltransferases (except Rad6) and their target sites on histone tails.

1.1.3 Histone acetyltransferases (HAT)

Acetylated histones are usually associated with transcriptionally active chromatin and deacetylated histones with inactive chromatin. The acetylation of histone tails could theoretically increase the access of transcription factors to DNA through structural changes in nucleosomes. The neutralization of the basic charge of the histone tails by

acetylation is thought to reduce their affinity for DNA and to alter histone-histone interactions. Moreover, coactivators and transcription factors are recruited by specific binding to acetylated histone tails. The highly conserved histone H3 lysines at amino-terminal amino acid positions 9, 14, 18 and 23, and H4 lysines 5, 8, 12 and 16, are frequently targeted for acetylation. As an exception to the hyperacetylation found in transcriptionally active regions, acetylation of H3 lysine 12 is linked to transcriptional silencing in yeast and *Drosophila* (Turner et al., 1992; Braunstein et al., 1996).

Strong molecular evidence for a direct link between acetylation and transcription was provided when the conserved transcriptional regulator Gcn5 was found to have histone acetyltransferase (HAT) activity (Brownell et al., 1996). Yeast and human Gcn5 is usually associated with other transcriptional adaptors or gene-specific activator proteins in multisubunit complexes (i.e. SAGA complex) that regulate its specificity and recruitment to target promoters. Numerous other coactivator proteins have been found to possess HAT activity, and there are currently several reported families of acetyltransferases, comprising over twenty enzymes. In human cells, the related proteins CBP [cAMP-responsive element-binding (CREB)-binding protein] and p300 bind to activator proteins involved in cell-cycle control, differentiation, DNA repair and apoptosis. CBP and p300 stimulate transcription by acetylating histones and are therefore termed 'coactivators'. The physical association between CBP and a histone methyltransferase activity indicates a functional cooperation of acetylation and methylation of histones (Vandel et al., 2000).

1.1.4 Histone deacetylases (HDAC)

Specialized regions of chromatin are transcriptionally inactive and form hypoacetylated, heterochromatin-like regions, i.e. telomeres, centomeres, and silent yeast mating-type loci. Inhibition of histone deacetylase (HDAC) activity and inactivation of sites for hypoacetylation in histone H4 are known to disrupt the formation of such highly condensed domains (Ekwall et al., 1997). Furthermore, a large number of HDAC have been identified, many of which act as corepressors of transcription. The yeast HDAC Rpd3 is recruited by repressor proteins to promoters, thereby contributing to repression by local deacetylation of chromatin (Wu et al., 2000). In yeast, heterochromatin formation is mediated by the HDAC Sir2 and the Sir3 and Sir4 silencing proteins (Imai

et al., 2000; Landry et al., 2000; Smith et al., 2000). Interestingly, HATs and HDACs seem to counteract the effects of each other by a constant acetylation and deacetylation. This global, antagonizing activity maintains an equilibrium level of histone acetylation throughout the genome. Probably, the genome-wide acetylation status of histone tails is adaptable to certain requirements of chromatin dynamic during the cell cycle.

1.1.5 Histone kinases

Histone phosphorylation contributes to processes such as transcription, DNA repair, and chromosome condensation. Gene activation in mammalian cells and during the heat shock response in *Drosophila* has been shown to correlate with phosphorylation on serine 10 of histone H3. Epidermal growth factor (EGF) treatment of fibroblasts leads to rapid phosphorylation of serine 10 by Rsk-2 and simultaneously induces the induction of early response genes such as *c-fos*. The mechanism by which phosphorylation contributes to transcriptional activation is not well understood. However, it has been shown that several HATs have increased activity on phosphorylated substrates. Thus, the transcriptional activation by histone kinases could be mediated by phosphorylation-dependent recruitment of acetylating co-activators. Phosphorylation of H2A is correlated with mitotic chromosome condensation. In yeast, the induction of DNA damage rapidly induces phosphorylation of H2A at serine 139 by the Mec1 kinase. The requirement of this histone modification for efficient non-homologous end-joining repair of DNA suggest the formation of a chromatin structure that facilitates the repair, or the surface-dependent recruitment of DNA repair proteins.

1.1.6 Histone methyltransferases (HMT)

Acetylations and phosphorylations of histones occur with a relatively high turnover and are therefore considered as short-term signals of the 'histone code'. By contrast, histone methylation has been regarded as a more long-term epigenetic mark, consistent with the relatively low turnover of the methyl group. Histone methylation occurs on lysine residues 4, 9, 27, and 36 in H3, and on position 20 in H4. In addition, lysine methylation is present in the highly variable N-terminus of the linker histone H1 and in

non-histone proteins. Each lysine can accept up to three methyl groups, adding another level of complexity to the 'histone code'. Suv(var)3-9 was the first identified mammalian HMT, which specifically methylates H3 at lysine 9 (Rea et al., 2000). The methyltransferase activity of Suv(var)3-9 lies within one invariant protein motif named the SET domain. The SET domain was initially identified as a 130-residue motif present in *Drosophila* SU(VAR)3-9, the *Polycomb*-group protein Enhancer of zeste [E(z)] and in the *trithorax*-group protein Trithorax (TRX). There are more than 70 gene sequences containing the SET domain in mammals, but only seven SET-domain gene sequences (named Set1 to Set7) in the budding yeast *S. cerevisiae*. Furthermore, budding yeast, unlike fission yeast, does not undergo H3 lysine 9 methylation. Comparison of the SET domains found in mammals led to their classification into four subfamilies.

The **SUV39 subfamily** includes the founding member, *Drosophila* Su(var)3-9, closely related to yeast Clr4. In mice, there are two orthologues named Suv39h1 and Suv39h2. Methylation by Suv39 at lysine 9 of H3 creates a binding site recognized by the heterochromatin protein HP1 [yeast Swi6] (Bannister et al., 2001; Lachner et al., 2001). Interestingly, Suv39 associates with HP1 and therefore creates its own binding site, a mechanism that allows the spreading of the methyl mark for repressive heterochromatin. Another member is G9a, which is closely related to Suv39 and represents a 'dual' HMT that methylates K9 and K27 of histone H3. Interestingly, methylation specific antibodies have revealed that G9a mono-methylates lysine 9, while Suv39 di- and tri-methylates lysine 9. Finally, ESET methylates lysine 9 on H3 *in vitro*, recent observations however suggest that the *in vivo* target of this HMT is the p53 protein.

The **SET2 subfamily** is defined by the SET domain of the founding member from *Saccharomyces cerevisiae* SET2, which methylates K36 on histone H3 (Strahl et al., 2002). Included in this subfamily are the three highly related members NSD1, NSD2 and NSD3. NSD1 binds hormone receptors such as retinoic acid receptors and thyroid hormone receptors. Thus, it is possible that NSD1 is a co-regulator of hormonally regulated gene transcription through specific interaction with nuclear receptors. The *Drosophila* ASH1 gene has a bromodomain, a Phd finger domain and a SET domain that suggests its classification within the SET2 subgroup. In addition, ASH1 is a TRX group gene homologue that also belongs to the trxG3 subgroup, which includes Trithorax, ASH1 and ASH2. The multiple methylation specificities towards H3 K4, H3 K9 and H4 K36 of ASH1 are intriguing but may be artifacts of the *in vitro* assays.

The third group is the **RIZ subfamily**, which includes the proteins RIZ, MDS-EV11, MDL1, BLIMP1, PFM1 and MEL1. None of the RIZ proteins has been shown to possess methyltransferase activity. However, a mutation in the SET domain of RIZ1 identical to a mutation that abolishes the methyltransferase activity of Suv39 (Cys106Thr) has a transforming effect. The fact that this mutation is found in tumors suggests that the RIZ1 protein might possess an enzymatic activity, impairment of which promotes oncogenesis.

The **SET1 subfamily** includes yeast SET1 that has the capacity to methylate lysine 4 on histone H3 (Roguev et al., 2001). In mice, there are two orthologues named SET1a and SET1b. This family includes the polycomb group (PcG) proteins EZH1 and EZH2, and the trithorax group (TrxG) proteins MLL (TRX1/HRX/ALL1), MLL2 (TRX2/HRX2), MLL3 and the related protein ALR. Finally, this family includes SET7 (SET9), which methylates H3 K4 and H4 K20. A defining structural feature of this family is a SET domain, at the very carboxyl terminus of the protein, which is mostly followed by a POST-SET domain. The two proteins that do not fit this definition are EZH1 and EZH2, which methylate H3 K27, while all other members are likely to methylate H3 K4. Therefore EZH1 and EZH2 may represent a subset of this family.

Set1 is the exclusive H3 K4 methyltransferase in the yeast genome, which does not contain homologues of the TrxG genes MLL and MLL2. The Set1 complex purified from *S. cerevisiae* comprises eight members (Roguev). Interestingly, two separate polypeptides, Bre2, containing a SPRY domain, and Spp1, containing a PhD finger, appear to be the homologue of Ash2, which contains both conserved motifs. Subsequent purifications of the 3 mammalian Set1, Mll and Mll2 complexes revealed a remarkable similarity in composition (Wysoka et al., 2003; Yokoyama et al., 2004; Hughes et al., 2004). All three complexes contain mammalian ASH2L (*Drosophila* Ash2 and yeast Bre2/Spp1), and the highly conserved WD40 repeat-containing proteins WDR5 and/or RBBP5 (yeast Swd2/3 and Swd1, respectively). In addition, the tumor suppressor menin associates with both MLL and MLL2 complexes and is required for the methyltransferase activity. The similar composition of the mammalian SET1, MLL and MLL2 complexes and the yeast SET1 complex could indicate an ancient and conserved biochemical machinery for histone H3 lysine 4 methylation.

1.1.7 Epigenetic regulation of cellular memory by the Polycomb and Trithorax group proteins

The maintenance of differential gene-expression patterns of specific cell types during DNA replication and at mitosis is believed to be accomplished by epigenetic mechanisms. In *Drosophila*, the antagonizing Polycomb group (*PcG*) and Trithorax group (*TrxG*) proteins are required to maintain gene expression patterns of important developmental regulators like the Hox genes during cellular proliferation. The molecular mechanism of this regulation is poorly understood. However, recent work has shown that at least part of the silencing function of the PcG complex ESC-E(Z) is mediated by its intrinsic activity for methylating histone H3 on lysine 27. Several studies have indicated that histone tail methylation can affect chromatin-based gene regulation and lead to the proposition that patterns of covalent modifications serve as an epigenetic code for transcriptionally active or silenced chromatin. Previous studies have shown that PcG mediated gene repression mediated by histone methylation can be propagated through DNA replication and mitosis, thereby guaranteeing the inheritance of silenced chromatin states. In contrast, much less is known about inheritance of the active state, which leads to the question:

Are there epigenetic mechanisms in mammals based on inheritance of active chromatin states?

It is unclear, if and how ‘active’ chromatin states are propagated and inherited through cell divisions, but mammalian SET1-like complexes are likely to contribute to these mechanisms. The goal of this thesis was a functional analysis of Mll2, a SET1-like histone methyltransferase, and to gain insights to mammalian mechanisms of inheritance of active chromatin states. For reasons that are discussed in **section 1.2**, this study used the mouse as model organism.

1.2 Manipulating the mouse genome

The availability of totipotent mouse embryonic stem (ES) cells and near-complete DNA sequence of the mouse genome(s) has greatly simplified the generation of transgenic mouse mutants. One reason for the use of the mouse relative to other model genetic organisms is that it is the closest genetically tractable organism. Indeed, despite the facility with which other model organisms can be dissected genetically (e.g. *D. melanogaster* and *C. elegans*), the mouse is valued for its relatively unique applicability to the genetic study of immunology, cancer, behavior, and mammalian development. At present, it represents the premier genetic model organism for the study of human disease and development.

The development of new methods for manipulating the mouse genome, including transgenic and embryonic stem (ES) cell knockout technology, combined with greatly improved genetic and physical maps for mouse has revolutionized our ability to generate new mouse models to study gene function.

1.2.1 Mammalian multipurpose allele

Hundreds of genes have been mutated by targeted mutagenesis in the mouse, and the field of biomedical research has benefited significantly from the study of these mutant mice. Despite the power of the targeted mutation technology, this approach has limitations. The creation of targeted mutations is still costly, labor-intensive and time consuming. Moreover, while the basic gene targeting experiment yields a null allele, it is often the case that more subtle mutations provide more information about gene function. These mutations can be gain-of-function alleles, hypomorphic alleles or hypermorphic alleles. In addition, recently developed technologies include conditional tissue-specific and/or inducible mutagenesis and protein complex purification using targeted insertion of protein tags. Instead of creating several mouse lines with different allelic variations for a single gene, an elegant enhancement is to combine more than one of those features in one multipurpose allele. A paradigm for such a multivalent

approach is a null allele that is convertible to a conditional allele *in vivo* by recombeneering the genome with site-specific recombinases (SSR).

1.2.2 Recombeneering the mouse genome with site-specific recombinases

Regulated somatic mutagenesis is essential for the analysis of gene function during development and in the adult organism. In mice transgenesis through oocyte injection or DNA recombination in embryonic stem (ES) cells allows mutations to be introduced into the germ line. However, the earliest phenotype of the introduced mutation can eclipse later effects and circumvent studies of gene function during subsequent development. A solution to this problem is temporally and/or spatially regulated somatic mutagenesis.

Recent work on somatic mutagenesis has focused on the use of site-specific recombination (Kilby et al., 1993; Rossant et al., 1995; Bedell et al., 1997). Two site-specific recombinases (SSRs), Cre recombinase from the *Escherichia coli* phage P1 and FLP recombinase from the 2 μ circle of *Saccharomyces cerevisiae*, have been shown to possess the properties required for genomic manipulations in a wide range of living systems including mice. Genomic manipulations with SSRs require expression of an SSR protein and introduction of at least two recombination target sites at chosen positions in the genome. The type of recombination event mediated by the SSR depends on the disposition of the recombination target sites, with deletions, inversions, translocations and integrations being possible (Kilby et al., 1993).

In addition, it was shown that the ligand-dependent characteristics of steroid hormone receptors could be imposed on SSRs by expressing recombinase-steroid receptor fusion proteins (Logie et al., 1995; Metzger et al., 1995). These fusion recombinases are inactive in the absence of a cognate steroid hormone, but respond rapidly to hormone administration, allowing regulation of their enzyme activities by administration of the appropriate ligand. In the absence of ligand, the hormone receptor domain interacts with the ubiquitous heat shock protein 90 (HSP90) and traps the recombinase fusion protein in an inactive complex. Upon ligand binding, the fusion protein is released from this complex and can now bind the target sites, where it catalyses the recombination reaction. Thus SSR-steroid receptor fusion proteins present an experimentally convenient way to determine the time of recombination by ligand administration.

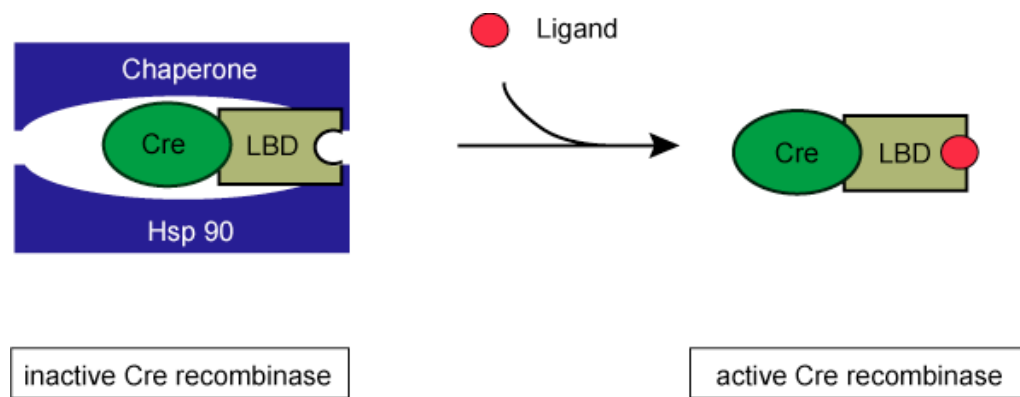


Fig. 2 *Temporal regulation of site-specific recombinase.*

The expressed protein is a fusion of Cre recombinase and the ligand binding domain (LBD) of the human estrogen receptor. The fusion protein is inactive because the LBD interacts with the ubiquitous Hsp90 complex. The fusion protein is released from the inactive state upon ligand binding by the LBD, allowing recombination between loxP sites in the genome. The LBD is mutated and does not bind to the endogenous hormone estrogen, instead activation is achieved with binding of the synthetic ligand tamoxifen.

Somatic mutagenesis in mice using SSRs requires, for precision, a near complete absence of background recombination. This is accomplished by expressing a fusion protein with a mutant estrogen receptor ligand-binding domain (EBD) that is insensitive to endogenous hormone β -estradiol but still responsive to the synthetic estrogen antagonist 4-OH-tamoxifen (Feil et al., 1997).

1.2.3 The Mll2 multipurpose allele

The mll2 allele used in this study serves three purposes of valuable merit. It is a null allele and a reporter for mll2 expression in its original configuration, but convertible to a conditional allele.

The strategy for the null allele is trapping of the endogenous transcript by a strong splice acceptor at the 5' end of the cassette (see section 2.2.1 for more detail). In the transcribed pre-mRNA exon 1 is spliced to the cassette instead to exon 2. The cassette comprises an IRES-LacZneo sequence that leads to expression of a LacZneo fusion protein under the promoter of mll2. A polyadenylation signal at the end of the cassette truncates the trapped transcript from which no mll2 protein is translated.

A null allele based on RNA splicing rather than genomic destruction of the gene gives an additional option, the creation of a conditional allele. For this purpose the cassette flanked by FRT sites is removed by the site-specific recombinase (SSR), Flp, which converts the null allele back to wild type. By using a second SSR, cre, a small genomic sequence including exon 2 can be deleted. By consequence, exon1 is spliced to exon3 in the pre-mRNA, creating a frame-shift mutation. The frame shifted mRNA has several stop codons and presumably does not produce full-length Mll2 protein. While the original allele is a constitutive null, the Flp recombined allele is a conditional that can be induced selectively to a null in a tissue and temporal specific manner by the cre recombinase.

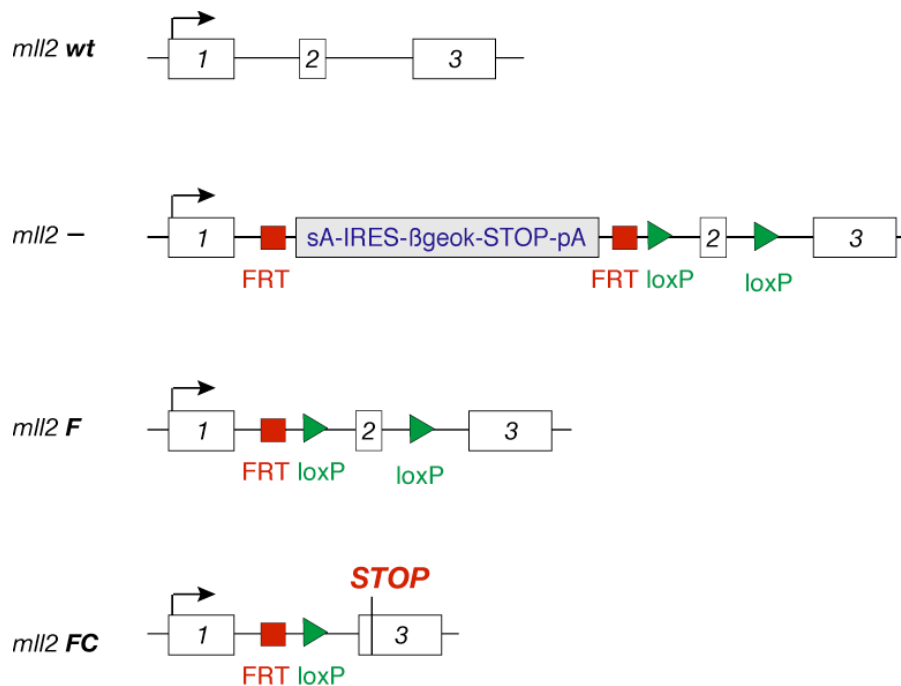


Fig. 3 The *mll2* multipurpose allele.

Shown is the *mll2***wt** allele from exon 1 to exon 3. The *mll2***-** allele was created by insertion of a synthetic exon, including IRES-LacZneo, a STOP codon and a polyadenylation signal, to intron 1. Mll2⁻ is a null allele by trapping and truncation of endogenous mRNA and a reporter for *mll2* expression by LacZ expression. By Flp mediated recombination, the null allele can be converted to the *mll2***F** allele, which is similar to wild type. The conditional allele *mll2***F** (Flp recombined) can be mutated by Cre recombinase, which removes exon 2 and creates the frame shifted allele *mll2***FC** (Flp & Cre recombined). In the processed mRNA transcribed from the *mll2***FC** allele, exon1 is spliced to exon 3. This creates a frame shift and a STOP codon, which prevents Mll2 protein translation.

1.2.4 Recombinogenic DNA engineering in *E.coli*

Section 1.2.1 described the benefits of multipurpose alleles in functional genomics. DNA engineering of these alleles often requires complex assembly of several elements creating very large molecules. Moreover, *Escherichia coli* vectors that contain large inserts, such as bacterial artificial chromosomes (BACs), offer several advantages for functional genomics. They can carry sufficient DNA to encompass most eukaryotic genes in a single molecule and are a valuable source for production of targeting constructs. However, DNA engineering by conventional cloning methods relies on the use of restriction enzymes, which precludes engineering of large molecules, as suitable restriction sites are often absent. Novel DNA engineering strategies that rely on homologous recombination *in vivo* in *E. coli* alleviate this limitation and allow a wide range of modifications of DNA molecules at any chosen position (Muyrers et al., 2001). Homologous recombination allows the exchange of genetic information between two DNA molecules in a precise, specific and faithful manner. These qualities are optimal for engineering of a DNA molecule regardless of its size. Homologous recombination occurs through homology regions, which are stretches of DNA shared by the two molecules that recombine. Because the sequence of the homology regions can be chosen freely, any position on a target molecule can be specifically altered, and virtually any DNA alteration can be achieved.

Recombinogenic engineering can be accomplished using ET recombination™ where recombination is mediated by phage-derived protein pairs, either RecE/RecT from the *Rac* phage or Red α /Red β , from γ phage (Zhang et al., 1998; Muyrers et al., 1999). RecE and Red α are 5'-3' exonucleases, and RecT and Red β are DNA annealing proteins (Kolodner et al., 1994). Red γ , another protein from the γ phage, is used to inactivate endogenous *E. coli* exonuclease *RecBCD* for protection of introduced linear targeting molecules. All three proteins can be applied to and induced in any *E. coli* host by transient transformation of an expression plasmid (Zhang et al., 1998).

With ET recombination, as illustrated in Fig. 4, a linear targeting DNA carrying short homology regions flanking a selectable gene (sm) is integrated into a circular target DNA. The length of homology required for efficient recombination is 35 – 60 nucleotides, and thus short enough to be made by oligonucleotide synthesis. In a very convenient application, the synthesized oligonucleotides also include polymerase chain

reaction (PCR) primers for amplification of the selectable gene. In the second variation represented in Fig. 4, the linear targeting molecule is a PCR-amplified plasmid backbone that contains a selectable gene and an origin of replication. The oligonucleotides used for PCR also contain homology regions that are chosen to define the exact boundaries of the DNA region to be cloned or subcloned. The advantage of this strategy is that the subcloned DNA is not PCR amplified, excluding the risk of PCR generated mutagenesis and allowing manipulation of DNA fragments of up to 40 kilobases.

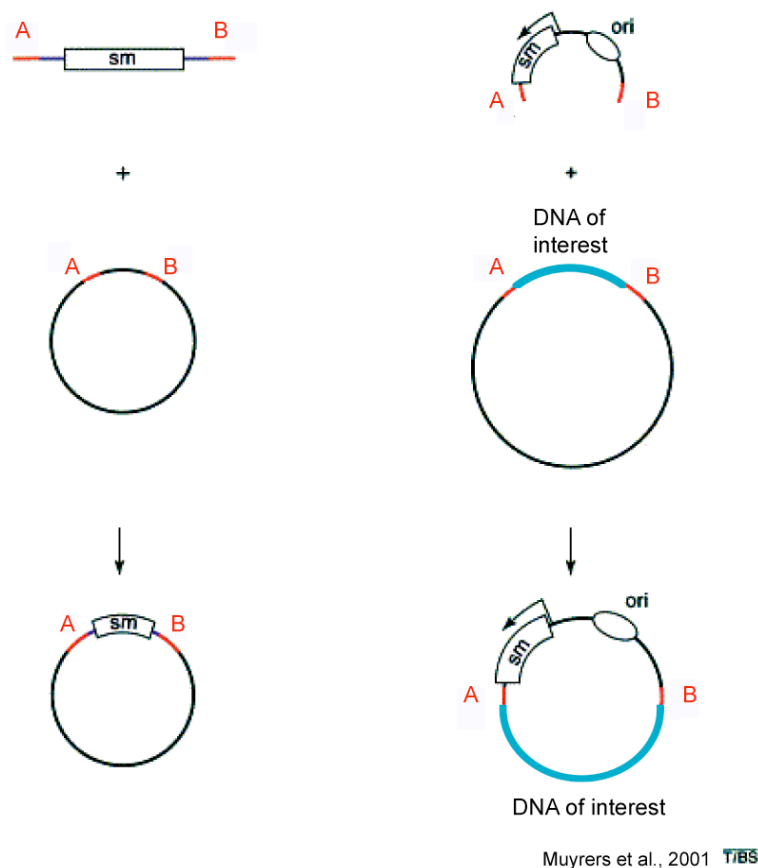


Fig.4 Two variations for recombinogenic DNA engineering.

A linear DNA is created (e.g. by PCR amplification) to include two regions, A and B, homologous to the regions in the targeting molecule, and a selectable marker gene (sm). The simplest exercise (left) involves insertion, by homologous recombination, of the linear targeting DNA into the target.

In a second variation (right), a DNA sequence is subcloned from a donor molecule (e.g. BAC). The linear DNA is a PCR amplified vector backbone, and includes an origin of replication (ori), a selectable marker (sm), and the homologie arms A and B. With this strategy, the subcloned DNA is not PCR amplified, excluding the risk of PCR generated mutagenesis and allowing manipulation of DNA fragments of up to 40 kilobases. (Muyrers et al., 2001)

2. Results

2.1 The Mll2 mouse line

Frank van der Hoeven generated this mouse line at EMBL in Heidelberg. My contribution to this work started with the analysis of the mouse line. Although I was not involved, I will briefly describe the production of the line in sections **2.1.1**, **2.1.2** and **2.1.3**.

2.1.1 Mapping of the mll2 gene.

Pierre-Olivier Angrand mapped the mll2 gene that spans approximately 35 kb of genomic sequence on chromosome 7. Three murine cDNA fragments named CF 28, CF 3.7, and CF14, were cloned and sequenced. The CF28 3.5 kb insert included incomplete exon1 and the missing sequence up to the initiating ATG was added by PCR. CF28 and CF3.7 had 2 kb overlapping sequence and were combined to a 5.5 kb sequence. The CF14 1.4 kb fragment confirmed exons 26 to 29 that were predicted by homology to the sequence of the murine homologue MLL. Mihail Sarov cloned the 3' end of the Mll2 cDNA including the SET domain.

2.1.2 Cloning of the mll2 targeting construct

A phage clone with genomic sequence of mll2 named X 2.2 was identified by hybridization to the murine mll2 cDNA CF28. A 6.1 kb HindIII fragment of X 2.2 was subcloned into pKS-bluescript and served as backbone for a targeting construct.

Next, a single loxP site was introduced in intron 2 of mll2. First, we inserted a loxP flanked PGK-neo cassette by Red/ET recombination. The two loxP sites were recombined by transient expression of Cre recombinase in *E. coli*. This removed the cassette and left a single loxP site in the plasmid. In the final step, a sa-IRES-lacZ-neo cassette flanked by FRT sites and a single loxP on the 3' end was introduced to intron 1 by Red/ET recombination. The final targeting construct had a 5' homology arm of 4.5 kb and a 3' homology arm of 1.6 kb. The 3' homology arm included one 35 bp loxP site, reducing the 3' flanking homologous sequence to 880 bp..

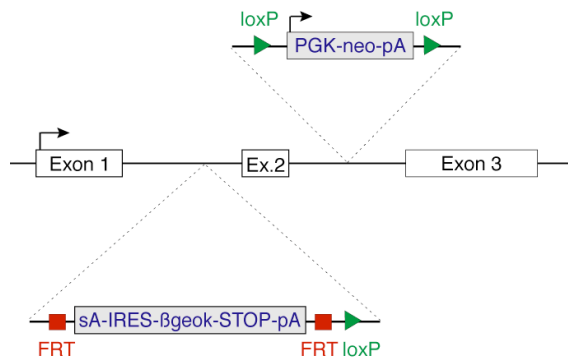


Fig. 5 Cloning of the *mll2* allele.

The selectable marker neomycin (neo), flanked by loxP sites, was introduced to intron 1 by Red/ET recombination. By transient expression of Cre recombinase in E.coli, the sm was removed, leaving a single loxP site in intron 2. Next, the cassette including sA-IRES-βgeok(LacZneo), two flanking FRT sites and a single loxP site, were integrated in intron 1 by Red/ET recombination.

2.1.3 Targeting of ES cells by homologous recombination

The targeting vector was linearized by NotI/SalI and the insert fragment purified. ES cells were electroporated with purified DNA and G418 resistant colonies were picked and expanded.

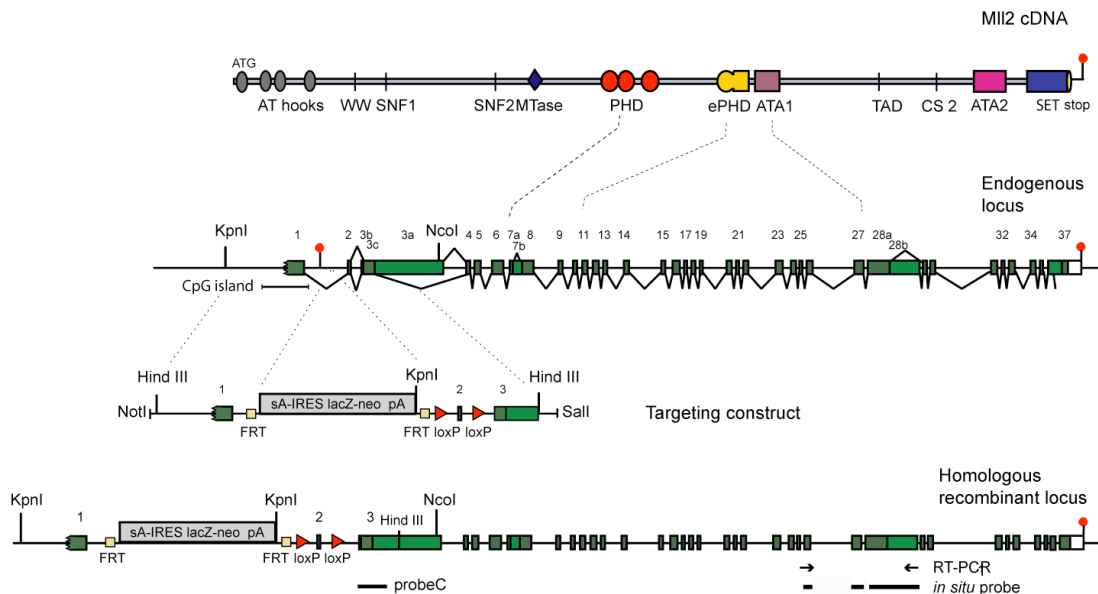


Fig.6 Targeted disruption of the mouse *mll2* gene.

Shown are the mouse *mll2* cDNA sequence, the genomic *mll2* wild type locus, the targeting vector, and the disrupted *mll2*- allele. The cDNA (8.5 kb) encodes several protein domains including four PHD fingers (PHD), ATA domains 1 and 2, the SET domain, and a sequence homologous to DNA methyltransferase (MTase). The *mll2* gene spans a genomic region of approximately 18 kb and has a CpG island at the transcription start site. The targeting construct was linerized with NotI/SalI and replaced 6.1 kb of endogenous sequence by homologous recombination. KpnI/NcoI-digested ES cells DNA was used for Southern analysis with probe C to screen for homologous recombinant clones. The probe hybridized to 4 kb and 2.6 kb restriction fragments generated from the wild type and the mutated allele, respectively.

The southern strategy used by Frank to identify homologous recombined clones is not known, but later Southern blotting with probe C of KpnI/NcoI digested tail DNA from wt and mll2 +/- mice confirmed the successful targeting (fig. 7).

2.1.4 Strains, crosses and genotypes of mice

The mll2 line was created by injecting targeted 129/ola ES cells into C57BL/6 blastocysts. Chimeric offspring was crossed to wild type C57BL/6 mice that gave birth to mll2 +/- mice with mixed background. Southern blotting of digested tail DNA confirmed correct targeting of Mll2 and excluded additional non-homologous insertions of the targeting construct. Intercrosses of heterozygote F1 mice did not yield homozygote offspring, indicating an embryonic lethal phenotype of Mll2 mutants. The line was kept in a heterozygote state with 5 consecutive crosses to C57BL/6 mice producing an inbreed background of 99 %. The genotyping of the Mll2 line was performed by PCR with sense primer 34 annealing in the neo gene and antisense primer 36 annealing in intron 2. This primer pair produces a 1.6 kb product from the targeted allele and no product from the wt allele.

Recombination of loxP sites flanking exon 2 was tested by crossing the mll2 line to the transgenic mouse strain PGK-Crem (Lallemand et al., 1998). In this strain, Cre is driven by the early acting PGK-1 promoter, but, probably due to cis effects at the integration site, the recombinase is under dominant maternal control. Consequently, when Cre is transmitted by PGK-Crem females, even offspring that do not inherit PGK-Cre recombine loxP sites. In the PGK-Crem female, cre activity commences in the diploid phase of oogenesis and is maternally inherited by the zygote. Thus, recombination occurs soon before the first cell division and is transmitted to replicating daughter cells. By coincidence, this transgenic line is X-linked (the Pgk-1 gene is located on the X chromosome). Advantageous for mouse colony management, males transmit the transgene to **all** their male offspring.

The mll2 null allele after cre recombination is still a null allele and was named mll2C (Cre recombined). As expected, no difference was observed between mll2 +/- and mll2C/+ mice. Successful recombination of loxP sites could be confirmed with primer pair 34/36, which produced a 800 bp smaller PCR product compared to the product from the unrecombined allele.

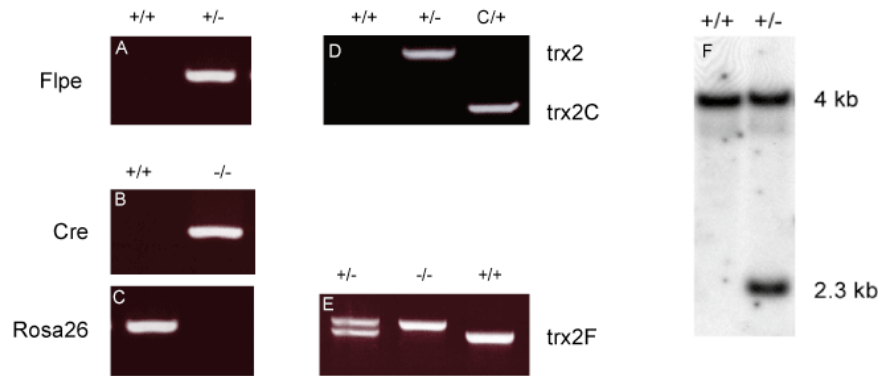


Fig.7 Genotyping of mice by PCR (A, B, C, D, E) and Southern blot (F). (A) Flpe-specific PCR for genotyping of the hATPC-Flpe line. Homozygote Flpe mice were identified by matings to wild type mice, in which they produced 100% transgenic offspring. (B) Cre-specific PCR for genotyping of the PGK-Crem and Rosa26-CreER(T2) line. Homozygous Rosa26-CreER(T2) mice were identified by PCR (C) with a primer pair flanking the insertion point of the targeting in the Rosa locus. (D) Genomic PCR for genotyping of the mll2 mouse line. The amplified PCR products are 1.6 kb and 0.8 kb from the mll2-allele and the cre recombined mll2C allele, respectively. (E) PCR to distinguish the Flp recombined allele mll2F from the mll2 wild type allele. The PCR product amplified from mll2F is 105 bp longer due to two loxP sites and a single FRT site. (F) Southern blotting of KpnI/NcoI digested tail DNA. Probe C hybridized to 4 kb and 2.6 kb restriction fragments generated from the wild type and the mutated alleles, respectively.

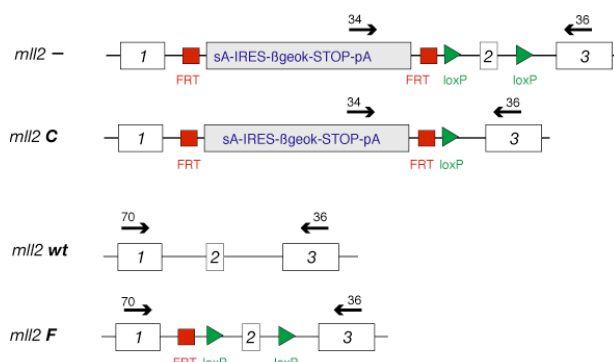


Fig. 8 Genotyping of mll2 alleles by PCR.

The primer pair 34/36 was used to identify the mll2- and mll2C alleles and produced a 1.6 kb and a 0.8 kb PCR product, respectively.

The primer pair 70/36 was used to identify the mll2F allele. The amplified PCR product was 1.5 kb, and could be distinguished from the 1.4 kb product of the wild type allele. Moreover, the primerpair was used to distinguish mll2-/- from mll2+/- embryos, as it amplified a 1.4 kb product from the wild type allele of heterozygotes. In contrast, the mutant embryos did not yield a PCR product, as the theoretical 7.9 kb product from the mll2- allele is not amplified.

We generated a conditional *mll2* line by crossing the original line to 2 different lines. First, we crossed *mll2*^{+/-} mice to the transgenic line hATPC-Flpe (Rodriguez et al., 2000). This line expresses the improved version of the Flp recombinase selected to recombine efficiently at 37°C and referred to as Flpe. The F1 offspring had only partially recombined FRT sites due to a lower efficiency of the enzyme compared to Cre, and a rather long distance of 6.5 kb between the target sites. However, an additional cross to hATPC-Flpe mice produced heterozygous Flp recombined offspring. We named the modified allele without the IRES-LacZneo cassette *mll2F* (**F**lp recombined). In contrast to the null allele, the *mll2F* allele is similar to wild type and was successfully breed to homozygosity. For genotyping, we used sense primer 70 annealing in exon 1 and antisense primer 36 annealing in intron 2 that produces a 1.5 kb PCR product from the wt allele. The PCR product from the *mll2F* allele is 102 bp longer due to the presence of one FRT site and two loxP sites.

Next, we crossed the *mll2F* line to the Rosa26-CreER(T2) line (Seibler et al., 2003). This line was created by targeting an inducible cre recombinase to the Rosa26 locus. The fusion protein is ubiquitously expressed and inducible by tamoxifen. Offspring heterozygous for *mll2F* and creER(T2) were crossed to *mll2F* homozygote and genotyped by PCR for both alleles. In addition, we crossed *mll2C*^{+/+} mice to Rosa26-creER(T2) mice. Finally, we crossed *mll2* F/F cre^{+/+} mice to *mll2C*^{+/+} and obtained *mll2C*^F:cre/cre mice. These mice have presumably the ideal genotype to efficiently induce loss of Mll2. First, the *mll2C* allele is already a null, leaving a single allele to be destroyed to create a k.o. Furthermore, homozygosity of the creER(T2) allele should favor efficient recombination due to higher concentrations of the protein. Mice were genotyped by PCR with cre specific primers 19 and 20. Homozygote cre allele was determined with primer pair rosa26 flanking the insertion point of the cre construct and producing a PCR product only in wild type and heterozygote mice.

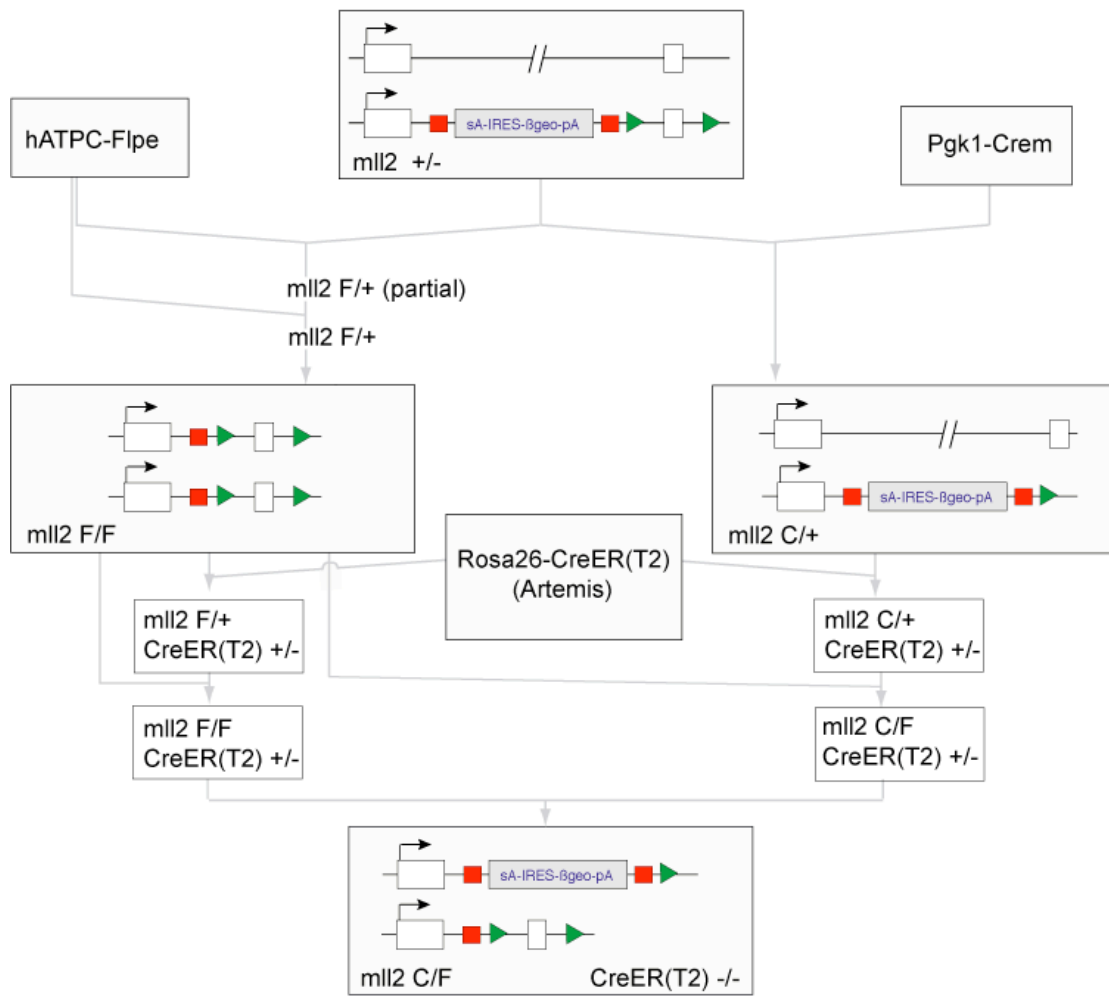


Fig. 9 *Matings of the mll2 mouse line.* Shown on top is the original *mll2*+/- line, which was obtained from matings of chimeric mice generated by blastocyst injections. Intercrosses of *mll2* +/- mice did not yield homozygous offspring, which indicated an embryonic lethal phenotype of homozygous embryos. Crossing the *mll2* line to three different lines generated a conditional *mll2* line. First, heterozygous *mll2* mice were crossed with PGK-Crem ((Lallemand et al., 1998) and produced *mll2* C/+ mice. Due to partial FLP recombination, *mll2* +/- mice were mated twice with hATPC-Flpe mice (Rodriguez et al., 2000) to generate *mll2* F/+ mice. The conditional *mll2*F allele is functional, and could therefore be intercrossed to homozygosity. Homozygous *mll2*F mice (and *mll2*C/+ mice) were mated to the ubiquitous, inducible Cre line Rosa26-CreER(T2) (Seibler et al., 2003). The F4 offspring from these matings were backcrossed to *mll2*F mice, yielding offspring without wild type *mll2* allele and heterozygous for Rosa26-CreER(T2). Intercrosses of this F5 offspring yielded mice with one null and one conditional *mll2* allele, and two Rosa26-CreER(T2) alleles.

The genetic background of the Flpe line was 75% C57BL/6 and 25% 129/ola when crossed to the mll2 line that had 87% C57BL/6 and 13% 129/ola backgrounds. The additional crossing of the partially recombined offspring to the Flpe line and subsequent crossing to Rosa26-creER(T2) with inbred 129/ola background produced conditional mice with a 39% to 61% C57BL/6 and 129/ola background, respectively.

Later, we crossed mll2F mice twice to C57B6 (wild type and Rosa26-creER(T2) to produce conditional mll2 mice with an inbred C57BL/6 background of 94%. With these mice the conditional genetic alteration was maintained on a standard background, a feature important for obtaining reproducible results and genetically defined controls.

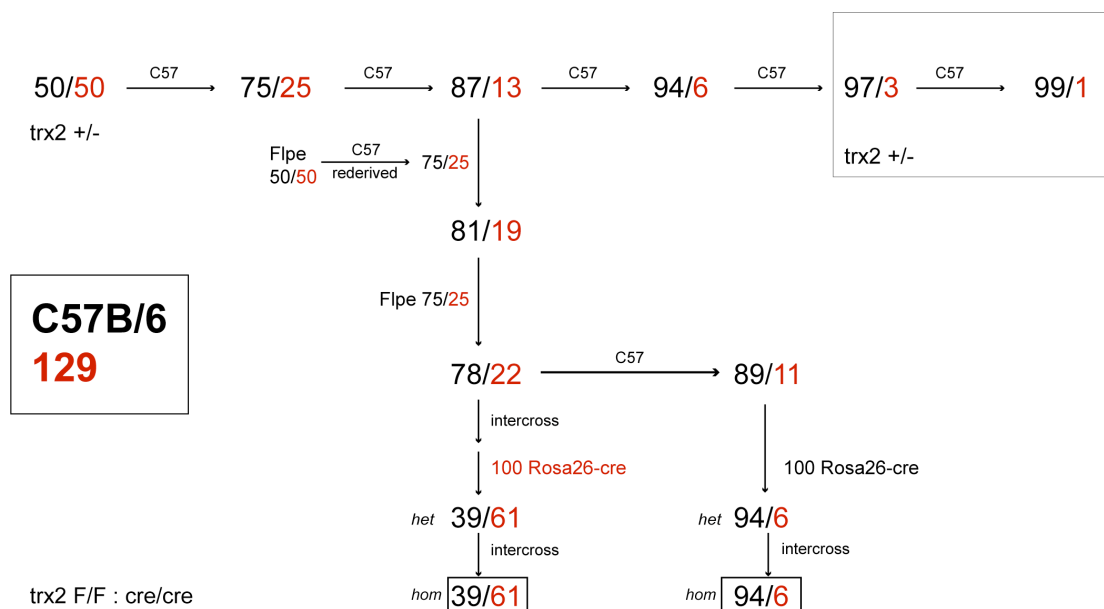


Fig.10 Genetic backgrounds of the mll2 mice. The mll2 line was obtained in a mixed 129ola/C57BL/6 background. An inbred strain was obtained by 6 to 7 crosses to C57BL/6 mice. The conditional line mll2F/Rosa26-CreER(T2) was generated twice, once with a mixed background (39 to 61), and once with a more inbred background (94 to 6) of C57BL/6 and 129/ola.

2.2 Constitutive mutagenesis of Mll2

The absence of Mll2 ^{-/-} mice from heterozygote crosses indicated an embryonic lethal phenotype of mutants and argued for an essential role of Mll2 during embryonic development. The goal of this study was to describe the embryonic phenotype and to gain insight into the roles of Mll2 in mouse development.

2.2.1 Validation of the null/reporter allele on RNA level

As described in section 1.2.3, the mll2 null allele leaves the genomic structure of the gene intact, but relies on trapping and truncation of the RNA transcript. The trap cassette is made of 1.8 kb of genomic sequence from the homeobox protein engrailed-2 (En2, ENSMUST00000036177/chromosome 5, BAC clone RP23-358F24) inserted between FRT and IRES of FRT-IRES-LacZneo-Stop-pA-FRT-loxP. The genomic sequence includes 1.65 kb of intron 1 and 158 bp of exon 2 of the En-2 gene and serves as splice acceptor (interestingly the En2 splice site is not properly predicted by the splice site detection software from www.cbs.dtu.dk/services/NatGene2/, therefore splice site prediction appears unfaithful). The null/reporter allele produces a polycistronic transcript from which 2 proteins are translated; First, a protein including 121 aa of mll2 (coded by exon1) fused to 40 frame shift mutated aa of En-2 (coded by a part of exon 2). Second, a LacZneo fusion protein is translated from the IRES sequence.

Such an allele design requires careful validation to exclude alternative splicing events that would ruin the strategy. Therefore, we wanted to confirm absolute trapping of mll2 transcript by the inserted trap cassette and efficient truncation at the newly introduced polyA site. If this was the case, no transcript spanning exon 2 to 37 should be detectable in mutant embryos.

We dissected E 8.5 embryos from mll2^{+/-} intercrosses. Genotyping by yolk sac PCR with primer pair 34/36 determined that 3/4 of each litter was carrying the null allele, and therefore potentially heterozygote or homozygote. A second PCR with primer pair 31/36, which flank the insertion point of the LacZneo cassette, detected 1/4 of embryos as homozygotes. These primers amplify a 720 bp product from the wt allele of heterozygotes, but not the theoretical 7.2 kb product from both null alleles of mutants.

This result indicated that the embryonic lethality occurs at later stages than E 8.5 in *mll2* mutants.

We extracted RNA from individual embryos and transcribed cDNA to perform RT-PCRs. The *mll2* specific primer pair 78/79 annealing to exons 26 and 29 did not amplify a product from cDNA of *mll2* mutants. However, the 1.6 kb product was amplified from *mll2*^{+/-} and *mll2*^{+/+} cDNAs with approximately twice the amount of product in the wild type. As control we used LacZ specific primers that amplified a product from *mll2*^{+/-} and *mll2*^{-/-} but not *mll2*^{+/+}. A third PCR with actin specific primers demonstrated the use of equal amounts of PCR template.

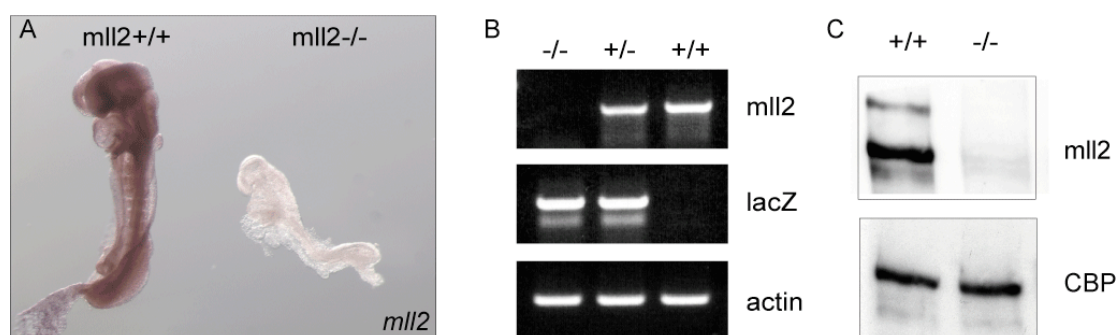


Fig.11 The *mll2* – allele is a null allele. (A) Expression of *mll2* at E8.5. The expression is ubiquitous in the wild type embryo and absent in the homozygous embryo. (B) RT-PCR analysis of E 8.5 embryos. An *mll2* specific primer pair amplified a reaction product from *mll2*^{+/-} and *mll2*^{+/+} embryos, but not from an *mll2*^{-/-} embryo. (C) Western blot analysis of wild type and *mll2*^{-/-} ES cells probed with an antibody that recognizes the N-terminus of Mll2 (amino acids 168 – 288). A strong band was detected in wild type extract probably corresponding to the predicted proteolytic 225 kDa Mll2 fragment processed by caspase1 (Hsieh et al.). The weaker band in wild type extract could correspond to the predicted 284 kDa unprocessed Mll2 fragment. No bands were detected in extracts from *mll2*^{-/-} cells.

Furthermore, we used whole mount *in situ* hybridization on embryos, with an *mll2* cDNA probe amplified by the RT-PCR primers 78/79. We observed ubiquitous expression of *mll2* in wild type embryos at E 8.5 d.p.c. Moreover, no signal could be detected in *mll2*^{-/-} embryos, further substantiating that no alternate splicing bypassed the synthetic exon.

Finally, we provided evidence that the null allele causes complete absence of Mll2 protein by using an *mll2* specific antibody and *mll2*^{-/-} ES cells. Julia Schaft generated the Mll2 antibody serum by immunization of two rabbits with synthetic peptide (aa 754 to 925). Julia Schaft generated *mll2*^{-/-} cells by targeting the second allele of *mll2*^{+/-} cells with a sA-IRES-LacZneo-hygromycin cassette. In a western blot we observed complete absence of Mll2 protein in double-targeted ES cells. An antibody specific for

CBP (Santa Cruz), a protein with similar size than Mll2, was hybridized to the stripped membrane to confirm loading of equal amounts of extract.

Next we wanted to compare the *mll2* null/reporter and the induced conditional *mll2* allele during embryonic development. If the design is correct, both alleles should give an identical embryonic phenotype. This experiment was a first validation of the conditional *mll2* allele, and a more detailed validation is described in sections 2.3.3, 2.3.4, and 2.3.5. We crossed the *Mll2*F line, where the *mll2* allele is flp recombined, to PGK-Crem (section 2.1.4; Lallemand et al., 1998). Offspring of these crosses with one (cre recombined) *mll2*FC allele were crossed to *mll2*+/- mice. Embryos from pregnant mothers were dissected and genotyped at various time points and phenotypes of *mll2*FC/- embryos were compared to *mll2*-/- embryos from previous dissections. Both alleles produced an identical embryonic phenotype, which confirmed that the frame shifted *mll2* allele is identical to the null allele. Genotypes from all dissections are summarized in table 2 in section 2.2.3.

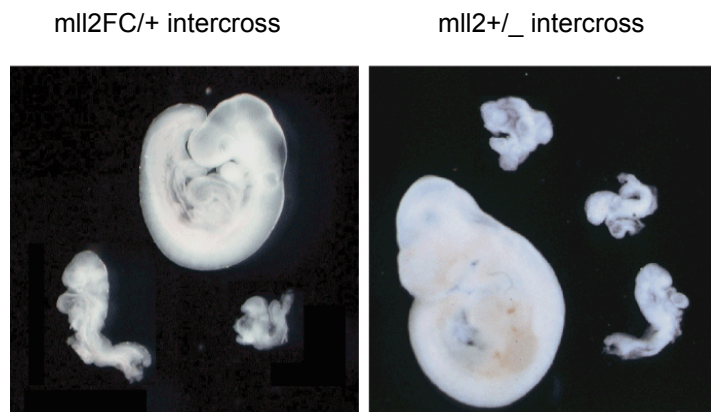


Fig. 12 *Mll2*^{-/-} embryos and *mll2*FC/FC embryos have an identical embryonic lethal phenotype. This validates the design of both alleles to be null alleles.

2.2.2 Embryonic expression pattern of *Mll2*

We dissected various litters from *mll2*+/- intercrosses at developmental stages E 6.5 to E 12.5 d.p.c. and performed LacZ staining for genotyping and expression pattern analysis. Results of β -Galactosidase stainings were confirmed by whole mount *in situ* hybridization of wild type embryos with an *mll2* specific probe described in section 2.1.1.

At gastrulation *mll2* expression was detected in the epiblast and visceral endoderm, but absent or weak in the trophectoderm. The almost ubiquitous expression pattern was found at all stages that we dissected and may persist throughout development. At E 9.5 *mll2* was detected in the ectoderm (surface ectoderm, neural tube, neural crest), endoderm (branchial arches) and mesoderm (mesenchyme and somites).

2.2.3 Phenotype of *Mll2* mutant embryos

Embryos from E 6.5 and 7.5 were genotyped by lacZ staining, with mutants staining more strongly than the heterozygotes due to the presence of two copies of the β -galactosidase gene. Embryos from later stages came from *mll2*^{+/-} to *mll2*^{C/+} crosses and were genotyped by yolk sac PCR. Due to the size difference of the PCR products amplified from the two different null alleles, primer pair 34/36 produced a double band in mutants (section 2.1.4).

Table 1 Embryonic lethality of the *trx2* mutant embryos

Embryonic day	Genotype			Resorbtion
	+/+	+/-	-/-	
E 6.5	8	13	6 (21%)	1 (4%)
E 7.5	8	18	9 (25%)	1 (3%)
E 8.5	27	44	30 (27%)	9 (8%)
E 9.5	32	71	36 (23%)	14 (9%)
E 10.5	24	51	19 (18%)	10 (10%)
E 11.5	5	10	3 (13%)	4 (18%)
E 12.5	3	7	0	4 (29%)

Table1. Genotype of mice resulting from *mll2* heterozygous intercrosses in C57BL/6J inbred mice

Table 2 Embryonic lethality of the *trx2* induced conditional embryos

Embryonic day	Genotype			Resorbtion
	+/+	FC/+	FC/FC	
E 9.5 (4 litter)	4 (12%)	18 (53%)	9 (26%)	3 (9%)
E 10.5 (3 litter)	6 (22%)	15 (56%)	5 (19%)	1 (4%)
E 11.5 (3 litter)	5 (24%)	12 (57%)	3 (14%)	1 (5%)
E 12.5 (3 litter)	4 (17%)	14 (61%)	0	5 (22%)
born pups (7 litter)	8 (31%)	18 (69%)	0	-

Table2. Genotype of mice resulting from *mll2*^{FC} heterozygous intercrosses in outbreed (C57BL/6 and 129/ola) mice. Both alleles produce an identical phenotype during embryogenesis.

At gastrulation (E 6.5) no obvious difference was observed between all 3 genotypes. However, at E 7.5 some mutants were retarded in development. While heterozygotes developed normally, the retardation was observed in all mutants at E 8.5. During further development the retardation of mutants compared to their wild type and heterozygote

littermates increased gradually. Interestingly, retarded mutant embryos still developed normally until E 9.5 and were morphologically identical to earlier stages of wild type embryos. However, from E 9.5 mutants had morphological abnormalities although they were still viable and continued developing. We observed widespread abnormalities rather than specific defects, e.g. anterior misshaping of the forehead but also posterior irregularities. An increase of resorptions to 10% at this stage indicates the earliest occurrence of lethality in mutants. Nevertheless, most mutants continue to develop and rarely turn between E 9.5 and E 10.5. Despite proper neurulation and closure of the head fold, the neural tube appears to be kinked, which is often a characteristic of lack of paraxial mesoderm. Indeed, while somites are visible at early stages, somite development is lacking in mutants at later stages. All mutants are hemorrhagic and dead by E 11.5 and fully resorbed by E 12.5.

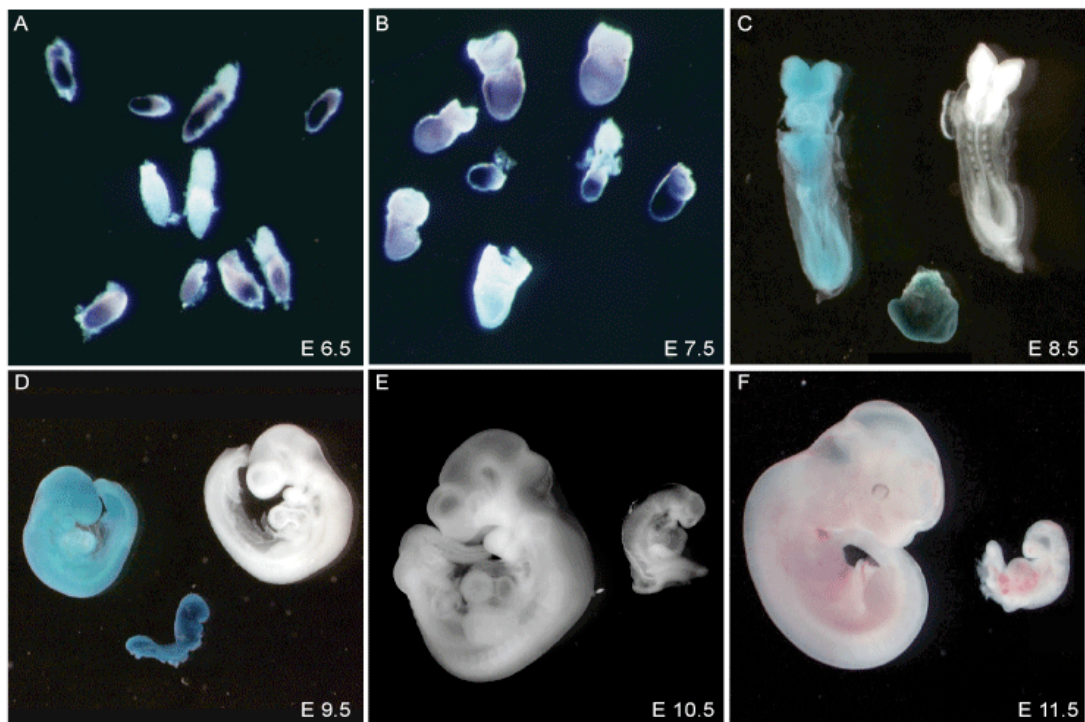


Fig. 13 *Mll2*^{-/-} embryos exhibit developmental delay and morphological abnormalities. Mutant embryos from litters shown in A, B, C, and D were identified by a strong LacZ staining due to two *mll2* null alleles. Individual embryos from litters C, D, E, and F were genotyped by yolk sac PCR and confirmed the LacZ results. (A) At 6.5 dpc, *mll2* mutants were identical compared to littermates (*mll2*^{+/-} and *mll2*^{+/+}). (B) The phenotype became first evident at 7.5 dpc when some mutants were retarded in development. (C) At 8.5 dpc, mutant embryos exhibited developmental delay but no morphological abnormalities. (D, E, F) Normal 9.5 dpc, 10.5 dpc, and 11.5 dpc embryos (*mll2*^{+/-} and *mll2*^{+/+}) compared with mutant *mll2*^{-/-} littermates. *Mll2*^{-/-} mutants had morphological abnormalities from 9.5 dpc and lethality occurred between 9.5 and 11.5 dpc.

Table 3 Typical somite numbers in wild type

E 8.0	4	somites	turning
E 8.4	8-9	somites	
E 8.5	10	somites	
E 8.7	12-13	somites	
E 9.0	16-17	somites	

Table 4 Retardation of *Mll2*^{-/-} mutants

trx2 ^{+/+} +/-	trx2 ^{-/-}	Δday	
E 7.5	E 7.0 - 7.5	0 - 0.5	
E 8.4	E 7.5 - 7.8	0.6 - 0.9	
E 9.5	E 8.3 - 8.5	1 - 1.2	
E 10.5	E 8.5 - 9.0	1.5 - 2	turning
E 11.5	/	/	

Table 3 & 4. *Developmental retardation of mll2^{-/-} embryos.* Table 3 summarizes typical somite numbers during developmental stages 8 to 9 dpc. Table 4 indicates the developmental stage of *mll2^{-/-}* embryos based on morphology and somite numbers. The developmental retardation was first obvious at 7.5 dpc and gradually increased until lethality occurred.

2.2.4 Histological analysis of *Mll2* mutant embryos

We embedded embryos in paraffin and performed saggital and transverse sections. Apoptotic cells and proliferating cells were labeled using terminal deoxyribotransferase (TdT) and an antibody recognizing Ki-67, respectably. No specific region of mutant embryos was apoptotic; instead we found an evenly distributed increase of apoptotic cells throughout the whole embryo compared to wild type controls. In contrast, the number of proliferating cells was similar in mutants compared to controls (data not shown). The increased ubiquitous apoptosis could explain the retardation of mutants, as more proliferation events would have to occur in those embryos to reach required cell numbers for progression in development.

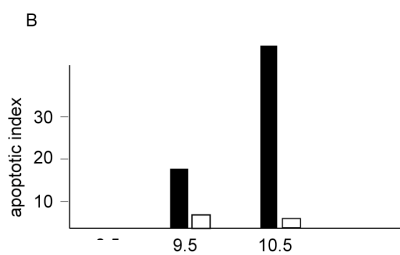
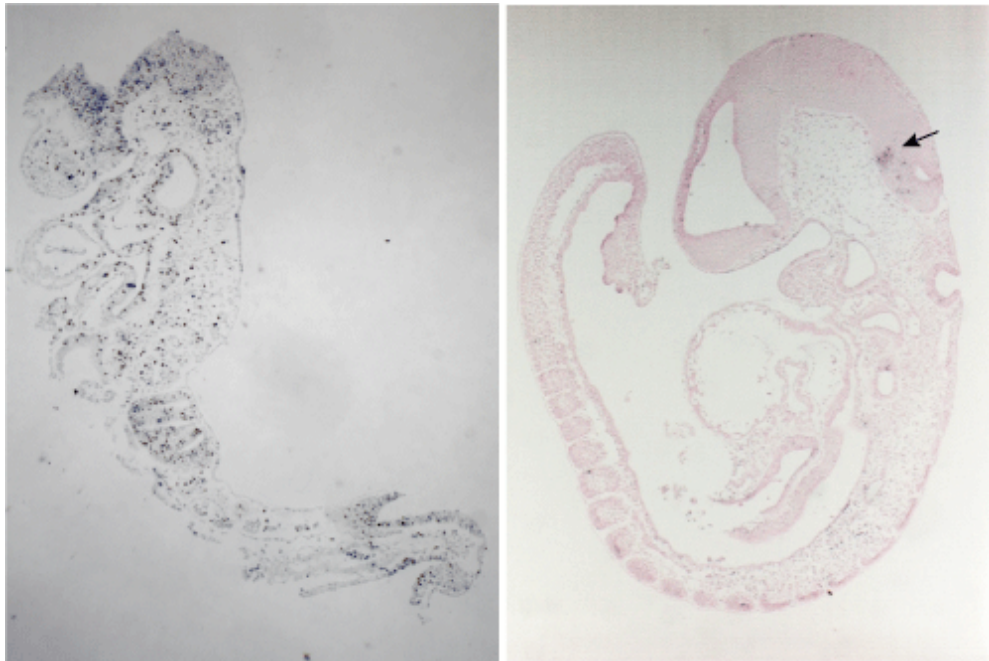


Fig.14 Analysis of apoptosis in *ml2* mutant embryos. TUNEL stained paraffin section of a E9.5 *ml2*^{-/-} embryo and a E9.5 *ml2*^{+/+} embryo. Positive cells are indicated by arrow. (B) For E9.5 and E10.5 embryos, apoptotic cells divided by the total number of cells yield the apoptotic index.

2.2.5 Molecular characterization of the *Mll2* embryonic phenotype

We used an extensive array of markers to analyze defects in *ml2* null mutant embryos. To account for the retardation observed in mutants we used $\omega\lambda\delta$ $\tau\psi\pi\epsilon$ embryos from different litters at suitable developmental stages as controls. As summarized in table 4, mutant embryos from litters dissected at E 9.5 are generally at a developmental stage corresponding to E 8.5. We therefore compared their gene expression patterns to wild type embryos from litters of this stage, rather than to their heterozygote and wild type littermates.

Defective longitudinal extension of paraxial mesoderm is the most likely cause of the kinky and compressed shape of the neural tubes in the mutant embryos. To establish whether the defects observed in somite development originate from defects in the

morphogenesis of the primitive streak, *Brachyury (T)* expression was assessed. In wild type embryos at E 7.5, *T* marks the entire proximodistal axis of the streak and nascent mesoderm (Wilkinson et al., 1990), and an identical expression was detected in *mll2* null mutants. At later stages, *T* expression was detected in the notochord and posterior (tail) mesoderm cells of both wild type E 8.5 and mutant E 9.5 embryos.

We then used the somite marker *mox1* and observed normal expression in paraxial mesoderm in wild type and mutants during early somitogenesis. However, *mox 1* expression was lost in mutant embryos at later stages. While mutants expressed *mox1* from the 1 to 8 somite stage, all mutants at later stages had lost expression. Interestingly, some mutants at the 10 somite stage showed a loss of *mox1* expression in anterior somites, while newly formed posterior somites still expressed *mox 1*. The somitogenesis of the mouse embryo is controlled by a cyclic biological clock, which leads to the formation of a new pair of somites every 2 hours. Thus, we could conclude that the loss of *mox 1* expression at the 10 somites stage had occurred 20 hours after formation of the affected somite. Moreover, *mll2* function was not required to determine the initial expression of *mox1*, but was soon required to maintain it.

Despite the abnormal development of the anterior region of *mll2*^{-/-} embryos, expression of the prospective forebrain and midbrain marker *otx2* (Ang et al. 1993) was appropriately detected although weaker in some mutants. However, expression of *six3*, a homeobox gene that is normally expressed in the forebrain (Oliver et al. 1995) was not detected in *mll2*^{-/-} embryos. Previous studies have shown that *otx2* activity in the anterior neuroectoderm is not essential for initiation of *six3* expression but is required for maintenance of *Six3* expression (Acampora et al. 1998; Kimura et al., 2000). Because *Otx2* expression was detected in mutants, the absence of *six3* expression seems to be directly related to *mll2* function. Previous studies have indicated that *Otx2* regulates *Wnt1* positively (Rhinn et al., 1999). In agreement with this observation, *wnt1* expression was detected as two sharp transverse rings immediately next to each other at the midbrain-hindbrain border by E 9.5 and E10.5 in wild type and mutants, respectively. We next examined the expression of *Hoxb1*, which is normally expressed in rhombomere 4, lateral mesoderm and posterior neuroectoderm at E9.5. In *mll2*^{-/-} mutants *hoxb1* expression was properly initiated at E8.5 but completely absent at E9.5. Thus, *Mll2* function is not required for initial expression of *Hoxb1* but for maintenance of expression.

Taken together, these data demonstrate that Mll2 is a maintenance factor of specific homeotic transcription factors. While initial expression of *mox1* and *hoxb1* was not affected, a role for maintenance of expression for these genes was observed. Moreover, no expression of the forebrain marker *six3* was observed, either because of a lack of forebrain development or a specific role of Mll2 for *six3* expression.

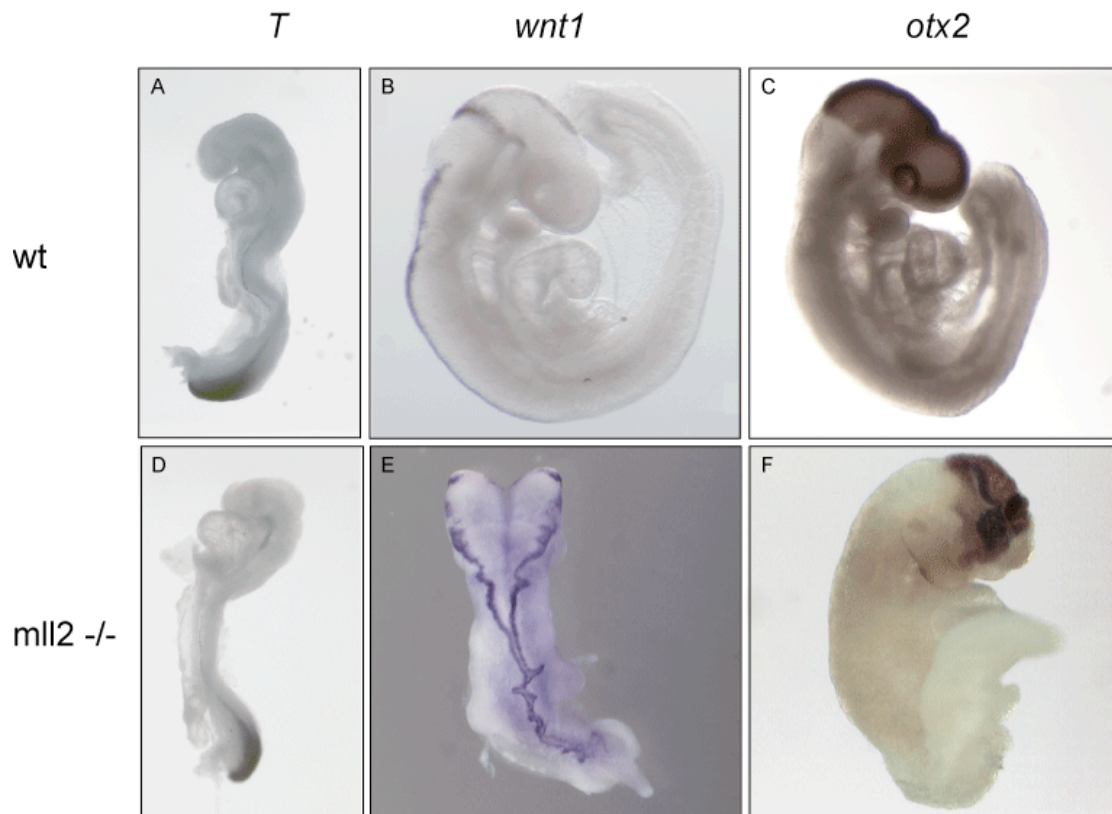


Fig. 15 *In situ* hybridization analysis of *T* (A, D), *wnt1* (B, E), and *otx2* (C, F). The expression of these markers was not affected in *mll2*^{-/-} embryos (D, E, F) compared to *mll2*^{+/+} embryos (A, B, C). (D) In E9.5 *mll2*^{-/-} mutant embryo, *brachyury* (*T*) expression in the streak and notochord was similar to the expression detected in wild type (A) E8.5 embryo. A normal expression pattern of *wnt1* was observed in E9.5 *mll2*^{-/-} mutant (E) compared to E10.5 wild type (B) embryo. The forebrain/midbrain marker *otx2* was normally expressed in E9.5 *mll2*^{-/-} mutant embryo (F). Compared to the wild type (C) E10.5 embryo, the mutant had an abnormally shaped head.

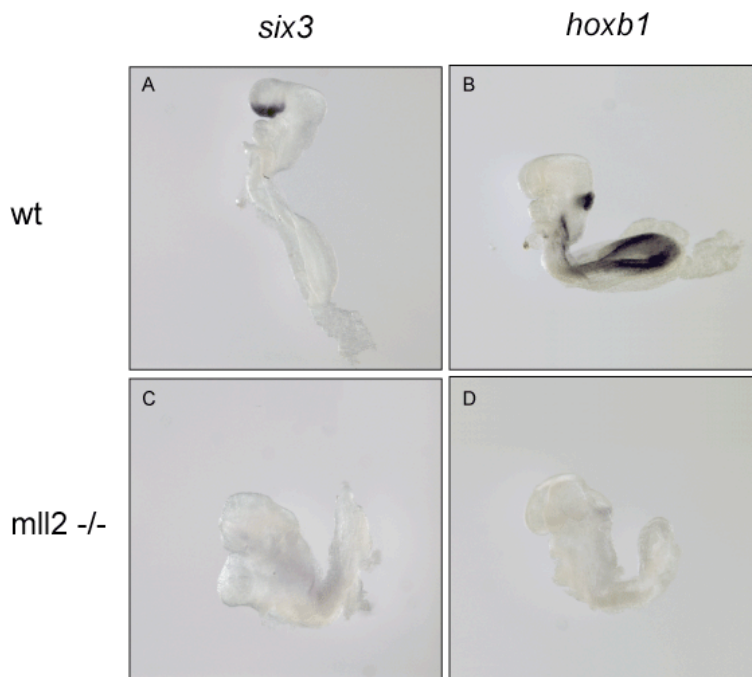


Fig.16 *In situ* hybridization analysis of *six3* (A,C) and *hoxb1* (B, D) indicated a defect in expression maintenance of these genes in *mll2*^{-/-} mutant embryos. E9.5 *mll2*^{-/-} embryos (C, D) where compared to E8.5 *mll2*^{+/+} embryos (A, B). *Six3* was detected in wild type (A) E8.5 embryo, but not in E9.5 *mll2*^{-/-} mutant embryo (C). *Hoxb1* was detected in E8.5 wild type (B) embryo. In *mll2*^{-/-} mutants, *hoxb1* was expressed from E7.5 to E8.5, but not at E9.5 (D).

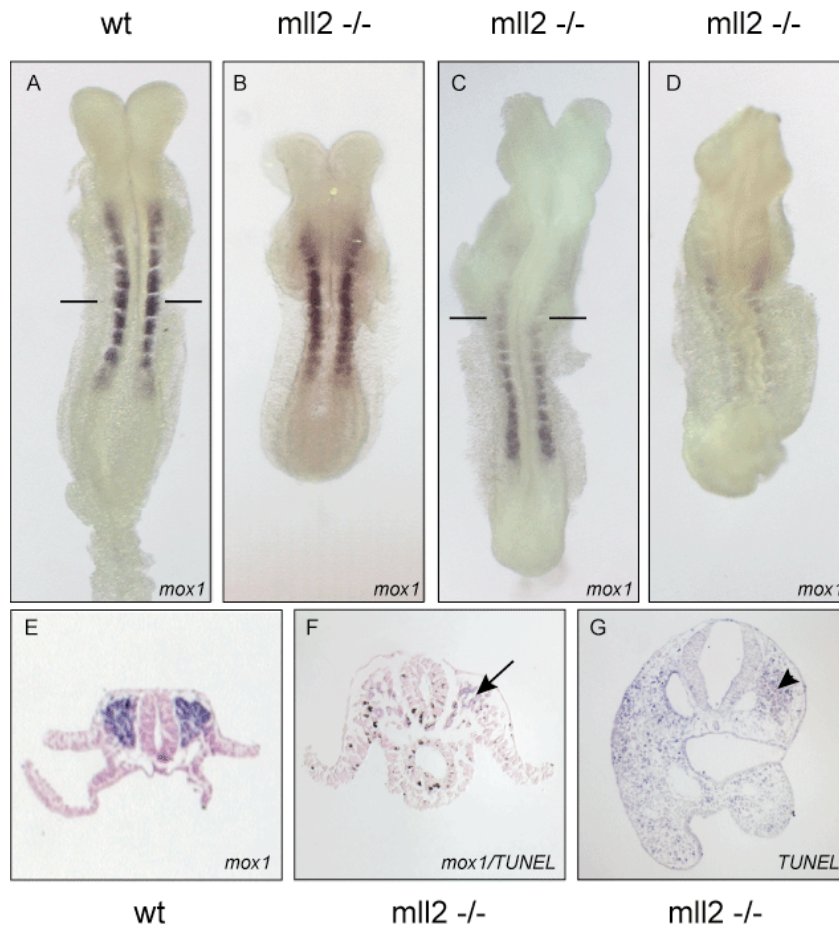


Fig. 17 In situ hybridization analysis of the paraxial mesoderm marker *mox1* indicated a defect in expression maintenance in *mll2*^{-/-} mutant embryos. Whole-mount embryos (A-D) and transverse sections (E-G) are depicted. (A) In a E8.4 wild type embryo (8 somites), *mox1* is expressed in the presomitic mesoderm and in somites. (B) In a E9.0 *mll2*^{-/-} embryo with 8 somites, *mox1* expression is normal. (C) In a E9.5 *mll2*^{-/-} embryo with 10 somites, *mox1* expression is lost in the 2 anterior somites. (D) In a E9.75 *mll2*^{-/-} embryo, no *mox1* expression is detected. Defective longitudinal extension of paraxial mesoderm is the most likely cause of the kinky and compressed shape of the neural tube in mutant embryos at this stage. (E) Transverse section of the E8.4 wild type embryo displayed in (A) shows *mox1* expression in paraxial mesoderm. (F) TUNEL stained transverse section of the E9.5 *mll2*^{-/-} embryo displayed in (C). Black apoptotic nuclei appear throughout the section. *Mox1* signal (arrow) is not decreasing because of apoptosis of paraxial mesoderm. (G) TUNEL stained transverse section of a E10.5 *mll2*^{-/-} embryo. Whole embryo section is positively stained with the highest amount of apoptotic cells in the paraxial mesoderm (arrow).

2.3 Conditional mutagenesis of Mll2

We used the conditional mll2F allele to perform induced mutagenesis in adult mice and cell culture. Mutagenesis is achieved by deletion of 815 bp of Mll2 genomic sequence by cre recombinase. The deletion includes exon 2 and creates a frame shift in the processed mRNA (section 1.2.1).

The goal of this study was ubiquitous mutagenesis of Mll2 in all tissues of embryos and mice. We therefore planned to generate an ubiquitous, inducible cre deleter line by targeting a ligand-regulated recombinase to the housekeeping gene topoisomerase I. This work is described in section 2.4.

As this work was ongoing, we obtained the similar cre deleter line Rosa26-CreER(T2). By targeting CreER(T2) to the Rosa26 locus, Seibler and colleagues created a line in which inducible cre recombinase is expressed in all tissues *in vivo* (Seibler et al., 2003). As this suited our purpose, we used this Cre line for all experiments described in section 2.3.

2.3.1 Induction of the conditional Mll2 allele *in vitro*

A homogenic cell population produced by *in vitro* cell culture is sometimes more beneficial for experiments than a heterogenic cell population extracted from *in vivo*. Organs are complex structures composed of blood vessels and many different cell types, which by consequence may produce high variations in the outcome of an experiment. In contrast, cells grown in tissue culture usually produce reproducible, robust results.

Different cell lines were generated from Mll2F/creER(T2) mice under the supervision of Konstantinos Anastassiadis. First, we obtained embryonic fibroblast (MEFs) by dissecting 6 embryos at E 13.5. All embryos had creER(T2); Embryos heterozygous for Mll2F gave rise to a control cell line and embryos homozygous for Mll2F the inducible mll2 null line. Second, we cloned ES cells from blastocysts. Five independent clones homozygous for Mll2F and creER(T2) were obtained.

In vitro mutagenesis of Mll2 was induced by adding 100 nM (10^{-7} M) 4-hydroxytamoxifen to the culture medium.

2.3.2 Induction of the conditional Mll2 allele *in utero* and *in vivo*

For *in vivo* and *in utero* inductions two protocols for administration of tamoxifen to mice were tested; We fed a tamoxifen/oil solution orally by gavage or injected (i.p.) 4-hydroxytamoxifen dissolved in oil. In agreement with previous studies (Kuehbandner et al., 2000), both protocols gave identical recombination efficiencies. We preferred the gavage protocol, as the LD50 of tamoxifen in mice is 15-fold higher via the oral route than by i.p. injection (200mg versus 5g/kg, Seibler et al., 2003). In addition, orally administered tamoxifen is probably efficiently metabolized to 4-hydroxytamoxifen in the liver of the mouse. We could therefore restrict the use of costlier 4-hydroxytamoxifen to *in vitro* inductions. The recombination efficiencies obtained with different concentrations of tamoxifen are described in section **2.5.3**.

As an alternative induction protocol, we tested injections (i.p.) of tamoxifen dissolved in 15% EtOH. The partial cre recombination achieved with this protocol was probably due to incomplete dissolving of tamoxifen in 15% EtOH. Increasing the EtOH concentration to 40% resulted in better dissolving, but was not used for injections, as this concentration would be toxic for the mice. However, the partial recombination achieved with injections of tamoxifen in 15% EtOH was beneficial for an experiment described in section **2.5.8**.

In addition to inductions of adult mice, we induced mutagenesis in embryos and newborn pups. Inductions in embryos at different stages of development were carried out by feeding pregnant females tamoxifen. Induction in neonates was obtained by feeding lactating females tamoxifen, which achieved efficient transmission via the milk (section **2.5.10**).

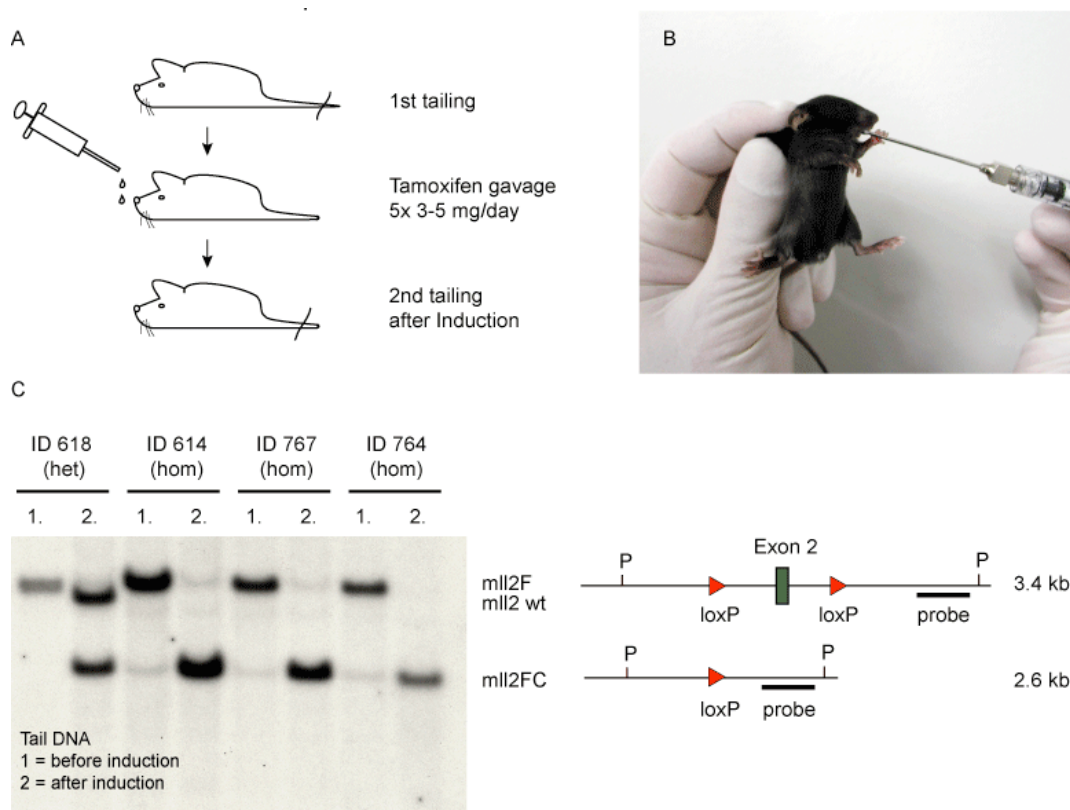


Fig. 18 Induced mutagenesis of *mll2* in vivo. (A) Mice were tailed, induced for 5 days by gavage of a tamoxifen/oil solution, and re-tailed 7 days after the last feeding. (B) The gavage is performed by applying 5mg tamoxifen dissolved in 50 μ l oil, which was heated to 37°C and fed with a feeding syringe. (C) Southern blot of PstI-digested tail DNA before (1) and after (2) induction. In three mice homozygous for the conditional allele mll2F (ID 614, 767, and 764), almost complete recombination after induction was observed. Hybridization with probe C detected a 3.4 kb fragment for unrecombined mll2F and a 2.6 kb fragment for recombined mll2FC.

2.3.3 Validation of the induced allele on DNA level

We analyzed the recombination rates of the conditional *mll2* allele using different concentrations of tamoxifen with the goal to achieve the highest possible rate in all tissues. Recombination was determined by PCR and southern blotting of PstI digested DNA from various organs and hybridization to probe C. A dose-response experiment indicated that the extent of recombination is highly dependent on the amount of tamoxifen given to the mice. A daily dose of 2.5 mg tamoxifen for 5 days resulted in partial recombination in most tissues and no recombination in the brain. However, the use of 4mg and 7mg yielded full recombination in all tested tissues and 30% or 50% recombination in the brain, respectively. The limited degree of recombination in the brain may reflect a lower local concentration of ligand due to the blood-brain barrier rather than a reduced expression level of CreER(T2) (Seibler et al., 2003). For further

induction experiments, we administrated 5 mg tamoxifen for 5 days, a treatment that caused no side effects on 28 tested wild type mice.

A background activity of CreER(T2) in untreated mice was detected in tail DNA of 15% of genotyped mice. The leakiness of CreER(T2) was only observed in some mice, with a recombination rate of up to 20% in the tail, while in most animals no background activity was detected. The mice with background activity were excluded from experiments.

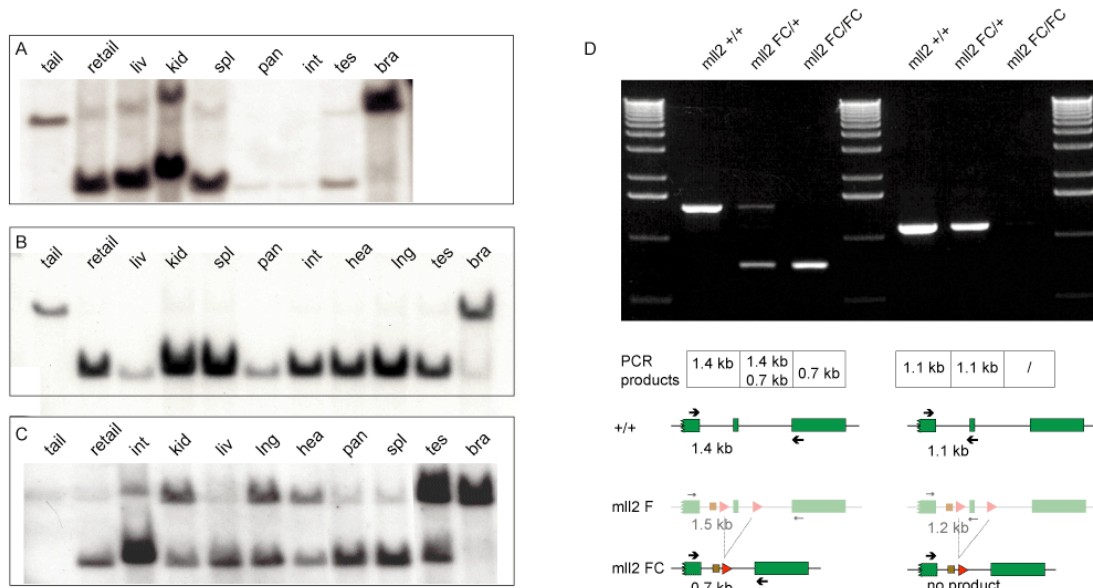


Fig. 19 *Recombination efficiencies obtained with different induction protocols.* (A, B, C) Southern blot with DNA from various tissues of three mice (mll2 F/F; RosaCreER(T2)+/-) induced with different protocols. (A) Gavage with 2.5 mg tamoxifen in oil yielded incomplete recombination in some tissues. (B) Gavage with 4 mg tamoxifen in oil yielded complete recombination in all tissues except the brain. Heterozygosity for Cre is sufficient to obtain complete recombination; indeed the tamoxifen concentration is the rate-limiting step during the induction. (C) Injection (i.p.) of 1 mg tamoxifen dissolved in 15% EtOH yielded partial recombination in all tissues. The partial recombination obtained with this protocol was used in an experiment described in section 2.5.8.

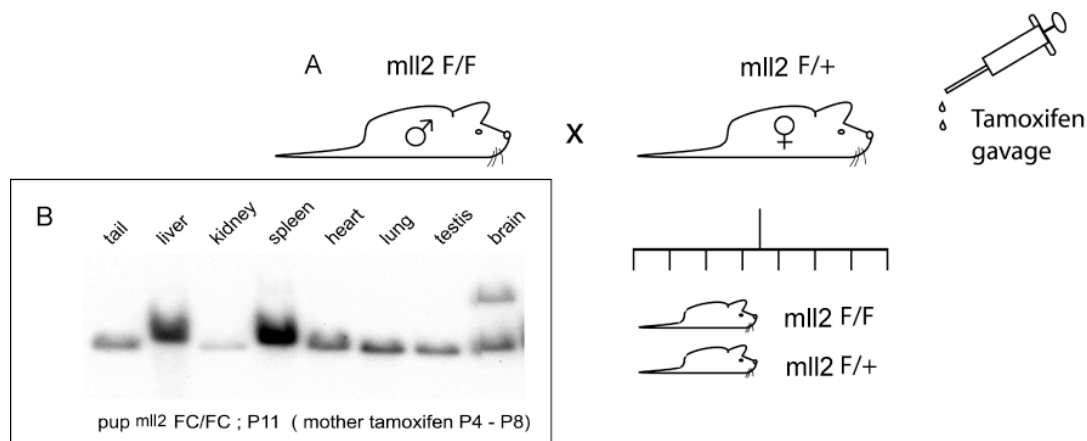


Fig. 20 Induction of breast fed pups by gavage of lactating mothers with 5x 5mg tamoxifen.

2.3.4 Validation of the induced allele on RNA level

The induced Cre recombination of the conditional *mll2* allele removes exon 2 (73 bp) and presumably results in splicing of exon 1 to exon 3 in the pre-mRNA. This abnormal splicing would create a frame shift and a nonsense codon in exon 3 that circumvents full-length *mll2* protein translation. Instead, a putative peptide of 140 amino acids could be translated from the frame shifted *mll2* mRNA, including 121 amino acids of wild type sequence coded by exon 1 and 19 amino acids of mutated sequence coded by exon 3. This hypothetical protein has a predicted low compositional complexity (SMART database), as it does not include any protein domain. Indeed, the most N-terminal protein domain of Mll2 is an AT hook coded by aa 149 to 159.

Exon 1

ATG GCG GCG GCG GCG GGC GGC GGC AGT TGC CCC GGG CCT GGC TCC GCA CGG GTT CGC TTC CCG GGC CGG CCG
M A A A A G G G S C P G P G S A R V R F P G R P
CTG GGT TGC GGC GGC GGC GGC GGC CGC GGC GGC CGA GGC AAC GGA GCC GAA AGA GTG CGG GTA GCC CTG CGG
L G C G G G G G G R G G R G N G A E R V R V A L R
CGC GGT GGC GCG GCG GGC CCG GGA GGA GGC GAG CCC GGG GAG GAC ACG GCC CTG CTC CGT TTG CTG GGT
R G G G A A G P G G A E P G E D T A L L R L L G
CTT CGC CGG GGC CTG CGC CGG CTC CGC CGC CTG TGG GCT GGT GCG CGA GTT CAG CGA GGC CGA GGC CGC GGC
L R R G L R R L R R L W A G A R V Q R G R G R G
CGG GGA CGG GGC TGG GGC CCG AAC CGA GGC TGC ATG CCG GAG GAA GAG AGC AGT GAC GGG GAA TCC GAG GAG
R G R G W G P N R G C M P E E E S S D G E S E E

Exon 3

GAG GTC GAG CCC CTC GGG GTC GGG GCC GCA AGC ATA AGA CGA CCC CCC TTC CTC CTC GCC **stop** TAG CAGATGTGACTCCT
E V E P L G V G A A S I R R P P F L L A
GTCCCCCAAGGCCCTACTCGGAACGGGGTGGAGGGGACAGAACGGATGGTGCAGGCACTGACTGAACCTTCTCCGGCGGTCCCAAGCACCCCA
ACCCCCCGAGCCGGGACGGGACGTGAACCTCTACTCCCCGACGGTCTCGGGGAAGGCCCCAGGACGGCCAGCCGGTCCCTGCCGGAAAAAGC
AGCAAGCAGTAGTGTAGCAGAAGCGGCTGTGACAATCCCTAAACCCGAGCCTCCGCCCCCTGTGGTTCC

Fig. 21 Analysis of the mRNA expressed from the frame shifted *mll2^{FC}* allele. RT-PCR was performed on several tissues of induced mice with a primer pair annealing in *mll2* exon 1 and exon 3. Sequencing of the PCR product confirmed the expected splicing of exon 1 to exon 3 in absence of exon 2. The created nonsense mutation in exon 3 and the hypothetically translated protein of 140 amino acids are indicated.

We analyzed the RNA produced from the induced conditional *mll2* allele by Northern blot and RT-PCR. Total RNA from various organs of induced mice was extracted 2 weeks after tamoxifen treatment. Mutant mice were heterozygous for CreER(T2) and homozygous for the conditional *mll2* allele, while control mice were heterozygous for CreER(T2) and the conditional *mll2* allele. Control mice were therefore exposed to tamoxifen treatment, activated cre recombinase activity and recombination of loxP sites, but retained one wt *mll2* allele after recombination.

We expected complete absence of *mll2* mRNA in induced mutants due to nonsense-mediated mRNA decay (NMD), which is triggered by premature translation termination. Surprisingly, we did not observe a marked reduction of *mll2* mRNA in induced mutants. However, due to the minimal size difference of 73 bp between the wt

and the frame shifted *mll2* mRNA, we could not conclude if the signal detected in mutants was frame shifted mRNA that resisted NMD or unrecombined mRNA transcribed before the induction.

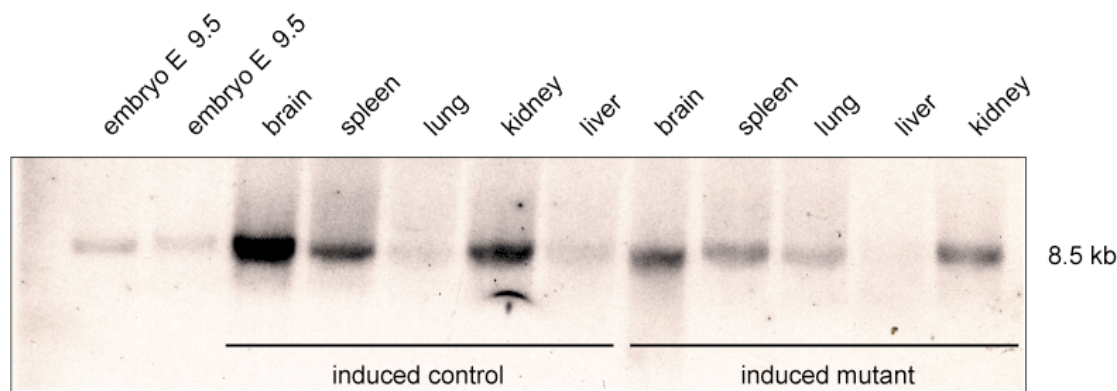


Fig. 22 Northern blot analysis of various tissues from induced mice. The mutant mouse (*mll2*^{F/F};*RosaCreER*(T2)^{+/-}) and the control mouse (*mll2*^{+/+}) were induced with 5 mg tamoxifen and sacrificed after 7 days for RNA extraction. Hybridization with probe CF14 detected the 8.5 kb *mll2* transcript in all tissues of both mice. Due to the minimal size difference of 73 bp between the wt and the frame shifted *mll2* mRNA, we could not conclude if the signal detected in mutants was frame shifted mRNA that resisted NMD, or unfeccombined mRNA transcribed before the induction.

We therefore used quantitative RT-PCR on tissue culture, mouse embryonic fibroblasts and ES cells, with primer pairs 145/146 and 145/147, which distinguish the wild type from the recombined allele, respectively. Both primer pairs were tested on serial dilutions of template to evaluate the PCR efficiencies. A similar slope of -3.4 for both assays in a Ct vs. concentration graph (data not shown) indicated a PCR efficiency of 95 %.

A PCR reaction is described by:

$$X_n = X_o (1+E)^n$$

X_n = concentration at cycle n
 E =PCR efficiency: $0 \leq E \leq 1$

With $E = 0.95$ and $n = -\Delta\Delta Ct$ we used $(1.95)^{-\Delta\Delta Ct}$ to calculate the expression levels of wt (unrecombined although induced) and frame shifted *Mll2* mRNA after induction compared to normal expression levels of *Mll2* in untreated cells.

After 2 - 4 days of treatment with 4-hydroxytamoxifen the wild type *Mll2* mRNA was detected at 0.3% and 0.7% compared to the expression level in untreated Mefs and ES cells, respectively. The residual unrecombined allele detected in ES cells could be a

contamination of wt feeder cells on which the ES cells were grown before they were selected for 3 passages to grow without feeder cells.

In agreement with the northern result with mouse tissues, the frame shifted mll2 mRNA was detectable in induced Mefs and ES cells. While the frame shifted mRNA was reduced to 23% compared to the expression of mll2 in uninduced Mefs, the reduction in ES cells was 82%.

Taken together these results demonstrate that the induction of the conditional Mll2 allele results in a reduction of wild type mll2 mRNA levels below the detection limit of 1%. The frame shifted mRNA is still transcribed and present in the cells after induction although at reduced levels.

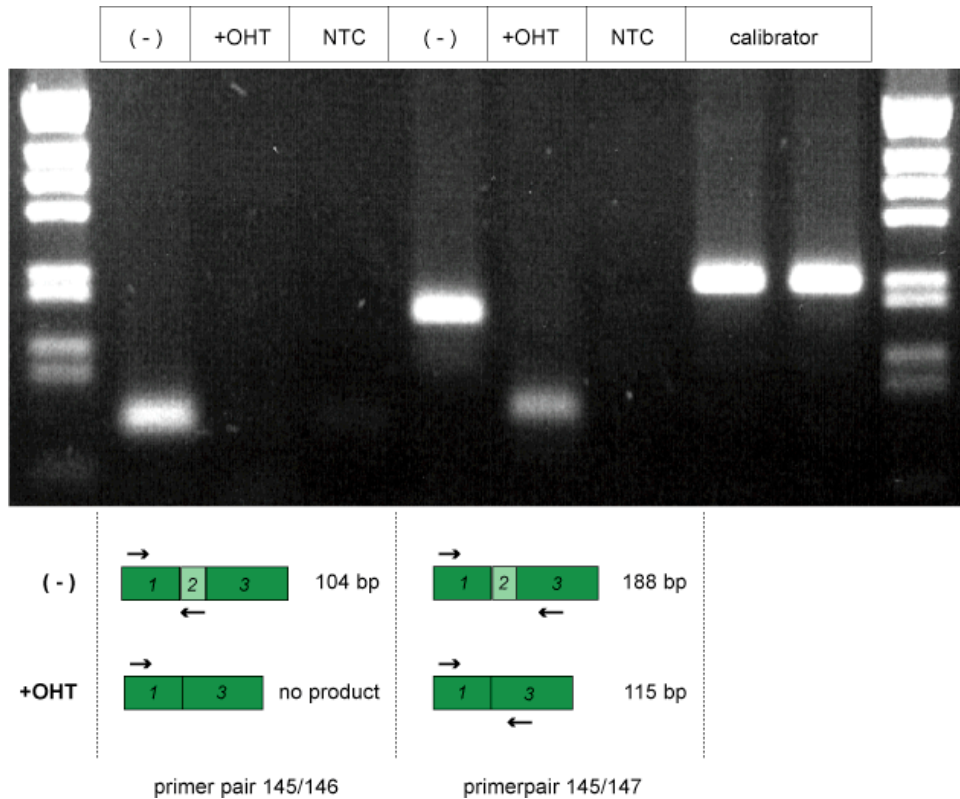


Fig. 23 Quantitative RT-PCR analysis to distinguish unrecombined *mll2F* RNA from recombined *mll2FC* RNA. The primer pair 145/146 was specific for unrecombined *mll2F* template and produced a 104 bp product. This assay was used to estimate if unrecombined *mll2F* allele was detectable after induction. The second primer pair 145/147 amplified products from both alleles, which could be distinguished by size difference. This assay was used to estimate if the frame shifted *mll2FC* RNA was detectable after induction. Both assays had identical amplification efficiencies and produced identical Ct values when used on wild type template (date not shown).

Table 5

	Induction	Primer	Δ Ct	$\Delta\Delta$ Ct	Expression -% -
wt allele	(-)	145/146	10.6	8.6	0.3 %
	(+OHT)	145/146	19.2		
frameshifted allele	(-)	145/147	10.9	2.2	23 %
	(+OHT)	145/147	13.1		

Table 5: *Mll2* RNA levels in tamoxifen induced *mouse embryonic fibroblasts* (MEF). While the wt RNA is detectable at 0.3%, the frame shifted RNA is detected at 23% compared to normal *mll2* expression level in untreated cells.

Table 6

	Induction	Primer	Δ Ct	$\Delta\Delta$ Ct	Expression -% -
wt allele	(-)	145/146	9.2	7.4	0.7 %
	(+OHT)	145/146	16.6		
frameshifted allele	(-)	145/147	12.2	0.3	82 %
	(+OHT)	145/147	12.5		

Table 6: *Mll2* RNA levels in tamoxifen induced *ES cells*. While the wt RNA is detectable at 0.7 %, the frame shifted RNA is detected at 82% compared to normal *mll2* expression level in untreated cells.

2.3.5 Validation of the induced allele on *protein* level

The essential validation of the conditional *mll2* knockout allele was to demonstrate that the induced frame shift mutation leads to a complete absence of Mll2 protein. Therefore the goal was to induce the frame shift by Cre recombination in (*mll2F/F*) ES cells and perform western blots with the Mll2 antibody. We used *mll2*^{-/-} ES cells that had been Flp recombined by Sandra Lubitz, creating ES cells homozygous for the conditional *mll2F* allele. The cells were electroporated with a newly engineered Cre expression plasmid (pCAGs-iCreIRESpuro) that confers puromycin drug resistance upon transformed cells. After growing cells for 2 days in selection medium (1µg/ml puromycin), approximately 300 resistant colonies from 3 independent experiments were picked and expanded. Cre recombination of loxP sites could be detected in all clones by amplification of a 716 bp PCR product with primer pair 145/147.

However, primer pair 145/146 detected a double band indicating unrecombined *mll2F* allele; because ES cells were grown on wild type feeders, a 1.1 kb product was amplified from the wild type allele. In addition, a second 1.17 kb PCR product indicated unrecombined *mll2F* allele in all clones. An XhoI digest of the PCR products ascertained the presence of unrecombined *mll2F* and produced two smaller fragments. This is due to the Xho site in the spacer of the FRT site that is not in the PCR product amplified from the wild type allele.

These unexpected PCR results indicated that Cre recombination had occurred in all clones and proved functionality of the newly engineered Cre expression construct. However, as unrecombined allele was also detectable in all clones, this led to the conclusion that only one of both *mll2F* alleles had recombined. This is considered to be a very unlikely event, as one would expect recombination of both loxP pairs if molecules of the recombinase were present in the cell. The *mll2*^{-/-} cells from Julia Schaft had indicated that the protein is not essential in ES cells. This excluded the possibility of a lethal counter selection of double recombined clones. We therefore suspected a mutation in the loxP site(s) of the second *mll2* allele that was targeted with sA-IRESLacZneo-hygro. This targeting construct was cloned from sA-IRESLacZneo, which has functional loxP sites (section 2.1.2). It is possible that the insertion of hygromycin gene by Red/ET recombination introduced a mutated loxP site with the

oligonucleotide. However, sequencing of the hygro targeting plasmid revealed no mutation in the loxP sites (sequencing by Jun Fu). Therefore, we assume that the 3' loxP site did not integrate during the targeting of the second *mll2* allele with the hygro construct.

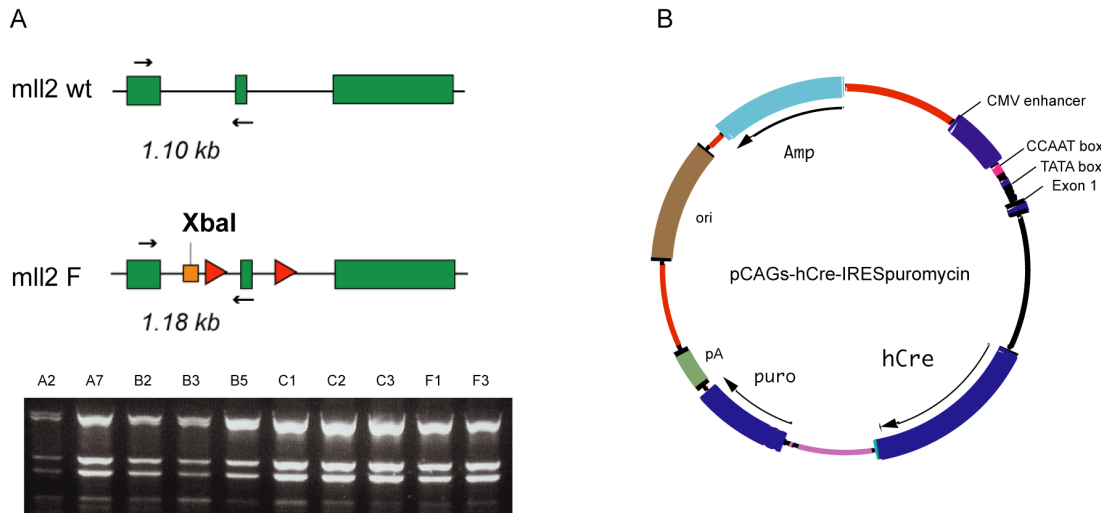


Fig. 24 *Cre* recombination of the conditional allele in *mll2*^{F/F} ES cells. (A) Shown are 10 clones that were puromycin resistant after electroporation of pCAGs-hCre-IRESpuromycin. Primer pair 145/147 detected *Cre* recombination in all clones. However, unrecombined *mll2*^F allele was also detectable by amplification of a 1.18 kb PCR product in all clones with the indicated primer pair. The PCR products were digested with *Xba*I, which yielded two smaller fragments in all clones (gel). As the *Xba*I site is in the spacer of the FRT site, this indicated that the PCR product originated from *mll2*^F and not from the wild type *mll2* allele from feeder cells. None of the > 300 resistant clones was recombined at both *mll2*^F alleles. We concluded that the *mll2*^{-/-} ES cells were generated with a mutation in the loxP site during the second round of targeting with the construct FRT-sA-lacZneo-hygro-FRT-loxP.

(B) Cloned eukaryotic *Cre* expression construct. The plasmid is functional for puromycin selection and *Cre* recombination.

Konstantinos Anastassiadis solved the problem by cloning ES cells from blastocysts of intercrossed mice homozygous for *mll2*^F and *Cre*^{ER(T2)}. *Cre* recombinase was induced in these ES cells by adding 10⁻⁷ M 4-OHtamoxifen to the medium, and complete recombination of loxP sites was detected by southern blot and PCR (data not shown).

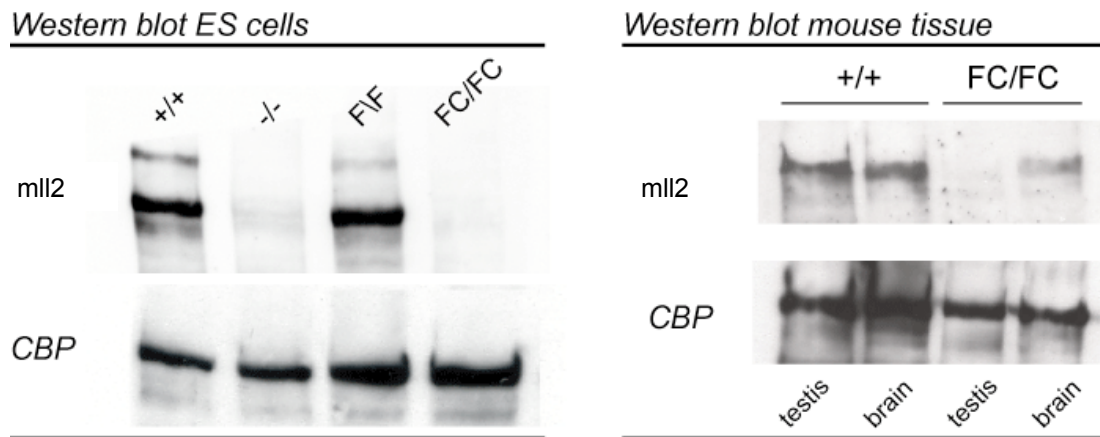


Fig. 25 *The frame shifted mll2FC allele is a null allele.* Western blot analysis of ES cells (A) and mouse tissue (B) probed with an antibody that recognizes the N-terminus of Mll2 (amino acids 168 – 288).

(A) A strong band was detected in wild type ES cells. Specificity of the antibody was demonstrated by absence of the signal in mll2^{-/-} ES cells. In conditional ES cells (mll2^{F/F}; RosaCreER(T2)^{-/-}), mll2 was detected before but not after induction with tamoxifen. (B) Mll2 is detected in testis and brain of induced wild type mouse. In contrast, mll2 is absent in testis of induced mll2^{F/F}; Rosa26CreER(T2) mouse. In the brain, low levels of mll2 are detected, which corresponds to the incomplete recombination observed in the brain.

Protein extracts from Mll2^{+/+}, Mll2^{-/-}, and Mll2^{F/cre} (induced and uninduced) ES cells were used in western blots with the Mll2 antibody. Mll2 was detected in wild type and uninduced Mll2^F cells, but absent in induced Mll2^{FC} cells. The absence of a signal in Mll2^{-/-} extracts proved the specificity of the Mll2 antibody.

In parallel, we have done western blots with protein extracts from various organs of wt and induced Mll2^{FC/creER(T2)} mice. Mll2 protein was detected in testis and brain extracts of wild type mice, but absent in testis extract from induced Mll2^{FC} mice. However, low levels of Mll2 were detected in brain extracts of induced mutants. This is in agreement with the incomplete DNA recombination observed in the brain, probably due to low penetration of tamoxifen into the organ.

Taken together, these results demonstrate that the induced frame shift of the conditional Mll2 allele leads to complete absence of the protein. By Cre recombination, Mll2 protein is efficiently knocked out in ES cells and most organs of the mouse, except for the brain.

2.3.6 Severe diarrhea in induced Rosa26-CreER(T2) mice

We induced 201 mice with 5x 5 mg tamoxifen per day administered by gavage. Of these, 127 mice were “mutants” homozygous for *mlh2F* and homozygous or heterozygous for Rosa26-CreER(T2). As controls, we used 29 wild type mice (C57BL/6) to assess possible side effects of the tamoxifen dose. Furthermore, we used 35 mice of the Rosa26-creER(T2) line (C57BL/6 and 129/ola) as controls for possible side effects of cre recombinase activity on the genome in the absence of loxP sites. As control for possible side effects of cre recombinase activity in the presence of one pair of loxP sites, we used 10 mice heterozygous for *Mlh2F* and Rosa26-creER(T2) where recombination occurred on one of both *Mlh2* alleles.

Gavages were well tolerated by 28 of 29 wild type mice (grey), which showed no abnormal behavior. One mouse had symptoms of adynamia on the 1st day of induction due to suffocation (blue tongue) caused by oil that had accidentally penetrated the lung. Dissection of the lung confirmed this diagnosis and proved the critical illness to come from improper handling of the feeding needle. With more practice, the experimenter never produced such a case again.

In contrast to the wild type mice, we observed a high rate of illness and lethality in all other mice. Due to the close observation after induction, only a few of the mice were found dead. In most cases, mice with symptoms of illness were sacrificed to avoid extended periods of suffering. The illness occurred between the 5th and the 15th day after induction, with most cases from day 8 to day 10. The first symptoms of illness were reduced motility and constant weight loss that indicated pronounced dehydration. During progression of the illness, mice sustained severe diarrhea observable at the anus of animals. Dissections of sick mice revealed that the entire intestine was filled with liquid. The gall bladder and stomach were distended and the gastric content of sick mice had on average twice the weight as in wild type mice.

Mouse strain	Conditional mll2	Rosa26-creER-T2	Total mice	Sick mice	Lethality %
C57BL/6-129	hom	hom	54	39	72
	hom	het	73	13	18
	het	het	10	0	0
C57BL/6	wt	hom	6	6	100
	wt	het	9	0	0
129	wt	hom	20	16	80
	wt	het	/	/	/
C57BL/6-129	wt	wt	29	1	3

mll2 mutant cre

mll2 wt cre

mll2 wt no cre

Fig. 26 *Toxicity of the Rosa26-CreER(T2) line.* Summarized are all tamoxifen induced mice grouped by genotypes. Possible side effects of the tamoxifen treatment were excluded with 29 wild type mice (grey). Lethality occurred in the Rosa26-CreER(T2) line that was wild type for mll2 (blue). The lethality of the cre strain is not significantly influenced by the strain (C57BL/6 or 129/ola), but strongly influenced by the number of Rosa26-CreER(T2) allele(s). For this allele, we observed a lethality of 18 % in heterozygous mice and 72 – 100 % in homozygous mice (blue and yellow).

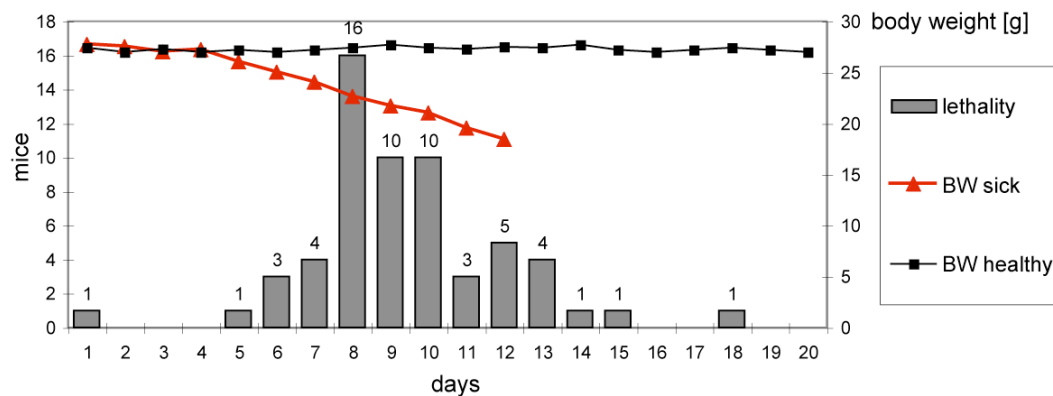


Fig. 27 *Illness and body weight of the Rosa26-CreER(T2) line.* Mice received tamoxifen gavage from the 1st to the 5th day. Illness and lethality occurred between the 5th and the 18th day with most cases from day 8 to day 10. Sick mice showed abnormal weight loss [▲] and reduced motility. When symptoms of illness were observed, mice were sacrificed to avoid extended periods of suffering.

Surprisingly, the gastrointestinal phenotype was not caused by mutagenesis of *Mll2*, as it also occurred in mice of the *Rosa26-CreER(T2)* line. In fact, the lethality seemed to originate from activated *CreER(T2)* protein. This conclusion is substantiated by the observation that the diarrhea occurred in 18% of mice heterozygous for *Rosa26-CreER(T2)*, but in 76 % of **all** homozygous mice. The 2 different strains that were used, C57BL/6 or 129/ola, did not produce a significant difference in disease. Furthermore, the oil was not the cause of the diarrhea; pups with *Rosa26-CreER(T2)* that did not receive oil but were induced by lactating mothers had an identical phenotype.

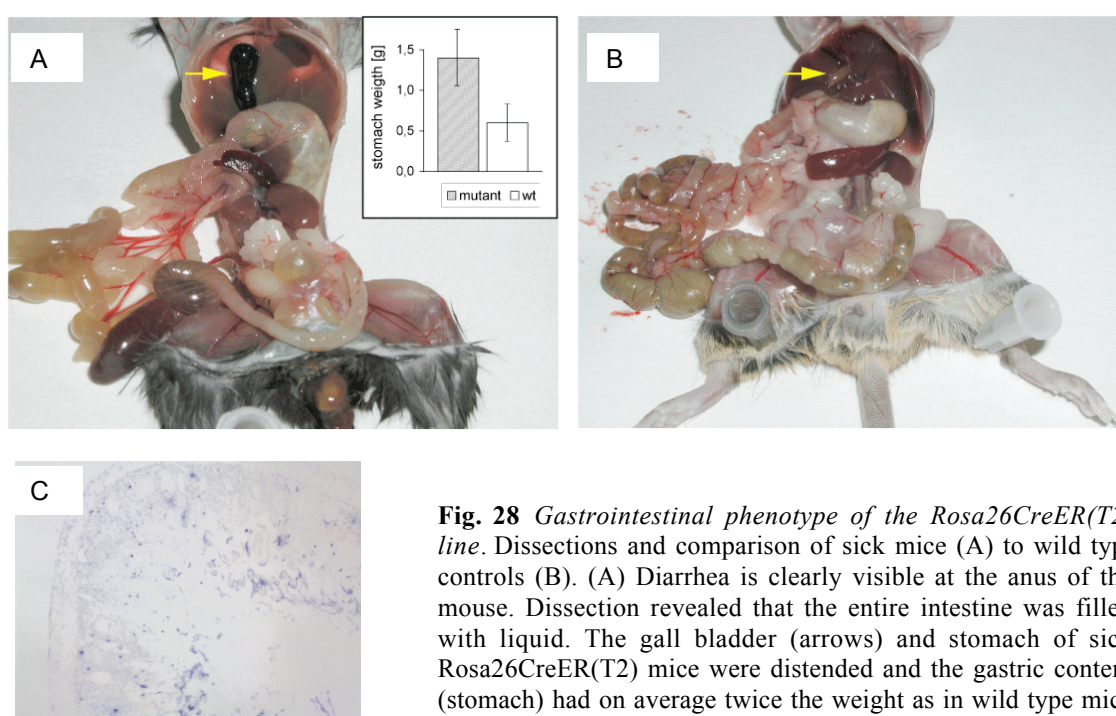


Fig. 28 *Gastrointestinal phenotype of the *Rosa26CreER(T2)* line.* Dissections and comparison of sick mice (A) to wild type controls (B). (A) Diarrhea is clearly visible at the anus of the mouse. Dissection revealed that the entire intestine was filled with liquid. The gall bladder (arrows) and stomach of sick *Rosa26CreER(T2)* mice were distended and the gastric content (stomach) had on average twice the weight as in wild type mice (box). (C) TUNEL staining of paraffin-sectioned intestine from sick mice did not reveal increased rates of apoptosis as a cause of the diarrhea.

We assumed that the diarrhea caused by the fusion protein is an effect of activated *ER(T2)* rather than an effect of *cre* activity. Several ubiquitous *cre* lines with no apparent phenotype exist; in contrast, the *Rosa26-CreER(T2)* is the first line that expresses the triple mutated *ER* in all tissues. It is unknown whether differently mutated versions of *EBD*, e.g. *ER(T1)*, would be deleterious or whether other *ER* versions would be more valuable for applications in the mouse.

2.3.7 Phenotype of Mll2 mutant embryos

The temporal flexibility of the conditional system allowed an extended analysis of the function of Mll2 during embryogenesis. As previously described in section 2.2.3, constitutive knock out of the protein results in a failure of gestation between E9.5 and E11. We induced mutagenesis at various stages of development to further define the period where Mll2 function is essential. Inductions of pregnant females by one to two daily doses of 5 mg tamoxifen at E4.5, E8.5 and E11 yielded complete recombination. In contrast, inductions of pregnant females by one dose of 5 mg tamoxifen at E17 resulted in incomplete recombination.

Interestingly, embryos induced at E4.5 and E5.5 recapitulated the phenotype of null embryos when dissected at E10.5. Previous tamoxifen inductions of ES cells had revealed that the recombination on DNA level is complete after 24 hours, which lead to absence of protein 72 hours later. Therefore, we assume that inductions *in utero* at E4.5 lead to absence of Mll2 protein at 6.5. The absence of protein from gastrulation is sufficient to recapitulate the phenotype of null embryos, which indirectly indicates that mll2 function is dispensable before.

In contrast, induction at E 8.5, which presumably leads to absence of protein at E 11.5, did not have any effect on embryos dissected at E13. Moreover, induction at E11, which presumably leads to absence of protein at E 14, did not have any effect on embryos dissected at E16. It cannot be concluded that Mll2 is dispensable from E11, as this would only be proven if inductions at E8.5 yielded viable pups. However, the normal morphological appearance of embryos induced at this stage strongly supports that conclusion.

♂		×		♀	
F/F	cre/cre	x	F/F	+/+	mutant
F/F	cre/cre	x	F/+	+/+	mutant / control
F/F	cre/cre	x	+/+	+/+	control
+/+	cre/cre	x	+/+	+/+	control (cre)
+/+	+/+	x	+/+	+/+	control (tam)

Fig. 29 Crossed genotypes for embryo inductions. Induced embryos where cre/+ to avoid the toxicity observed in adult mice homozygous for Cre. Moreover, induced females did not have Cre.

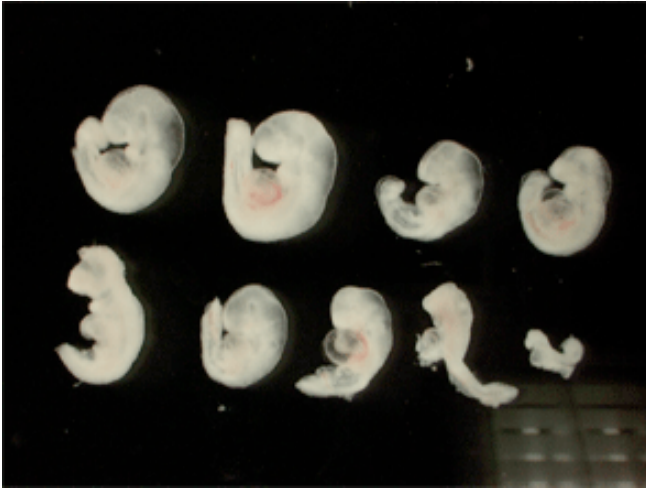


Fig. 30 Mutant embryos (Mll2F/F;cre/+) induced at E4.5 and dissected at E 10.5 recapitulate the phenotype of Mll2 null embryos.



Fig. 31 Control embryos (Mll2F/+;cre/+) induced at E8.5 and dissected at E13.5 served as control to exclude possible side effects of tamoxifen.



Fig. 32 Mutant embryos (Mll2F/F;cre/+) induced at E8.5 and dissected at E13.5 are morphological identical to induced control embryos (Mll2F/+ ; cre/+)



Fig. 33 & 34 Control (top) and mutant (Bottom) embryos induced at E11.5 and dissected at E16 are morphologically identical. Minor hemorrhage (top panel) was observed in control embryos.

2.3.8 Phenotype of Mll2 mutant mice

Except for the diarrhea, which is an artifact of the Rosa26-CreER(T2) line, the Mll2 mutant mice showed no conspicuous abnormalities compared to control mice. We monitored the health state of all induced mice by weekly hematological examination. The hematological profile generated with **HEMAVET™** included:

Leukocytes (total count/differential count of the five types of white blood cells:
lymphocytes, monocytes, neutrophils, eosinophils, basophils).

Erythrocytes

Hemoglobin

Haematocrit

Average cell volume

Average Hb content of erythrocytes

Reticulocytes

Platelets

Average platelet volume

All values of mutants were in the normal range and showed no significant variation with induction, except the white blood cell counts. This value multiplied by 1000x represents the total number of leukocytes in a microliter of blood. In the C57BL/6 strain the white blood cell count (WBC) is usually between 2 and 18 (Russell et al., 1951), thus more variable than in adult humans where the average WBC is 4.5 to 10.

The WBC of our 12 control (wild type) mice did not vary significantly with induction. The average value was 4 before induction with a small standard deviation of ± 2 . During tamoxifen treatment we observed a minor increase to 6, but similar values as before induction in the second and the third week. In contrast, the average WBC of mutants decreased with induction. The average WBC of mutants was 11 before induction and, although much higher than in control mice, still within the normal range of 2 – 18. However, this value dropped to 4 during induction and to 2 in the first week after. Whereas some mutants had only a slight decrease of WBC, some mutants dropped below 2 and had values that placed them at risk for a fatal infection.

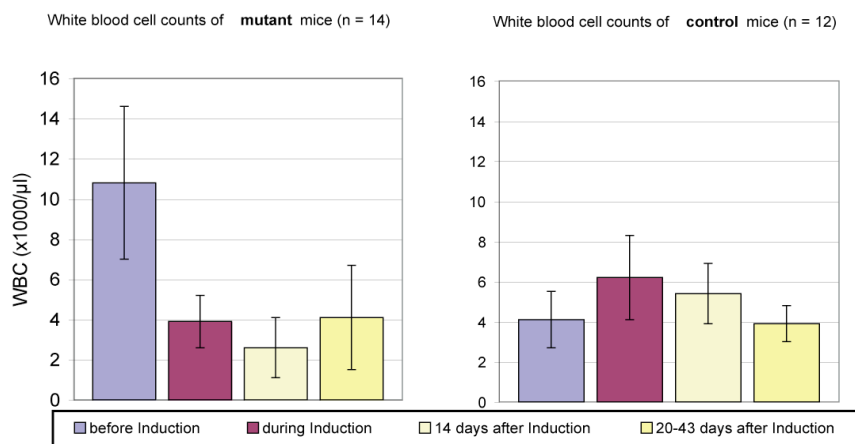


Fig. 35 White blood cell counts (WBC) are significantly reduced with induced mutagenesis of *mll2*.

The total number of white blood cells of mammals is highly dynamic and depends on physiological conditions. In response to an acute infection, trauma, or inflammation, white blood cells release a substance called colony-stimulating factor (CSF). CSF stimulates the bone marrow to increase white blood cell production. In a person with a

normal functioning bone marrow, the numbers of white blood cells can double within hours if needed. In contrast, while the average lifespan of white blood cells range from 13 to 20 days, they can be rapidly eliminated by apoptosis after an infection.

An increase in the number of circulating leukocytes is rarely due to an increase of white blood cell production. When this occurs, it is most often due to dehydration and hemoconcentration. Intriguingly, we observed a decrease of WBC in most mutants including mice that showed signs of dehydration from diarrhea. A possible explanation is that white blood cells are efficiently recruited to the gastrointestinal tissue in mutants with diarrhea, which in consequence caused a reduction in the peripheral blood system. Another hypothesis was that the loss of Mll2 triggered apoptosis in white blood cells. However, southern blotting with DNA from blood cells of induced mutants revealed complete recombination of the conditional allele (data not shown). This indicated that Mll2 is not essential in Leukocytes. Furthermore, recombination was complete in haematopoietic stem cells (HSC) that achieved steady-state hematopoiesis in absence of Mll2. These observations indicate that Mll2, unlike its orthologue MLL, is not essential in haematopoietic cell lineages.

The reduction of WBC occurred only in a fraction of induced mutants; therefore these observations are not conclusive. Furthermore, we do not know if this effect is due to mutagenesis of Mll2 or the toxicity of CreER(T2), as our control mice did not have CreER(T2). In contrast to the polymorphic effect on leukocytes, we did observe sterility uniformly in all induced mutants. Furthermore, the infertility did not happen in control mice with CreER(T2). The infertility of mutant females (2.3.9) and mutant males (2.3.10) is described in the following sections.

2.3.9 Infertility of mutant females

In order to analyze the infertility of Mll2 mutant females, we have to be familiar with the major cell types of the murine ovary. Thus, this section starts with a brief review of the origin of female germ cells and their maturation during oogenesis and folliculogenesis.

The formation of the ovary commences with the migration of the *primordial germ cells* (PGC) from the yolk sac into the intermediate mesoderm of the gonadal ridge. Although PGC may be found as early as day 8, they arrive at the gonadal ridge about gestation

day 11 to 11.5 (Baker, 1972). As the sex cords proliferate to form the ovary proper, the germ cells also proliferate via mitotic divisions and form "*oogonia*" beginning on gestation day 13. Subsequently, oogonia begin synchronized meiotic divisions and are then referred to as "*primary oocytes*". Meiotic prophase is divided into the leptotene stage (condensation of chromosomes), which occurs on or about day 14 of gestation, the zygotene stage (synaptonemal complex) between days 14 - 17, the pachytene stage (crossing-over) between days 15 - 19, and the diplotene division from day 17 of gestation to day 5 postpartum. In contrast to male meiosis where a diploid germ cell (4n) yields 4 haploid spermatozoa (1n), the female meiosis yields a single oocyte (1n) and the redundant chromosome sets are eliminated during both meiotic divisions by formation of 2-3 polar bodies. In the first week after birth, the mouse ovary contains about 7500 to 10 000 oocytes, which are arrested at the diplotene stage of meiosis I. Stromal cells surround the oocytes to form follicles, a process starting at E18 and referred to as "*folliculogenesis*". Concomitant with the growth of oocytes, the granulosa cells transform to acquire a cuboidal shape, forming primary follicles. Follicles are composed of an oocyte surrounded by granulosa cells, a basement membrane, and a concentric layer of thecal cells admixed with fibroblasts and myoblasts. Although vessels do not penetrate the basement membrane, blood-borne products (e.g. applied tamoxifen) freely diffuse across it to reach the granulosa cells and oocyte. After birth, cohorts of primordial follicles are periodically recruited to enter into a 3-week growth phase. The proliferation of granulosa cells results in pre-antral follicles composed of multilayer of granulosa cells surrounding the oocyte within the follicular basement membrane. Concurrent with the development of follicles, there is marked and continuous loss of oocytes, and by puberty, the mouse ovary contains about 2500 to 5000 primordial follicles. It is believed that these primordial follicles in the newborn mouse ovary represent the entire complement of germ cells available for reproduction, however this issue has recently been challenged (Johnson et al., 2004).

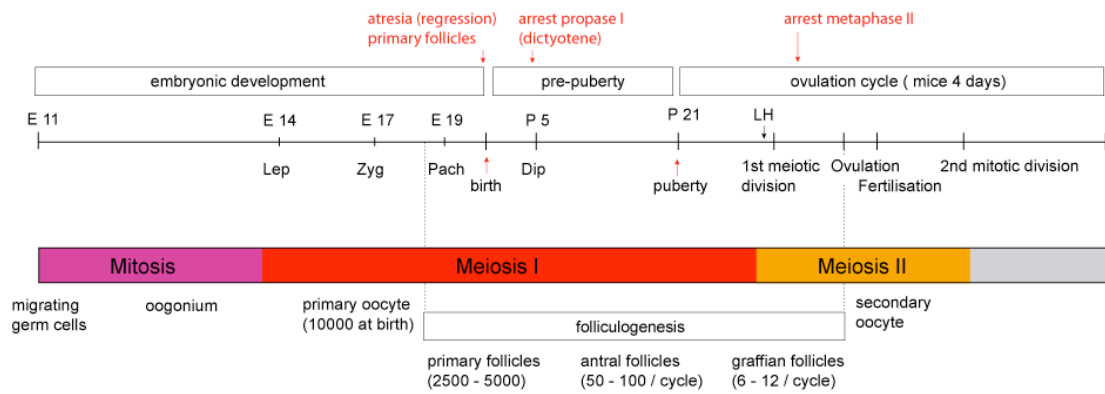


Fig. 36 *Maturation of female germ cells during oogenesis and folliculogenesis.* Migrating primordial germ cells enter the gonadal ridge at E11 and become mitotic oogonia. At E14, oogonia begin synchronized meiotic divisions and are then referred to as *primary oocytes*. Stromal cells surround the oocytes to form follicles, a process starting at E18 and referred to as “*folliculogenesis*”. At birth, the mouse ovary contains about 7500 to 10 000 oocytes, which are arrested at the diplotene stage of meiosis I. Concurrent with the development of follicles, there is marked and continuous loss of oocytes, and by puberty, the mouse ovary contains about 2500 to 5000 primordial follicles. In the mature mouse (5-6 weeks), the ovaries enter the estrous cycle with ovulation of oocytes every 4 days, which corresponds to the menstrual cycle of 28 days in humans. Within a cycle, meiosis I is resumed before ovulation. Arrest in meiosis II followed by ovulation marks the end of folliculogenesis. Fertilization of the secondary oocyte triggers completion of the second meiotic division.

After puberty, further growth of follicles is accelerated by gonadotrophins, namely FSH, leading to the formation of *antral follicles* (Kumar et al., 1997). Although oocytes within large antral follicles are competent for maturation, they remain arrested due to their interaction with the surrounding granulosa cells (Bornslaeger et al., 1986). In the mature mouse (5-6 weeks) the ovaries reflect a cycling reproductive status with ovulation of oocytes every 4 days, which corresponds to the menstrual cycle of 28 days in humans. Within a cycle, a preovulatory LH surge affects the maturation of the oocyte. This allows meiosis, held in abeyance since entering prophase weeks before, to resume approximately 24 hours before ovulation. In response to this LH surge, fully grown oocytes complete the first meiotic division, extrude the first polar body containing a set of chromosomes, and become arrested at metaphase II (Richards et al., 2002). With occurrence of meiosis II the oocyte is now referred to as a *secondary oocyte*. The LH surge is responsible for ovulation of the oocyte marking the end of folliculogenesis (Lee et al., 1996). While meiosis I is completed before ovulation, meiosis II does not continue into the second cell division until the occurrence of fertilization. If a sperm penetrates the oocyte, the fertilization triggers completion of the second meiotic division and formation of a second polar body.

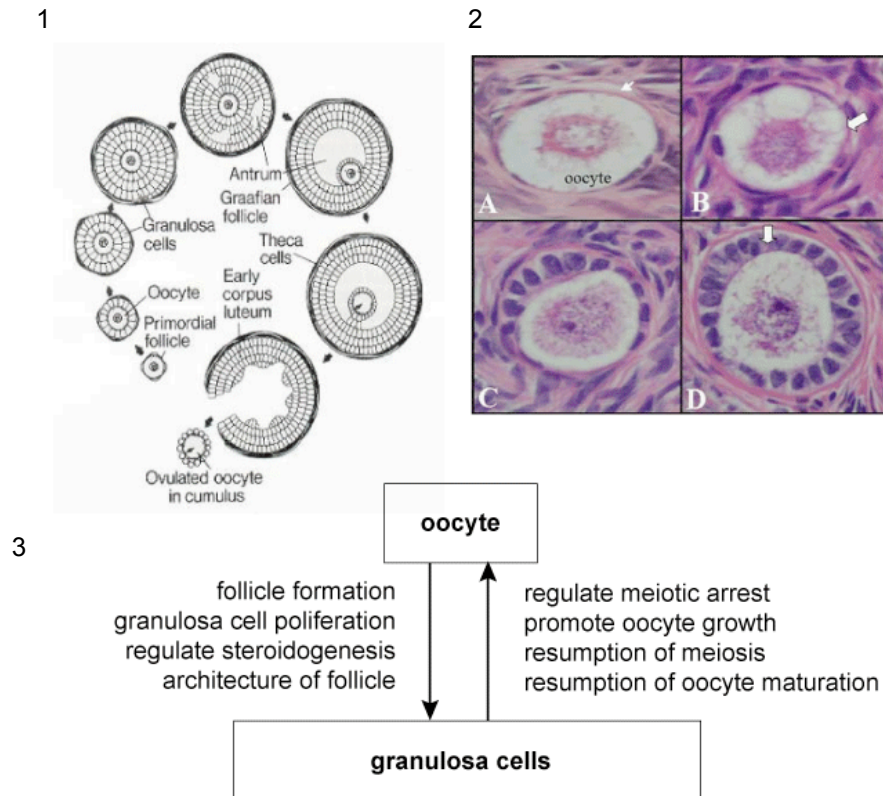


Fig. 37 Folliculogenesis. (1) Diagrammatic representation of follicular growth and ovulation (From Baker, 1972, Reproduction in mammals, Cambridge Univ. Press). (2) Photomicrographs of early stages of human prenatal folliculogenesis. A) Primordial follicle; arrow, squamous granulosa cell. B) Recruitment showing the primordial-to-primary transition; arrow, cuboidal granulosa cell. C) Primary follicle with multiple cuboidal granulosa cells. D) Fully grown primary follicle at the primary-to-secondary transition stage; arrow, formation of a secondary layer of granulosa cells. All photos are 40x and were found on the web at www.endotext.org. (3) Multiple cross regulations occur between the oocyte and the granulosa cells.

Since the majority of follicles (approximately 80%) that are recruited for growth in any given cycle degenerate rather than ovulate, cell death is a common and normal histological feature of the ovary. The process of follicular degeneration is referred to as “*follicular atresia*” and is characterized by granulosa cell death, which is morphologically and biochemically comparable to apoptosis (Hughes and Gorspe, 1991; Hsueh, 1994; Richards, 1980; Hirshfield, 1989). It is unclear, what determines which follicles will be ovulated and which will undergo atresia.

We used 10 females homozygous for the conditional Mll2 allele and heterozygous for Rosa26-CreER(T2) and 3 control females heterozygous for the conditional Mll2 allele and Rosa26-CreER(T2). All females were bred with wild type males prior to induction and produced offspring. After induced mutagenesis of Mll2 by tamoxifen gavage, mating to the previously used wild type males assessed the fertility of females.

Moreover, we included a wild type female in all matings to verify the virility of males. Although these control females became pregnant in the first week of breeding, all tamoxifen treated mice (mutants and controls) did not during 3 - 4 weeks after induction. This temporal infertility is probably caused by the antagonistic effect of tamoxifen on the estrogen receptor and not due to the absence of Mll2, as it was also observed in the 3 heterozygous Mll2F females. However, these control females recovered from infertility and became pregnant in the 3rd and the 4th week after induction, while the 10 mutant females never produced any offspring over a period of 8 months. We concluded that the absence of Mll2 protein caused sterility of the females. The adult ovary at the time of induction includes primary follicles that contain oocytes arrested in meiosis I, which periodically mature by resuming the 1st meiotic division with subsequent ovulation and arrest in metaphase II. The sterility of mutants indicated that Mll2 is involved in this process.

To further characterize the phenotype, we induced 4 mutant females with a different tamoxifen induction protocol that yielded incomplete recombination. Instead of oral feeding of 5 mg tamoxifen, these mice received i.p. injections of 1 mg tamoxifen dissolved in 20 % ethanol. Southern blotting with DNA from various organs of these females revealed that recombination had occurred in only approximately 50 % of the cells (fig. 19 C). This was probably due to a rapid precipitation upon injection and therefore poor metabolism of tamoxifen dissolved in an aqueous solution, as i.p. injections of 1 mg tamoxifen dissolved in oil performed in other mice yielded complete recombination. Interestingly, the partially recombined females were still fertile and produced offspring during 4 months of subsequent breeding. We genotyped the offspring and observed that the induced females had transmitted the recombined haplotype mll2FC. This indicated that primary oocytes that had recombined proceeded through meiotic telophase I and ovulated in the absence of Mll2. It is theoretically possible that a diploid primary oocyte recombined only one of both conditional Mll2 alleles. With meiotic division this could yield a recombined haploid secondary oocyte and a polar body with the unrecombined allele. As most of the cytosol is distributed to the oocyte while the polar body contains only one set of chromosomes, the recombined oocyte would probably contain sufficient levels of Mll2 until fertilization and transcription from the male genome. Moreover, it is possible that Mll2 protein translated in the oocyte before the recombination is very stable for extended periods, therefore our results do not provide final evidence that Mll2 is dispensable in oocytes.

However, it is possible that chimeric recombination obtained with the partial induction protocol produced primary follicles with few unrecombined granulosa cells. Although the oocyte recombined, there could possibly have been enough unrecombined granulosa cells to exert an essential, Mll2 dependent function on the oocyte. An experiment to test this hypothesis should use cell type-specific Cre recombination of the conditional mll2 allele. This could be achieved by crossing the Mll2F line to oocyte specific Cre lines, [GDF-9-iCre, Zp3cre, or Msx2Cre (Lan et al., 2004)], or a granulosa cell specific Cre line [AMH-Cre (Lecureuil et al., 2002)]. These experiments are currently being discussed.

2.3.10 Infertility of mutant males

Before description of the infertility observed in induced Mll2 mutants, this section will start with a short introduction to the male germ line (Cooke et al., 2002). In both man and mouse, the adult testis carries out two essential functions: it produces mature, haploid spermatozoa and it secretes steroid hormones, the most important of which is the androgen testosterone. Spermatogenesis, that is, the development of mature spermatozoa from diploid spermatogonial cells, takes 35 days in the mouse (fig. 40 A). Normal spermatogenesis and therefore fertility depends on interaction between the somatic cells (Sertoli, Leydig, and peritubular) and the germ cells, and also on hormonal support from the pituitary gland. Germ cells mature in the testis in the seminiferous tubules, highly organized structures that contain germ cells at all stages of maturation, with the most mature cells lying closest to the central lumen. Each Sertoli cell exists in close association with germ cells at multiple stages of their development (fig. 38 B). Maturation of germ cells is usually subdivided into three phases: mitotic proliferation of *spermatogonia*, meiotic division of *spermatocytes*, and differentiation of *spermatids* during spermiogenesis, which culminates in the release of mature spermatozoa (spermiation). In contrast to female germ cells, which proliferate exclusively during fetal development, the male germ cells are mitotically active in adults.

Two classes of spermatogonia have been identified by functional criteria: spermatogonial stem cells (A_{single} or A_s), which can colonize a recipient testis after germ cell transplantation, and differentiated spermatogonia (type A or B), which are not able to colonize the testis (De Rooij, D.G. 2001). These differentiated diploid spermatogonia undergo several mitotic divisions before they leave the stem cell niche, a compartment defined by tight junctions between Sertoli cells. During a lengthy meiotic prophase divided into the leptotene, zygotene

and pachytene phases, they are now referred to as spermatocytes. At the end of meiotic prophase, they undergo the final meiotic divisions to form haploid spermatids. Thereafter, the spermatids undergo spermiogenesis, during which the nucleus of the germ cell is remodeled and compacted into the form that is found in the mature spermatozoa. Spermatogenesis culminates in spermiation, when the mature spermatozoa are released from the Sertoli cell into the lumen of the seminiferous epithelium.

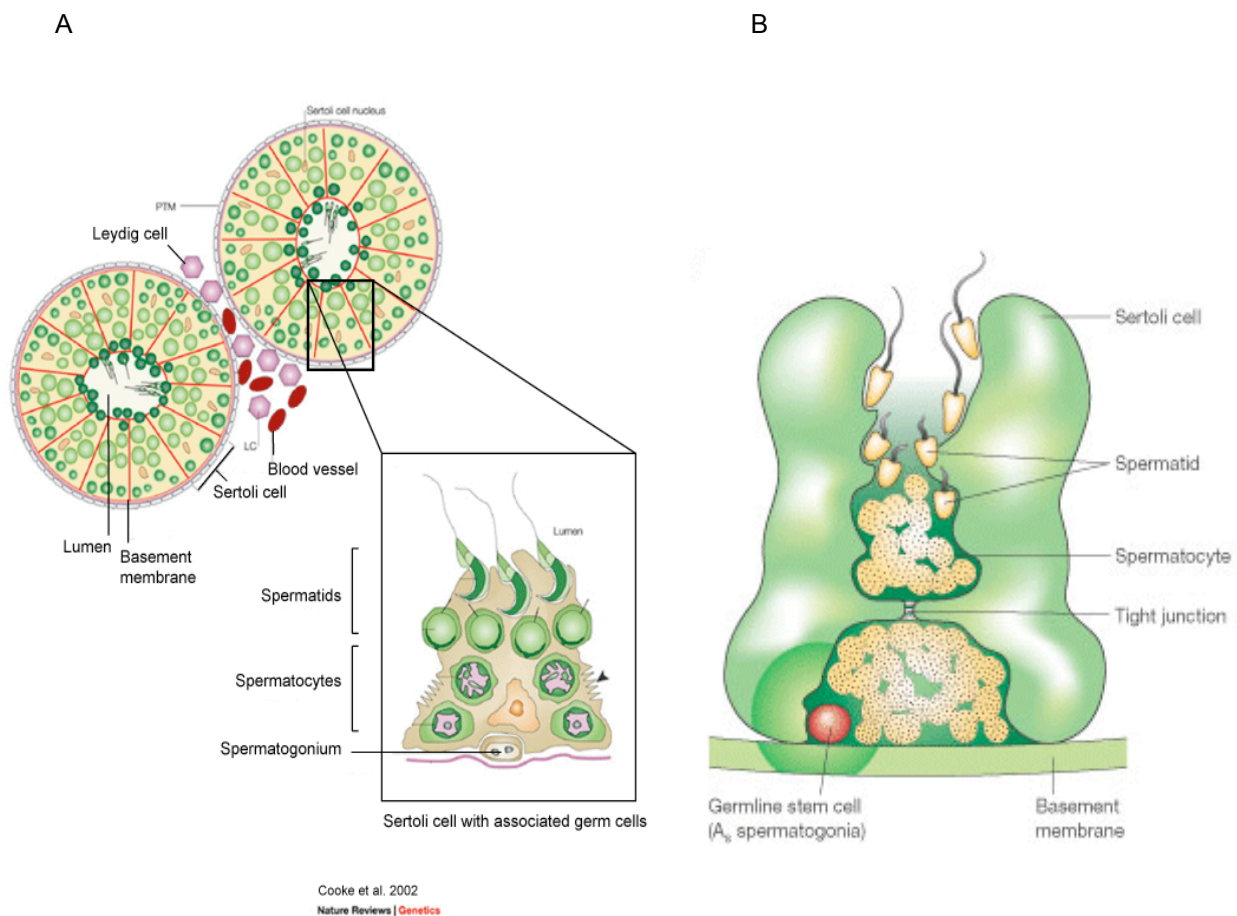


Fig. 38 *Organization of the testis.* (A) A diagrammatic cross-section through testicular tubules, showing the germ cells (green) at different stages of maturation developing embedded in somatic *Sertoli cells* (each Sertoli cell is outlined in red). *Leydig cells*, where testosterone is synthesized, are present in the interstitium. Shown in the box is a single Sertoli cell with its associated germ cell. Spermatogenesis comprises mitotic proliferation of *spermatogonia*, meiotic division of *spermatocytes*, and differentiation of *spermatids*. PTM, peritubular myoid cell. (B) Male germ cell niches. Germ cells are represented in yellow. The stem cell (spermatogonia), also known as a single (A_s) cell, is shown in red and constitutes a minority of the basal germ cells in contact with the basement membrane. Note that tight junctions between Sertoli cells (green) define two compartments: the stem cells and the pre-meiotic cells (spermatogonia) are found on one side of the junction, whereas the meiotic (spermatocytes) and the post-meiotic (round and elongating spermatids) cells are found organized in strict order of maturation towards the lumen. Figures A and B are published in Saunders et al. (2002) and Spradling et al. (2001).

For a fertility experiment, we used 11 males homozygous for *mlI2F* and heterozygous for *Rosa26-CreER(T2)* and 9 control males heterozygous for *mlI2F* and *Rosa26-CreER(T2)*, which were successfully mated to females before induction. Induction was performed by gavage of 5 mg per day tamoxifen for 5 consecutive days (see section 2.3.2). As described previously, mutant mice showed no exterior distinctive features compared to control mice. However, we had observed infertility of males (and females) in a previous experiment. Therefore, we mated 11 mutant and 9 control mice to 2 wild type females each after induction to assess fertility. Furthermore, we replaced the females with new females once per week for 8 weeks to determine a time lapse of the infertility.

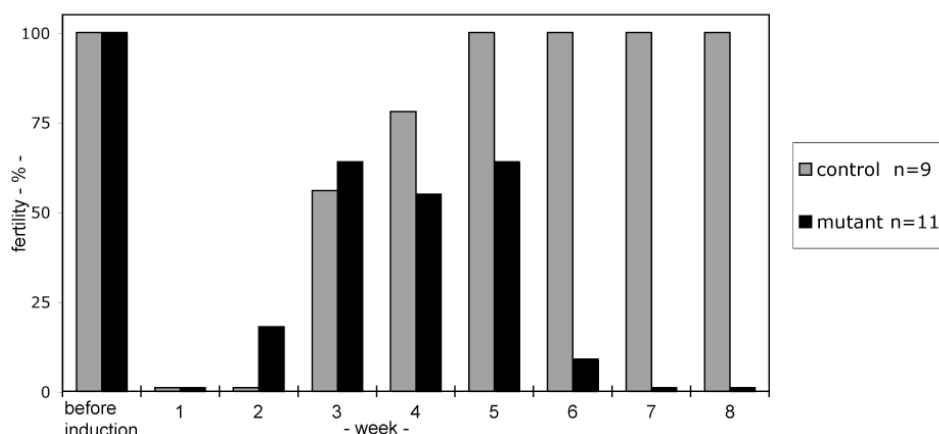


Fig 39 *Fertility of induced control and mutant mice.* Fertility was evaluated by weekly breeding of males to 2 females for a period of 8 weeks after induction. Fertility was temporally reduced in mutants and controls during 2 weeks after the tamoxifen treatment. Mutants and controls recovered fertility in the 3rd week, but mutants only became permanently infertile from the 7th week.

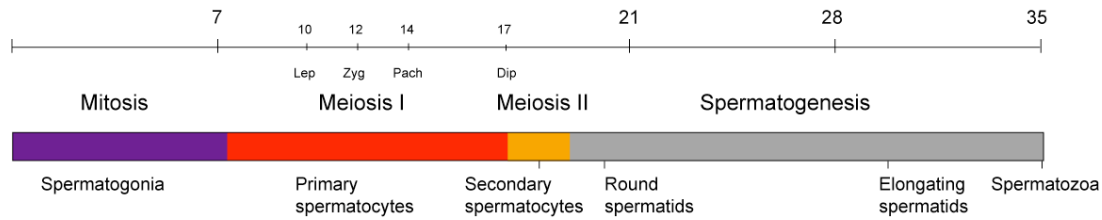
Similar to what we observed in induced females, there was temporary infertility in both mutant and control mice, which was probably a side effect of the tamoxifen treatment. Control mice recovered fertility gradually with 56% in the 3rd week, 78% in the 4th week, and 100% of individuals being fertile in the 5th week after induction. While older mice (3 - 4 months) recovered fertility in the 3rd week, younger mice (2 months) recovered more slowly. This could have been due to the lower body weight of the younger mice, which in consequence received a higher relative tamoxifen dose, as all mice were induced with 5 mg tamoxifen.

Of the mutants, 18% were fertile in the 2nd, 64% in the 3rd, 55% in the 4th, and 64% in the 5th week after induction, producing similar rates of recovery as in control mice.

However, not all mutants recovered fertility as controls did. Furthermore, there was subsequently a dramatic loss of fertility with 1/11 male fertile in the 6th week and all males sterile from the 7th week. We determined the transmitted *mll2* haplotype by genotyping the offspring from mutant crosses. Offspring derived from fertilizations during the 2nd and the 3rd week (day 7 to 22) after induction had the unrecombined *mll2F* allele, while offspring conceived during the 5th, 6th, and 7th week had the recombined *mll2FC* allele. This observation allowed determination of recombination success during tamoxifen treatment in different germ cell types. While spermatogonia and primary spermatocytes of early prophase I (leptotene to pachytene) did recombine, later stages of primary spermatocytes, secondary spermatocytes and spermatids did not. We assumed that *Rosa26-CreER(T2)* was not expressed at the cell stages where no recombination was obtained. Alternatively, the particular conformation of the DNA in these cells could explain the absence of recombined *mll2FC* allele. The formation of synaptonemal complexes and chiasmata during meiosis I could inhibit intrachromosomal recombination. Interchromosomal recombination, which could be the favored recombination event due to close pairing of homologous chromosomes, would not create the *mll2FC* allele. However, the existence of spermatocyte-specific and spermatid-specific Cre deleter lines (*Pgk2-Cre*, Ando et al., 2000; *Sycp1-Cre*, Vidal et al., 1998 & Chung et al., 2004; *Protamine1-Cre*, O’Gorman et al., 1997) argues against this possibility. Furthermore, Cre recombination is obtained in primary oocytes of adult females, which are arrested at the diplotene stage of meiosis I.

The induced mutants lost fertility between days 35 and 42 after induction, which corresponds exactly to a complete cycle of spermatogenesis. This indicated that the earliest phase of spermatogenesis was disturbed by mutagenesis of *Mll2*, as it required a full cycle to become striking. Moreover, offspring conceived in the 5th and the 6th week originated from germ cells that were spermatogonia A or B at the time of induction. Although these cells recombined, they underwent meiotic division, which indicated that *Mll2* is not required during meiosis and subsequent spermiogenesis.

A



B

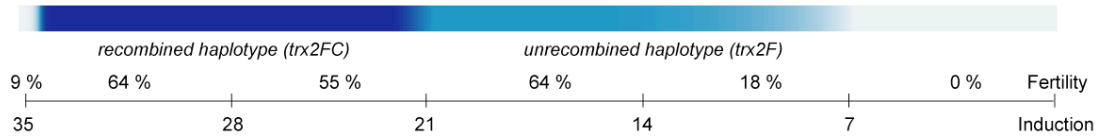
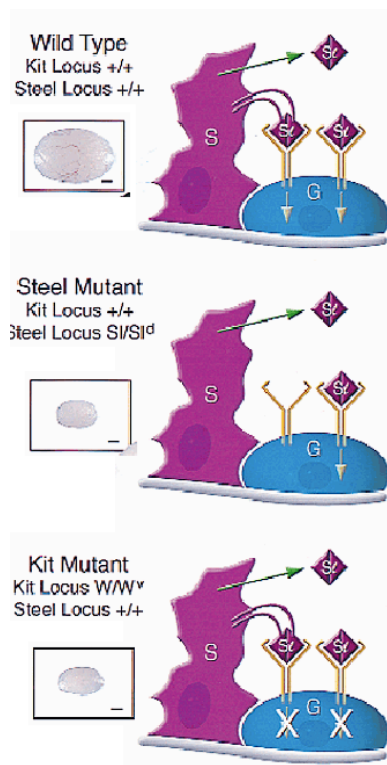


Fig. 40 Stages of spermatogenesis. (A) Spermatogenesis is a highly organized cyclic process with distinct phases: mitosis (purple), meiosis (red and orange), and spermiogenesis (grey). The time course shown indicates the duration of the maturation phases. (B) Fertility and transmitted haplotype of induced *mll2FC/FC* mice. Infertility in the first week after induction is also observed in control mice and a side effect of tamoxifen. The unrecombined *mll2F* allele is transmitted in the 2nd and 3rd week after induction, indicating that no cre recombination occurred in spermatocytes beyond the pachytene stage and spermatids. The recombined *mll2FC* allele is transmitted in the 4th to the 6th week after induction, indicating that cre recombination had occurred in spermatogonia and spermatocytes of the leptotene and zygotene stage. *Mll2* was not required for meiosis and spermiogenesis, as recombined spermatogonia succeeded in maturation and fertilized oocytes. The infertility of mutant males after 7 weeks indicated an essential function of *mll2* in spermatogonia.

Even though we determined the infertility to be related to spermatogonia, we could not



conclude whether the cause was a defect intrinsic to the germ cells or a defect in Sertoli cells. A model for defective Sertoli cell function is observed in the sterile mouse mutant *Steel*, which has mutated SCF/c-kit ligand. In contrast, the mouse mutant *Kit* has a mutated c-kit receptor, a defect of the germ cell that disrupts the same pathway and provokes an identical phenotype (Ogawa et al., 2000; Chabot et al., 1988; Geissler et al., 1988; Sorrentino et al., 1991; Flanagan et al., 1991). Whether *Mll2* function is required in Sertoli cells and/or spermatogonia could be addressed by the use of cell type specific cre recombinases. Therefore we are currently crossing the *mll2F* line with the inducible, germ cell specific Cre line PrP-CreER(T2) (Weber et al., 2003).

2.3.11 Histological analysis of testis

None of the eleven *ml12FC/FC* males produced any offspring 7 weeks after induction. To define the infertility phenotype, the histology of the testes from the induced males was examined. Testes of the mutants were atrophic and histological examination revealed smaller seminiferous tubules compared with controls. Spermatocytes were present in mutant testis but their number appeared reduced. Some seminiferous tubules were completely devoid of germ cells and contained only Sertoli cells, suggesting that the germ cells were undergoing rapid degeneration. In contrast, the Leydig cells in mutant testis appeared to be normal.

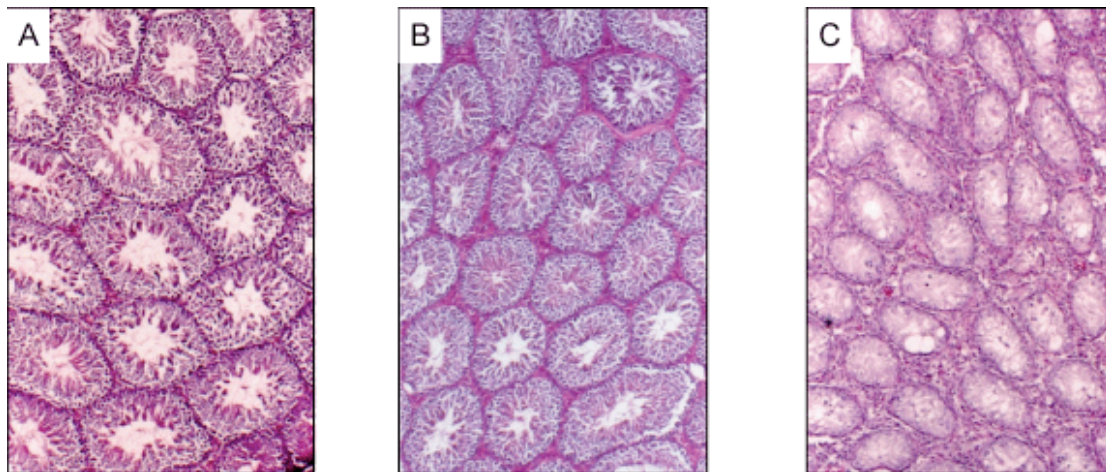


Fig. 41 *Histology of testes.* Testis sections were stained with haematoxylin and eosin. (A) In wild type control males (no tamoxifen) all stages of germ cells can be identified in the seminiferous epithelium. (B) Sections from tamoxifen treated heterozygous control mice (*ml12FC/+*; *Rosa26CreER(T2)+/-*) were similar to wild type controls. (C) In testis sections from mutant males (*ml12FC/FC*; *Rosa26CreER(T2)+/-*) 5 months after tamoxifen induction seminiferous tubules are completely devoid of germ cells. The interstitial Leydig cells surrounding the tubules appear to be increased in number, probably because of the decrease in the number of germ cells.

To determine if the loss of germ cells from seminiferous tubules was associated with cell death, the TdT-mediated fluorescein-dUTP nick-end-labeling (TUNEL) assay was used to detect the single and double strand DNA breaks that occur during apoptosis. Although very few apoptotic germ cells were seen in control testes, a large number of apoptotic germ cells were detected in mutant testes. Apoptotic cells were located exclusively in the peripheral region near the base of seminiferous tubules and therefore confined to spermatogonia. We induced several mutant *ml12F* males and examined the histology and extent of apoptosis in testis at several time points after induction. The

meiotic and post-meiotic germ cells appeared normal after induction, but the overall number of germ cells decreased with time because of the degeneration of spermatogonia. Increased apoptosis of spermatogonia was first observed 6 days after the beginning of tamoxifen treatment and was most prominent from the 15th to the 30th day. We immunostained testis sections with Ki-67 antibody, a marker for mitotically active spermatogonia. The positively stained cells in wild type sections were identified by their relative location in the seminiferous tubules to be spermatogonia of all stages. These include the self-renewing spermatogonia *A_{single}*, which differentiate to form spermatogonia *A_{paired}*, divide to form 4, 8, or 16 spermatogonia *A_{aligned}*, then differentiate to spermatogonia *A₁*, resume division to form spermatogonia *A₁* to *A₄*, divide to form intermediate spermatogonia (*In*) and finally divide to form spermatogonia type B. In testis sections of mutant males, no positive cells were detected 5 months after tamoxifen induction. These results confirmed the conclusions that the timing of infertility indicated a disruption of the earliest, mitotic phase of spermatogenesis in mutant mice. Furthermore, the complete lack of Ki-67 positive cells demonstrated a decay of the germinal stem cell (*A_{single}* cell) in the absence of *Mll2*.

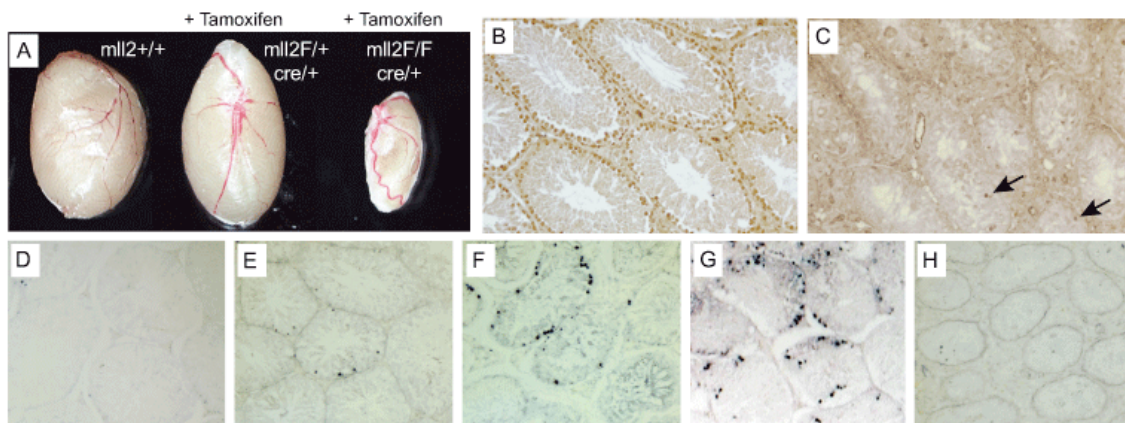


Fig. 42 *Defective spermatogenesis in Mll2^{FC/FC} males.* (A) Shown are 2 control testis of a wild type male (no tamoxifen) and a heterozygous male (*mll2^{FC/+}; cre/+*, with tamoxifen). Only the testis of the mutant male (*mll2^{FC/FC}; cre/+*, with tamoxifen) is atrophic. Testis section of wild type (B,D) and mutant (C,E-F) males. (B,C) Ki-67 immunostaining in tubules 5 month after tamoxifen induction. (D-H) TUNEL staining 6 days (D,E), 15 days (F), 25 days (G) and 5 months after tamoxifen induction.

2.3.12 Molecular characterization of the male infertility

To gain further insight in the infertility phenotype of *Mll2*^{-/-} males, we analyzed the expression of both *mll* and *mll2* in the testis by LacZ staining and *in situ* hybridization. LacZ stained cryosections of testis from *mll2*^{+/-} mice indicated expression of β -galactosidase in all germ cell stages, but not in Leydig cells. *In situ* hybridizations on wild type testis with probes specific for *mll2* and the close homologue *mll* were performed by collaborators (K. Loveland, Monash, Melbourne). Sense transcripts were used as controls and indicated low background for both probes. Antisense *mll2* cRNA signal was present in spermatogonia and spermatocytes, but absent in post-meiotic germ cells or somatic cells, including Sertoli cells. In contrast, the antisense *MLL* cRNA probe exhibited a strong signal in the pachytene spermatocytes, and a fainter signal in the round and early elongated spermatids. This partial exclusive expression pattern of both homologues in the testis could explain the restriction of the adult *mll2* phenotype to germ cell. Indeed, the rather surprising absence of abnormalities in other tissues of *Mll2*^{FC/FC} mice could be due to functional and spatial redundancy to *mll*. To substantiate this hypothesis, it remains to be excluded that *mll* is expressed in spermatogonia. Therefore, we are currently planning to isolate type A spermatogonia using the STAPUT method, which utilizes gravity sedimentation on a bovine serum albumin (BSA) gradient. RT-PCR analysis on a purified cell population will determine if *mll* is expressed in spermatogonia.

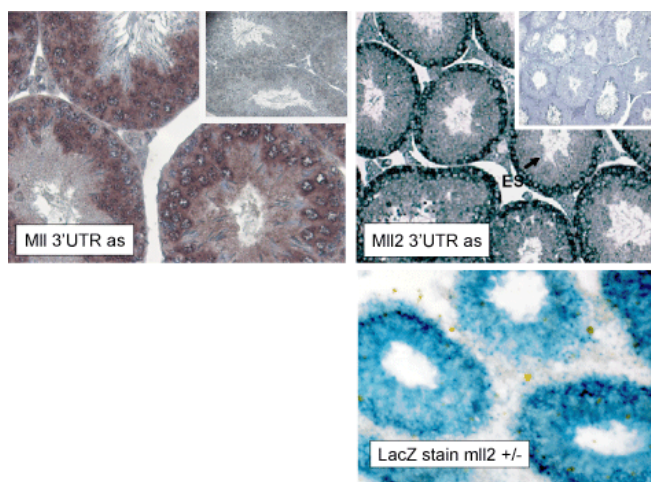


Fig. 43 Expression of *Mll* and *Mll2* in the testis evaluated by *in situ* hybridization on paraffin section and LacZ staining of *Mll2*^{+/-} testis cryosection. The strongest hybridization signal with the *Mll2* probe is observed in mitotic germ cells, while the strongest signal obtained with the *Mll* probe is detected in meiotic germ cells.

Next, we wanted to investigate if the infertility of mutant males is caused by a disturbance of the hormonal regulation of spermatogenesis. Testicular function is influenced both by endocrine (extra-testicular) and paracrine (intra-testicular) factors. The gonadotrophins luteinizing hormone (LH) and follicle-stimulating hormone (FSH), which are the main endocrine hormones, are secreted by the pituitary gland and signal through receptors (LHR and FSHR) expressed by Leydig and Sertoli cells, respectively. The paracrine regulation of spermatogenesis is thought to be provided by steroids, such as testosterone and oestradiol, which are both synthesized by Leydig cells, and by proteins, such as inhibin and activin, which are synthesized by the Sertoli cells. Several studies have indicated that deprived endocrine and paracrine support of the testis leads to reduction of testosterone concentration and complete infertility.

We tested testosterone levels of serum from 6 mutant mice and 2 control mice before, and at several time points after tamoxifen induction (experiments performed by Konstantinos Anastassiadis and Stefan Glaser in collaboration with Rattenberger). Blood samples were taken at a fixed time (11 a.m.) and plasma was collected by centrifugation. Testosterone concentrations were determined by a solid-phase ^{125}I -radioimmunoassay in 0.1 ml of plasma. The testosterone concentrations of induced mice were similar to the concentrations (2 to 5 ng/ml) previously measured in the C57BL/6 strain (Sayegh J.F. et al., 1990, Hampl et al., 1971). No difference in testosterone concentration was observed between induced mutant and control mice for up to one year after tamoxifen treatment. Thus, a perturbation of endocrine and/or paracrine signaling was not the cause of infertility in *mll2*FC/FC mice. Due to the incomplete recombination of the conditional *mll2* allele in the brain of induced mutants, a defective signaling of the pituitary gland was very unlikely. However, the normal testosterone levels indicated undisturbed paracrine signaling in the testis and functional Leydig cells in the absence of *mll2*.

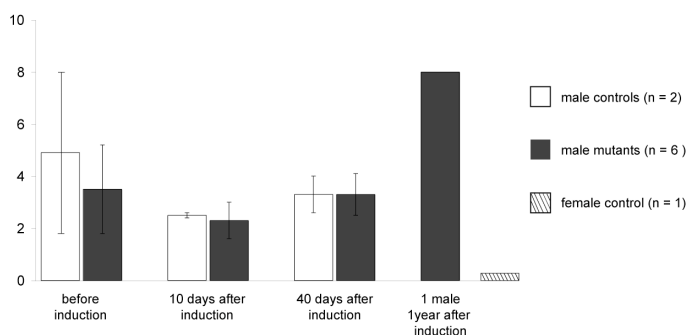


Fig. 44 *Normal testosterone levels in *mll2* mutant mice.* Blood samples were collected at different time points and testosterone levels [ng/ml] were determined from 100 μl serum. A control sample from a female yielded a value below 0,4 ng/ml

As *mll2* is strongly expressed in spermatogonia but absent in Sertoli cells, the infertility of *mll2* mutants is probably caused by an intrinsic defect in spermatogonia. Thus, these data indicated an essential function for *mll2* in spermatogonia. We wanted to determine if *mll2* is also essential in the fetal precursors of spermatogonia, the primordial germ cells (PGC). In the mouse, PGC arise early in embryogenesis, first becoming visible at E 7.5 in the extraembryonic mesoderm, posterior to the primitive streak. They subsequently become incorporated into the epithelium of the hindgut, from which they emigrate (E 9.5) and move first into the dorsal mesentery (E 10.5), and then into the genital ridges that lie on the dorsal body wall (E 11.5) (Gomperts et al., 1994). Simultaneous with the migration, PGC enter a period of proliferation from E 8.5 to E 13.5. After this time, PGCs in the male gonad undergo cell cycle arrest until a few days after birth, whereas in the female gonad, PGCs enter meiosis and arrest in prophase of meiosis I (McLaren, 2000). The high content of tissue non-specific alkaline phosphatase (TNAP) in PGC can be used as a rough marker to trace their development, however the widespread expression of another alkaline phosphatase gene in the embryo limits this application. Studies based on the detection of alkaline phosphatase (ALP)-positive cells detected about 8 cells at E7.0, 50 to 80 cells at the end of gastrulation, and about 125 cells at E8.0 (Ginsburg et al., 1990). Other studies detecting PGCs by alkaline phosphatase assays detected 50 cells at E 8.5 and 180 – 200 cells at E 9.5. PGC at later stages were detected using anti-PECAM antibody (Schmahl et al., 2000; Yao et al., 2002) and detected 2000 cells at E11.5, 5000 cells at E12.5, and 7000 cells at E13.5 (Atchison et al., 2003).

Interestingly, *mll2* seems to be dispensable in PGC, as (ALP)-positive cells were detected in E9.5 and E10.5 *mll2*^{-/-} embryos. However, fewer PGCs were seen in *mll2*-deficient male embryos. No abnormal or ectopic PGC migration was noted in *mll2*^{-/-} embryos, indicating that the PGC number did not decrease as a result of defective migration. The observed reduction of PGC number supports the concept that the absence of *mll2* increases apoptosis in various cell types and tissues including ES cells (Sandra Lubitz, unpublished results), developing embryos (section 2.2.3), and spermatogonia (section 2.3.11)

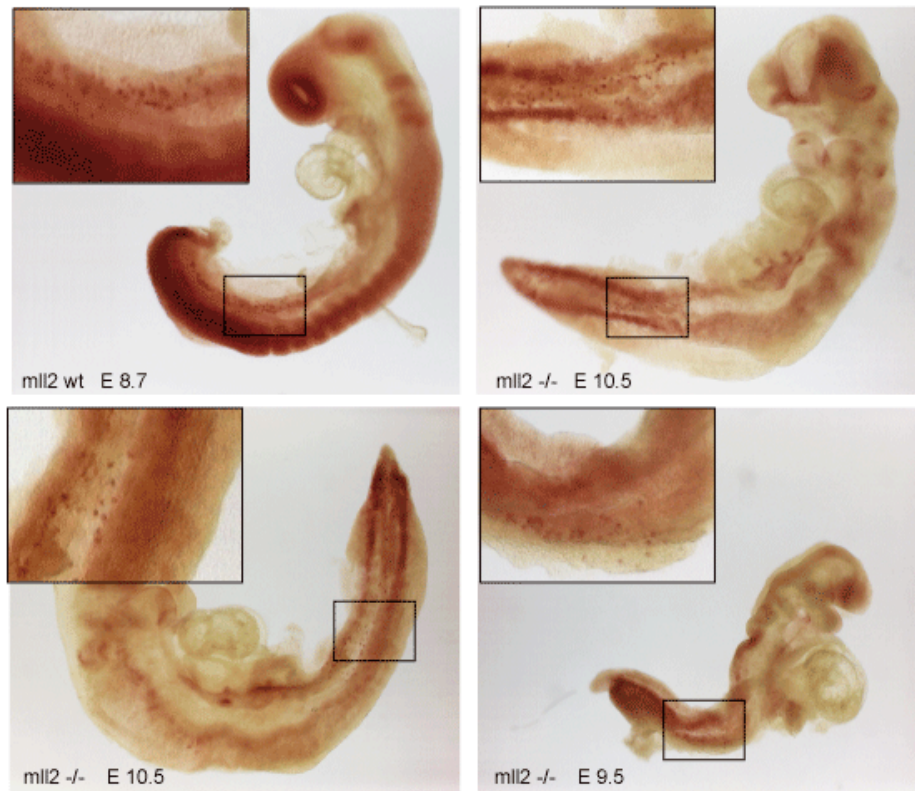


Fig. 45 Alkaline phosphatase staining of Mll2 ^{-/-} embryos revealed a decreased number of migrating primordial germ cells compared to wild type embryos.

2.4 Generation of an ubiquitous, inducible Cre mouse line

The goal of this project was the generation of a mouse line expressing an inducible SSR-steroid receptor fusion protein in all tissues. To achieve ubiquitous expression we decided to introduce the recombinase gene by DNA recombination into ES cells. A precise insertion by targeting an endogenous, ubiquitously expressed gene of the mouse would increase the chance of achieving omnipresent expression and be preferable to random integration of transgenes.

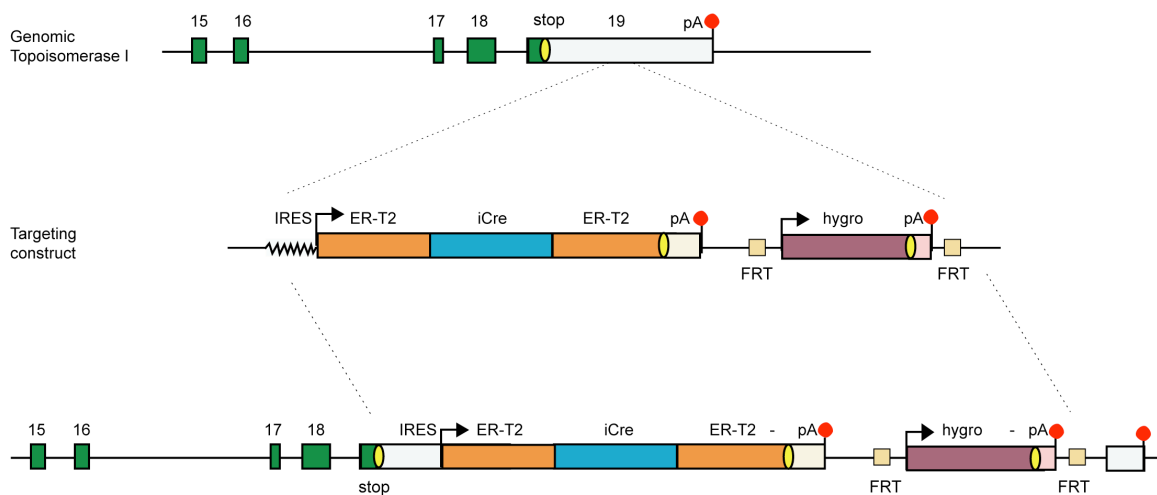


Fig. 46 Targeting to create an ubiquitous, inducible Cre line. By targeting IRES-ER(T2)-Cre-ER(T2)-hygro to the 3'UTR of topoisomerase I (topI), the homologous recombined locus expresses a polycistronic transcript (topI and cre) under the promoter of a house keeping gene.

Topoisomerase I belongs to the group of housekeeping genes, which are expressed in all nucleated cells. We designed a strategy for targeting a construct into the 3' UTR of this gene, thereby creating an allele for a polycistronic mRNA. By translation of both proteins, topoisomerase I and the CreER(T2), ubiquitous expression of the inducible recombinase would be achieved. Furthermore, the polycistronic approach would presumably not disturb expression of the targeted gene and the line could be maintained in a homozygous state.

2.4.1 Cloning of the targeting construct Topoisomerase I-ER(T2)-Cre-ER(T2)

The goal of this cloning was a construct with the coding sequence of Cre recombinase fused to two N- and C-terminal ER(T2)s. ER(T2) is a modified version of the estrogen receptor sequence with three amino acid substitutions (G400V/M543A/L544A). These substitutions render the ligand-binding domain insensitive to endogenous hormone β -estradiol but still responsive to the synthetic estrogen antagonist 4-OH-tamoxifen (Feil et al., 1997). An IRES was placed before the promoterless ORF to ensure its translation. For screening of ES cells by drug resistance the selectable marker hygromycin was placed at the 3' end of the construct. Flanking FRT sites allow removal by the site-specific recombinase Flp. Between all elements of the construct are one or two rare cutters, so that new variations of different alleles can be generated easily from this construct.

We generated ER(T1) and ER(T2) based on EBD (G400V) by a triple PCR strategy. The first reaction introduced the mutations L539A/L540A for T1 and M543A/L544A for T2 in the antisense primer, while the second PCR reaction carried the mutations in the sense primer. In the third reaction, both templates were used with the sense primer of the 1st and antisense primer of the 2nd reaction to generate the fused product.

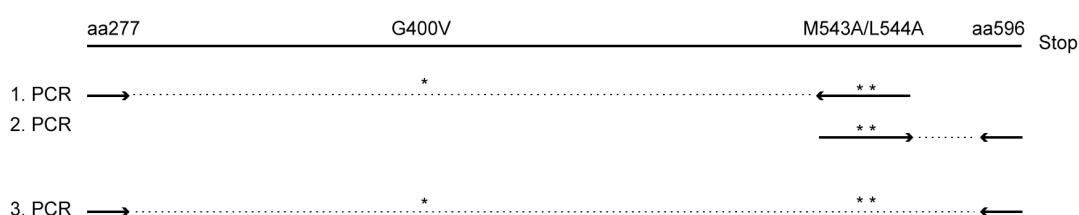


Fig. 47 Engineering of ER(T2) based on ER(G400V) by PCR. Two mutations (M543A and L544A) were introduced with primers in two separate PCRs. In a third PCR, a fusion of these two templates was generated by using sense primer of the 1st PCR and antisense primer of the 2nd PCR.

Next we introduced two ER(T2) into pBKC-iCreGBD (gift from Michael Huebner). This plasmid provided the improved Cre gene (iCre), where mammalian codon usage was applied to the prokaryotic coding sequence (Shimshek et al., 2002). First we replaced GBD by a BsiWI/EcoRI digest with one C-terminal ER(T2). Second, an additional N-terminal ER-T2 was cloned BstXI/EcoRV. This sequence coding a fusion protein with two ligand-binding domains is possibly less prone to leakiness.

In parallel we used Red/ET recombination to insert a PCR amplified chloramphenicol gene flanked by SgfI and AscI/PacI into pIRES-EGFP (Clontech). In a second Red/ET recombination we introduced this reamplified Cm-IRES sequence into pBKC-ER(T2)-hCre-ER(T2) setting the right frame between both elements.

In a third Red/ET reaction we introduced a PCR amplified hygromycin gene flanked by FRT sites and the restriction sites PmeI/NotI and FseI/SbfI. This selectable marker has a dual promoter for both prokaryotic and eukaryotic expression. Next we introduced 200 bp of PCR amplified sequence homologous to genomic topoisomerase I by restriction digest cloning using AscI/PacI on the 5' end and FseI/SbfI on the 3' end. This two-step conventional cloning was necessary because the construct was too large to be amplified in one PCR to introduce flanking homologous sequence. The final step was integration of the construct into a plasmid with genomic sequence of topoisomerase I by Red/ET recombination, creating a targeting construct with flanking genomic sequence for targeting in ES cells.

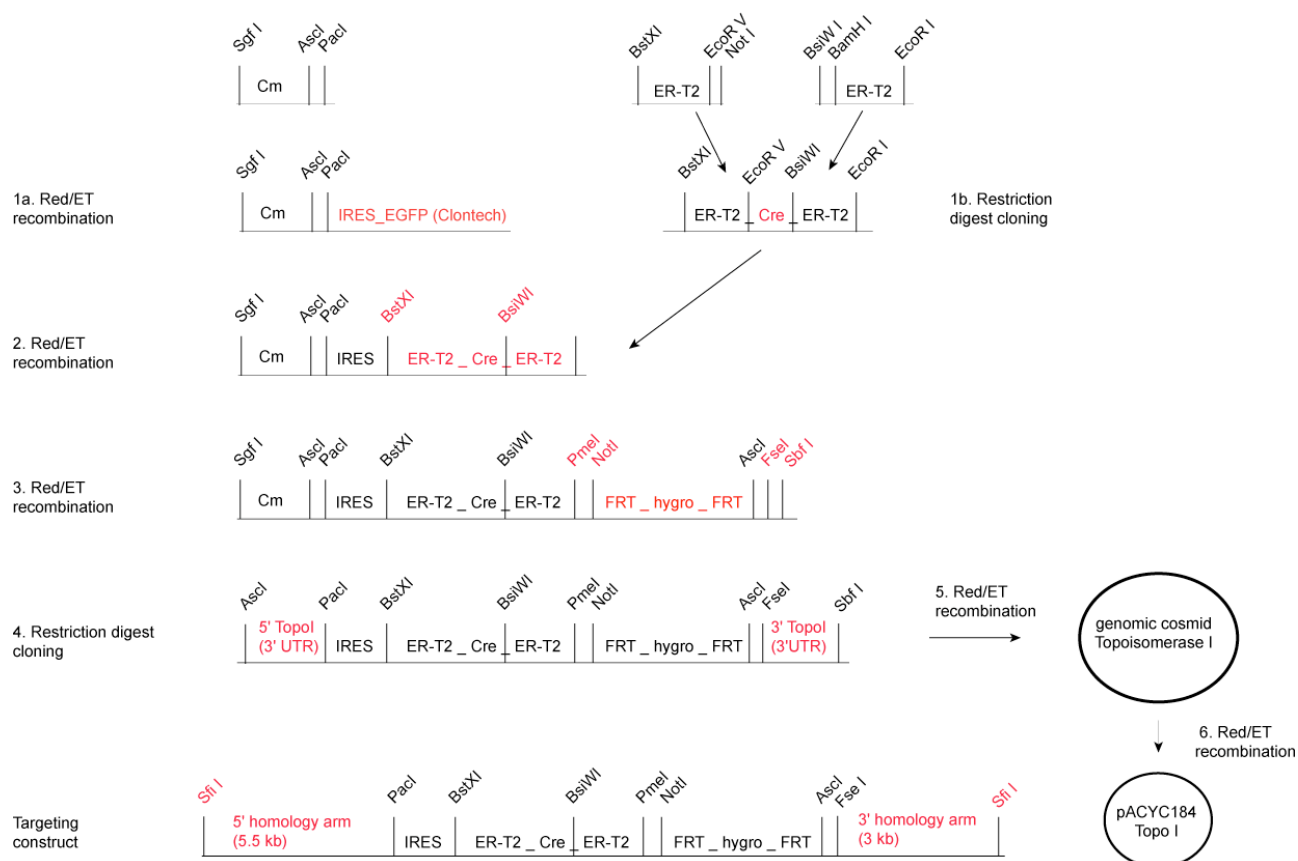


Fig. 48 Cloning of the targeting construct *Topoisomerase I-ER(T2)-Cre-ER(T2)*. (1a) Insertion of *Cm* into *pIRES-EGFP* by Red/ET recombination. (1b) Insertion of N-terminal and C-terminal *ER(T2)* in *pBKC-hCreGBD* by restriction digest cloning. (2) Insertion of *Cm-IRES* in *pBKC-ER(T2)hCreER(T2)* by Red/ET recombination. (3) Insertion of *FRT-hygro-FRT* into *pBKC-IRES-ER(T2)hCreER(T2)* by Red/ET recombination. (4) Insertion of two *topoisomerase I* homology arms by restriction digest cloning. (5) Insertion of the construct into a cosmid with genomic *topoisomerase I* sequence by Red/ET recombination. (6) Subcloning of a targeting construct with suitable homology arms for targeting in ES cells by Red/ET recombination.

2.4.2 Cloning of genomic topoisomerase I sequence

The goal was to obtain a clone with genomic sequence of *topoisomerase I* that would serve as a backbone to create a targeting construct for a *TopoI-ER(T2)CreER(T2)* allele. This work was done in the year 2000 before release of the mouse genome sequence therefore we did not have any sequence information on *topoisomerase I*. For more recent targeting projects we used sequenced BAC clones from the RCPI library, but at the time this work was done, those were not yet available. Instead, we used a 750 bp probe of *topoisomerase I* 3'UTR (from Julia Schaft) to screen 11 filters of a mouse 129/ola cosmid library. This screen identified 4 cosmids:

Cosmid 1: **MPMGc121G19773Q2**

filter: 78-2-249

coord. : 28 210, 26 208

Cosmid 2: **MPMGc121E12757Q2**

filter: 78-2-249

coord. : 61139, 64 138

Cosmid 3: **MPMGc121H03498Q2**

filter: 78-5-154

coord. : 228 124, 229 122

Cosmid 4: **MPMGc121I04703Q2**

filter: 78-2-219

coord.: 105 118, 102 117

Library 129/ola mouse cosmid

Library No: 121

Creator: Carola Burgtorf, Annette Poch, Michael Wiles

Source: Spleen

Vector: Lawrist 7 (**not** Lorist)

Host: DH5 alpha (E.coli)

Growth conditions: 37°C, kanamycin

The 4 clones were analyzed by restriction digest (EcoRI/SapI) and hybridized to the 3'UTR Topoisomerase I probe used for the screen. The probe hybridized to a 1.75 kb fragment in cosmids 1, 2 and 3 but not cosmid 4. The 1.75 kb EcoRI/SapI fragment could also be detected on the same blot from mouse tail genomic DNA. Therefore cosmids 1, 2 and 3 were identified as positive clones, while cosmid 4 was negative.

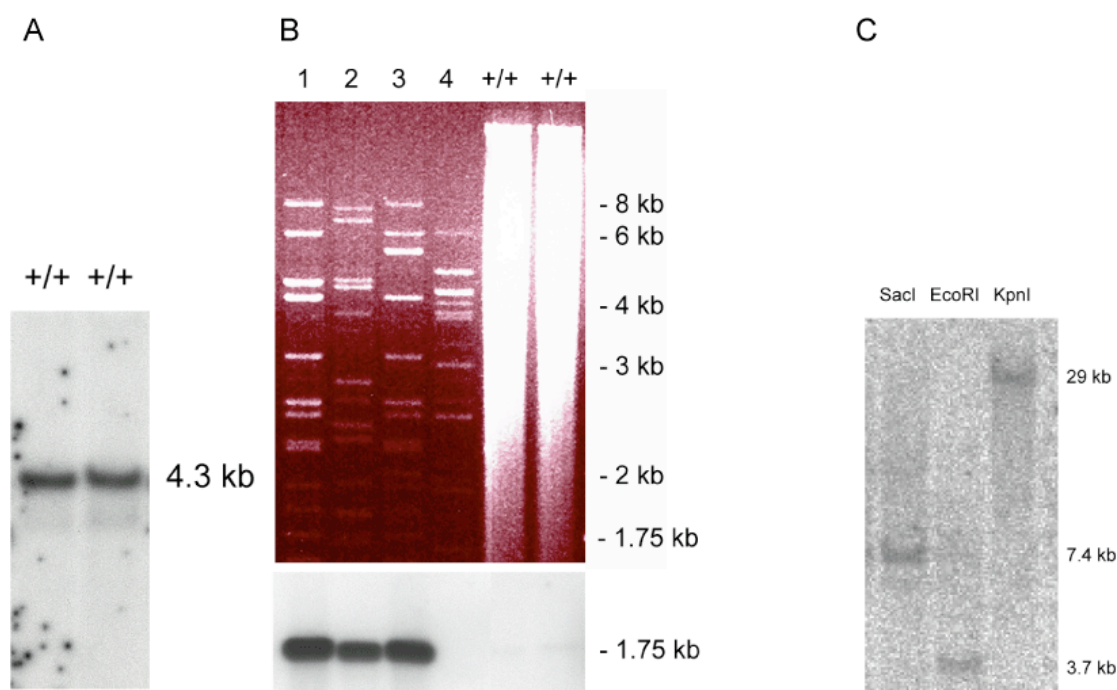


Fig. 49 *Genomic topoisomerase I DNA.* (A) Southern blotting of PstI digested mouse tail DNA hybridized with a 750 bp topoisomerase I 3'UTR probe detected a single 4.3 kb fragment. This probe was used for screening of a cosmid library containing mouse genomic sequence. (B)

Next we wanted to do an approximate mapping of the cosmids 1/2/3. In our design the final construct for ES cell targeting had a minimum of 3 – 5 kb of homology arms to achieve a high rate of homologous recombination. We were therefore searching for an adequate clone with a minimum of 3-5 kb of genomic sequence flanking the 3'UTR of topoI, which was our chosen integration locus for the ER(T2)Cre-ER(T2) construct. The size of the cosmid backbone (Lawrist 7) was 5 kb with one XhoI site and two SfiI sites flanking the insert. We used these enzymes and southern blotting with the 3'UTR topoI probe for mapping. An XhoI digest of cosmid1 gave 4 fragments of 23, 12, 9.5 and 7 kb, and the probe hybridized to the largest fragment. To find out where in this 20 kb fragment the TopoI 3'UTR was located, we introduced the ER(T2)-Cre-ER(T2) construct into the cosmid by Red/ET recombination. The size of the construct is 6 kb with a single XhoI site. Hybridizing an XhoI digest of this modified cosmid with a probe of the construct detected two fragments, of 18.5 and 8 kb. These two fragments together correspond to the 20 kb fragment, to which 6 kb (construct) and an XhoI site were added. We could therefore identify the insertion point of the construct at 5.5 kb of the 20 kb fragment, giving sufficient sequence on both sides of the construct. Next we

wanted to exclude the possibility that the 5.5 kb at the 5' end included the 5 kb backbone of the cosmid, reducing the genomic sequence to 0.5 kb. An XhoI/SfiI digest produced a 5 kb band (backbone) but the 8 kb fragment to which the construct probe hybridized was unaltered. From this we concluded that the construct was flanked by at least 5.5 kb at the 5' and 15 kb at the 3' end.

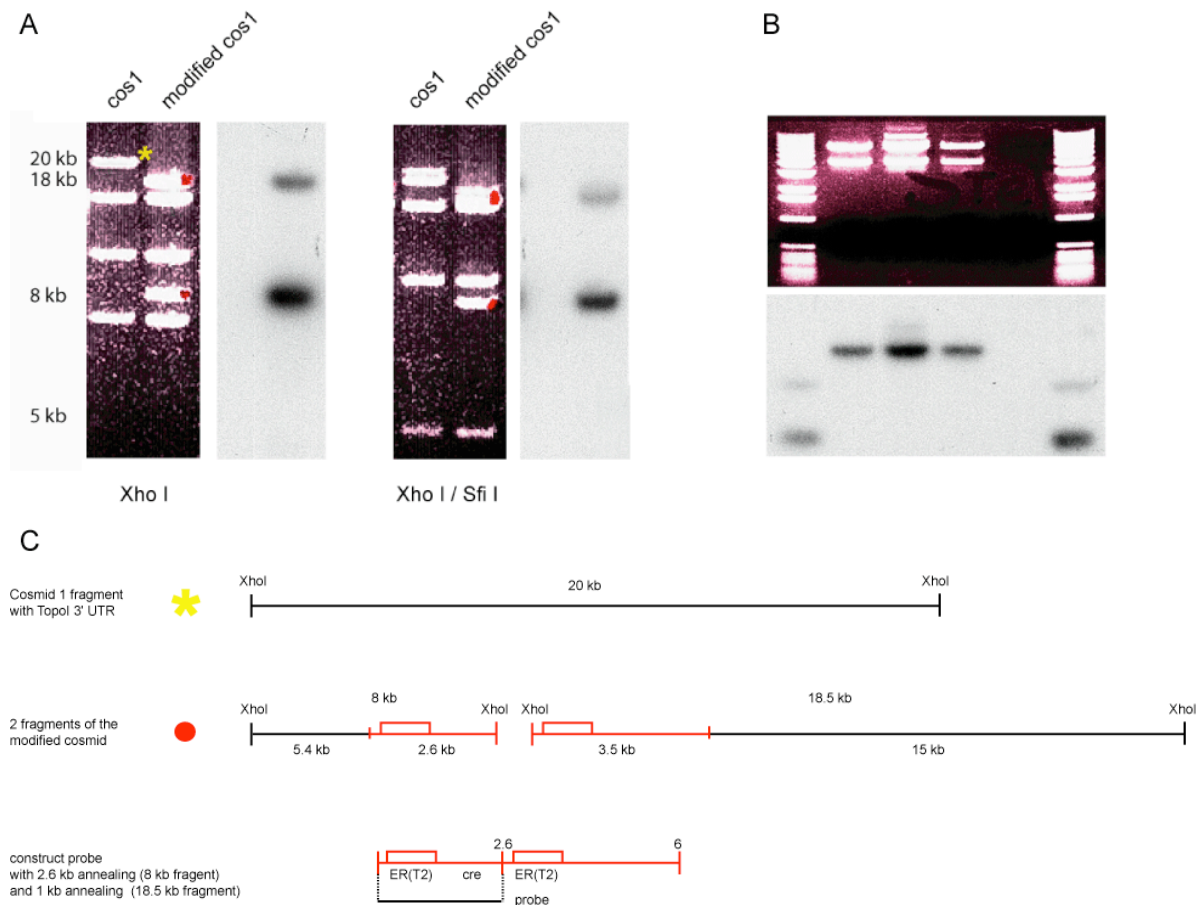


Fig. 50 Mapping of the cosmid containing genomic topoisomerase I sequence.

In the final cloning step we wanted to subclone the construct with suitable homology arms from the cosmid into a p15 origin plasmid by Red/ET recombination. This targeting construct would have homology arms according to the design of the southern strategy to screen for homologously recombined ES cell clones.

To perform this cloning we needed sequence information from the external ends of the cloning insert to create the 50 bp homology arms of the PCR primers. To obtain the sequence from the 5' end, we subcloned the 8 kb XhoI fragment from the modified cosmid into the pCI plasmid for end sequencing. Since this 8.5 kb fragment included 2.5 kb of inserted mll2 construct, by end sequencing the insert we obtained sequence information from the region 5 to 6 kb from the start of the construct. At the 3' end, we performed 3 rounds of primer walking sequencing to create a homology arm of 3 kb.

The cloning of the targeting construct was performed by transformation of pBAD α β γ Amp into the DH5 α cells with the modified cosmid. The PCR amplified backbone of pACYC184-kanamycin including two 50 bp homology arms was transformed after inducing Red protein expression, and 10 kanamycin resistant colonies were analyzed and showed the expected restriction digest pattern.

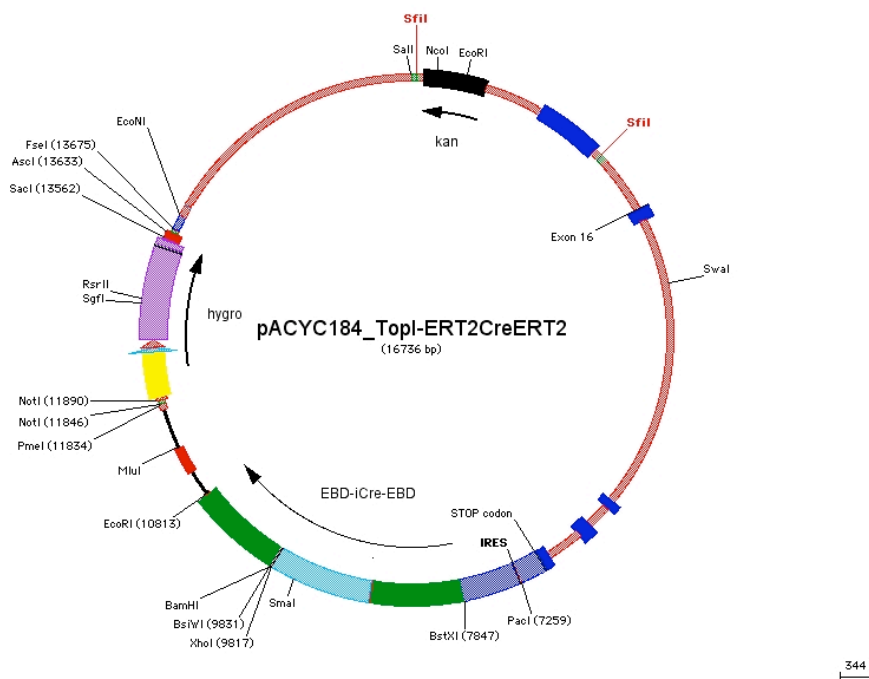


Fig. 51 Final targeting construct for the *Top1-ER(T2)-Cre-ER(T2)* allele

2.4.3 Repair of a point mutation in the TopI-CreER(T2) targeting construct

During the cloning of the targeting construct most intermediate cloning products were verified by sequencing. Nonetheless, a final sequencing of the whole construct before electroporation of ES cells revealed a point mutation in the IRES sequence (G to A). It turned out that this sequence, which was PCR amplified in the first cloning step, had never been sequenced before. We decided to repair the mutation in a two-step Red/ET recombination by first inserting a streptomycin/chloramphenicol cassette. In the second step we generated two final variations of the construct: (i) by reintroducing only a 150 bp IRES fragment we removed the N-terminal ER(T2) (ii) by reintroducing a 1.1 kb IRES-ER(T2) fragment we obtained the original construct design with N- and C-terminal ER(T2). As the recombinase fusion protein with two ERs could have disadvantageous induction properties (E. Cassanova, personal communication), we wanted to compare the two versions.

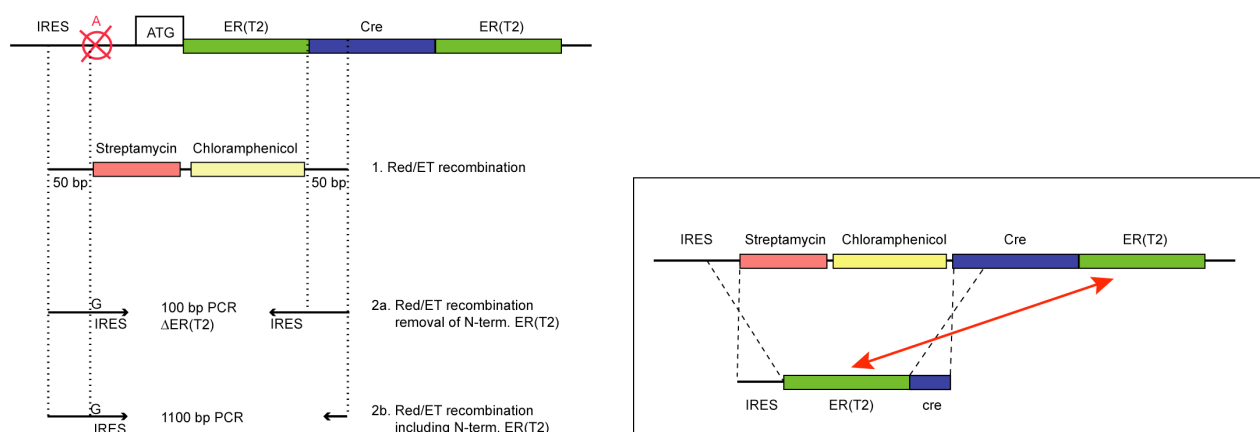


Fig. 52 Two-step Red/ET recombination used to repair the point mutation (A) in the IRES sequence. First, a counter selection cassette (Streptomycin/Chloramphenicol) is introduced. The second step was performed in two variations in order to obtain a cre fusion with a single ligand binding domain or two ligand binding domains. Shown in the box is the most probable recombination event (red arrow), which is the undesired recombination between the homologous ER(T2) sequences (1 kb). However, the correct recombination was obtained at a frequency of > 1%.

2.4.4 Targeting of ES cells by homologous recombination

The 2 final targeting constructs, IRES-ER(T2)-Cre-ER(T2) and IRES-CreER(T2) were linearized by SfiI digest separating inserts from plasmid backbones, purified from an agarose gel and extracted with phenol/chloroform. ES cells were electroporated and grown in selective medium with 200 µg/ml hygromycin. Although the experiment was repeated twice no drug resistant colonies survived the selection.

This failure is probably caused by a stretch of 35 bp missing in the promoter of the hygromycin gene and thus creating a hypomorphic allele. Sequencing identified the missing nucleotides, but since the original PCR template, pGK-P-hygro, had never been sequenced, we assumed the plasmid file to be incorrect. After failing to obtain resistant ES colonies, we sequenced pGK-P-hygro and realized that the gap had occurred during the PCR amplification in our cloning of the hygro cassette. Comparisons with the murine Pgk-1 promoter, from which this promoter for hygro is derived, revealed that the gap mutation is 49 bp upstream of the transcription start. This could indeed be a plausible explanation for a hypomorphic allele that did not confer drug resistance under the selection conditions used.

The repair of the presumed defective hygromycin promoter can be easily achieved in a single cloning step by replacing a 1 kb NotI/SgfI fragment from the targeting constructs with the same fragment from pGK-P-hygro.

We did not continue this project at this stage because we did receive an inducible cre deleter mouse line from colleagues, which had targeted CreER(T2) to the Rosa26 locus. This locus is known to give ubiquitous expression therefore this mouse line would presumably fulfill our requirements.

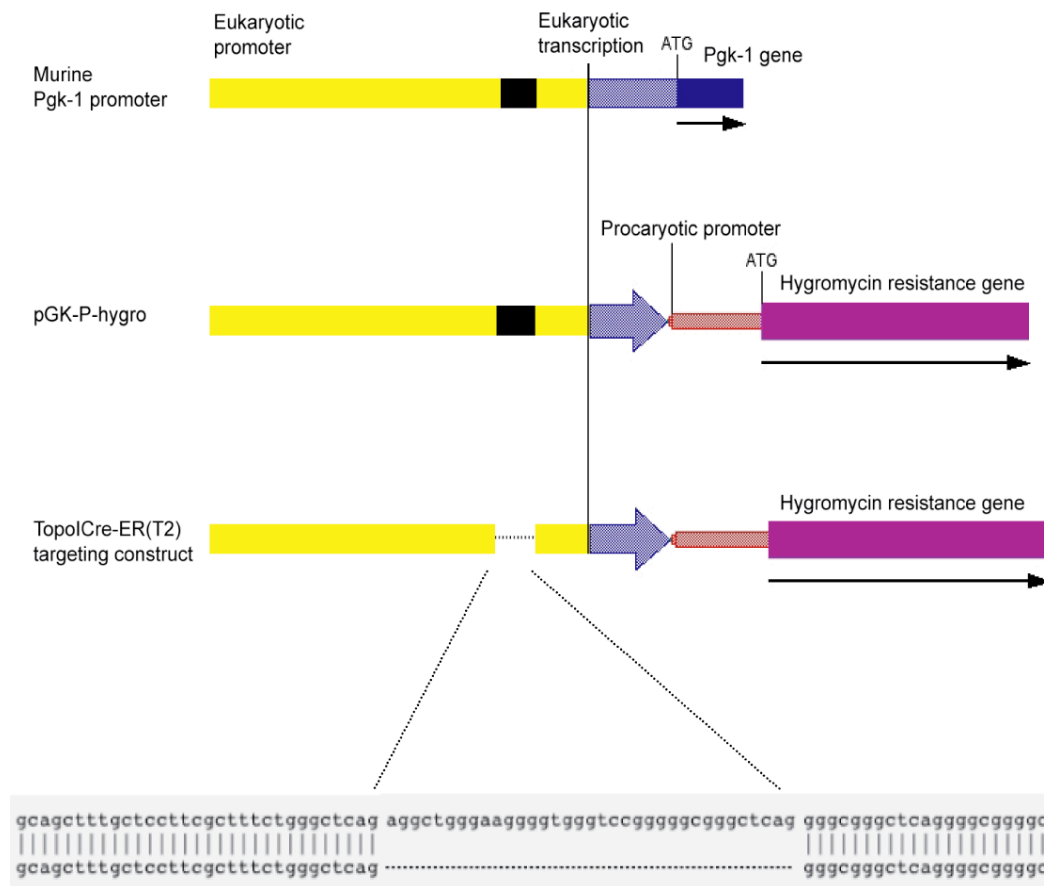


Fig. 53 Deletion in the hygromycin promoter of the *TopoI-CreER(T2)* targeting construct probably responsible for the unsuccessful targeting in ES cells. The repair of the defective hygromycin promoter can be achieved in a single cloning step by replacing a 1 kb *NotI/SgfI* fragment from the targeting constructs with the same fragment from pGK-P-hygro.

3. Discussion

3.1 The Mll2 multipurpose allele

The mll2 allele used in this study is versatile in its application. It is a **null allele** and a **reporter** for mll2 expression in its original configuration and convertible to a **conditional allele**. The inclusion of multiple features within one (i.e. multipurpose) allele is achieved by (i) leaving the genomic organization of the locus intact, (ii) insertion of a trap/reporter cassette that creates a null/reporter allele based on RNA splicing, (iii) removal of the trap/reporter cassette by site-specific recombinase to restore functionality of the allele, (iiii) conditional excision of an exon catalyzed by site-specific recombinase to create a frame shifted allele. The incontestable merit of a multipurpose allele is that the engineering of one targeted mutation can address several allelic purposes. However, a null allele based on RNA splicing rather than destruction of the genomic structure of the gene can comprise unforeseeable drawbacks. It is impossible to reliably predict the splicing events that are going to occur from a locus where a trap cassette has been inserted. In our targeting construct, we used 1.8 kb genomic sequence of the homeobox gene engrailed 2 as splice acceptor, which included the entire intron 1 and 158 nucleotides of exon 2. Although this sequence should provide a strong splice acceptor, it could not be excluded that the splicing of exon1 of mll2 to the trap cassette would be partial. An incomplete trapping of the transcript due to alternative splicing bypassing the trap cassette could result in production of the full length mRNA and therefore impede the creation of a null allele. However, no such transcript could be detected in mll2 ^{-/-} embryos and ES cells, indicating that the splicing of exon 1 to the trap cassette was complete. Interestingly, RNA splicing is not only sequence specific but appears to be influenced by the position of the trap cassette (probably dependent on mRNA secondary structure). While a trap cassette inserted in the 5' end of a gene often results in complete trapping, insertions in the 3' end of genes often produce incomplete trapping (German gene trap consortium, unpublished communication). Therefore, our approach to introduce the trap cassette in intron 1 of mll2 and having previously excluded alternative splicing of exon1 presumably contributed substantially to the successful creation of the null allele.

The *mll2* conditional allele was created by Flpe mediated excision of the trap cassette. This was achieved by breeding *mll2*^{+/-} mice to hATPC:Flpe mice (Rodriguez et al., 2000). Flpe recombination was partial in the F1 offspring, probably due to a rather long distance (6.5 kb) between the FRT sites. However, an additional cross to hATPC-Flpe mice produced heterozygous Flpe recombined offspring. In contrast to the null allele, the *mll2*F (Flpe recombined) allele is similar to wild type and could be bred to homozygosity.

Conditional mutagenesis of *mll2* *in vivo* and *in vitro* was induced by Cre mediated excision of loxP flanked exon 2. The presumed splicing of exon 1 to exon 3 in the *mll2*FC transcript (Flpe & Cre recombined) would create a frame shift and a nonsense mutation in exon 3. Cloning and sequencing of an RT-PCR product confirmed the exclusive splicing of exon 1 to exon 3. Surprisingly, the frame shifted *mll2* transcript was still detectable at reduced levels by Northern blot and RT-PCR and not fully eliminated by nonsense-mediated mRNA decay. This raised the issue if N-terminally truncated *mll2* protein could still be translated from the mutated transcript. The initiation of translation occurs by assembly of ribosomes at the 5' end of an mRNA. Subsequently, the ribosomes “scan” the mRNA to find the initiating AUG triplet. In this process, it is not always the most 5' AUG that is preferred as translation start site, but usually the triplet embedded in what most resembles a Kozac consensus sequence (ccA/Gcc AUG G). In the *mll2* transcript, the 3rd methionine-coding triplet (position 948), which is downstream of the created stop codon, corresponds to a Kozac consensus sequence. In an adversarial scenario, ribosomes would assemble at the 7'cap, skip the created stop codon and start in frame translation at the 3rd AUG triplet, which would yield a negligibly shorter protein (Δ 316 aa). However, this possibility was excluded by demonstrating complete absence of Mll2 protein by western blot in tissue of induced mice (except brain see section 2.3.3) and ES cells.

The null allele and the frame shifted allele are identical in the sense that both are null alleles. However, the mechanisms behind the two alleles are quite different. While the *mll2*⁻ allele relies on trapping and truncation of the endogenous transcript, the *mll2*FC allele relies on frame shifting of the transcript. We compared the two alleles by breeding them to homozygosity in mice. The observed embryonic lethal phenotype was identical and additionally proved both alleles to be equivalent.

As described in section 2.2.1 the transcript of the null allele produces two proteins; The LacZneo fusion protein is translated from the IRES while a presumed 161 aa protein is

translated from the endogenous translation start site. This protein consists of 121 aa of Mll2 coded by exon 1 and 40 mutated aa coded by frame shifted exon 2 of the engrailed 2 gene that served as splice acceptor for the trap cassette. It is unlikely that this new protein has a gain of function effect and influences the phenotype, as it does not include any conserved protein domain. Moreover, *mll2*^{+/-} embryos that produce this truncated protein from one null allele did not show any abnormality. However, a dosage dependent effect of the 161 aa protein cannot be fully excluded. Indeed, a similar protein consisting of 121 aa coded by exon 1 of *mll2* and 19 mutated aa coded by frame shifted exon 3 is translated from the *mll2*^{FC} transcript. The similarity of both alleles in embryogenesis could therefore not exclude the possibility of an influence of the proteolytic side products of both alleles.

We conclude that the multipurpose *mll2* allele successfully accomplished three different purposes. Its design therefore represents a valuable enhancement to currently applied strategies in mouse genetics.

3.2 The Rosa26-CreER(T2) allele

The embryonic lethal phenotype of *mll2*^{-/-} embryos between E8.5 and E11 obliged us to apply a conditional knockout strategy to study the function of the gene at later time points. We used the ability of the Cre recombinase to catalyze the excision of DNA flanked by loxP recognition sequences to mutate Mll2. Temporal control of Flp- and Cre-mediated recombination has been achieved with a recombinase fused to the hormone-binding domain of the mutated estrogen receptor (Logie et al., 1995; Metzger et al., 1995 and section 1.2.2). The fusion protein becomes active upon administration of the synthetic ligand tamoxifen, but not in the presence of the natural ligand 17 β -estradiol (Feil, 1996). For this analysis, we have used the mouse strain Rosa26-CreER(T2) (Seibler et al., 2003) that utilizes a triple mutated ligand binding domain ER(T2) with approximately 10 fold higher binding affinity to tamoxifen than the single mutated ER(T) domain used for the Rosa26-CreER(T) line (Vooijs et al., 2001). The ubiquitous expression of Cre-ER(T2) from the Rosa26 locus allowed induced mutagenesis of Mll2 in all tissues of embryos, neonates and adult mice.

Partial Cre recombination without administration of the ligand was detected in tail DNA of approximately 15% of mice with the conditional *mll2F* and the *Rosa26-CreER(T2)* allele. Thus, the leakiness of ligand regulated Cre occurred only individually and is not a general feature of the system, as is the case for the tetracycline inducible system tet-on (Gossen et al., 1995). The observed ligand-independent Cre activity may be a consequence of inappropriate nuclear transport or proteolysis of the Cre fusion protein, sufficient to catalyze a low level of recombination. The leakiness could be fully eliminated from the analysis by excluding the partially recombined mice.

We have cultured mouse embryonic fibroblasts (MEFs) and ES cells homozygous for the *mll2F* and the *Rosa26-CreER(T2)* alleles and tested the *in vitro* induction of the Cre recombinase by using serial dilutions of 4-hydroxytamoxifen (4-OHT). The recombination of the *mll2F* allele in ES cells was over 97% after 24 hours treatment with 100 nM 4-OHT (data not shown, see diploma thesis of Daniela Röllig). By using an Mll2 specific antibody that was validated using *mll2*^{-/-} ES cells (see thesis of Julia Schaft), we observed complete absence of the protein after 5 days of 4-OHT treatment. A more detailed analysis of Mll2 protein levels at earlier time points of induction indicated that the protein is lost after 72 hours of 4-OHT treatment. Thus, the approximate half-life of Mll2 protein in ES cells is 48 hours (diploma thesis Daniela Röllig).

For induction of the *mll2F* allele *in vivo* two protocols for administration of tamoxifen to mice were tested; Oral feeding of a tamoxifen/oil solution (gavage) or injection (i.p.) of 4-hydroxytamoxifen dissolved in oil. In agreement with previous studies (Kuehbandner et al., 2000), both protocols gave identical recombination efficiencies. We preferred the gavage protocol, as the LD50 of tamoxifen in mice is 15-fold higher via the oral route than by i.p. injection (200mg versus 5g/kg, Seibler et al., 2003). In addition, orally administrated tamoxifen is probably efficiently metabolized to 4-hydroxytamoxifen in the liver of the mouse. We could therefore restrict the use of costlier 4-hydroxytamoxifen to *in vitro* inductions. We analyzed the recombination rates of the conditional *mll2F* allele using different concentrations of tamoxifen with the goal of achieving the highest possible rate in all tissues. A dose-response experiment indicated that the extent of recombination is highly dependent on the amount of tamoxifen given to the mice. A daily dose of 2.5 mg tamoxifen for 5 days resulted in incomplete recombination in most tissues and no recombination in the brain. However, the use of 4mg and 7mg yielded full recombination in all tested tissues and 30% or 50%

recombination in the brain, respectively. The limited degree of recombination in the brain may reflect a lower local concentration of ligand due to the blood-brain barrier rather than a reduced expression level of CreER(T2) (Seibler et al., 2003). The standard protocol for all further induction experiments was gavage of 5 mg tamoxifen per day for 5 consecutive days, a treatment that caused no side effects on 28 tested $\omega\lambda\delta$ $\tau\psi\pi\epsilon$ mice.

In addition to induction of adults, we induced recombination in embryos and neonates by feeding pregnant or lactating females tamoxifen, respectively. Previous studies describe the induction of a ligand regulated Cre-ERTM *in utero* by a single, intraperitoneal injection of tamoxifen into a pregnant mouse at E8.5 postcoitum (Danielian et al., 1998; Hayashi et al., 2002). The transgenic CAGGCre-ERTM line used displayed dose-dependent recombination (0.5 to 9 mg i.p.), with higher doses giving more LacZ reporter activity (50 to 95 %). However, injections of tamoxifen doses above 3 mg at E8.5 caused pregnancies to fail after E 13.5, presumably due to the anti-estrogenic properties of tamoxifen (Jordan et al., 1990). The cytotoxic effect of tamoxifen on pregnancy was not observed in inductions at later developmental stages (E 11.5 and 14.5). The limitation of that study is the high concentration of ligand required to activate the CreERTM, which is quite close to the tamoxifen concentration that interferes with the maintenance of early pregnancy. Moreover, the obtained recombination was variable and incomplete.

Due to the higher binding affinity of the ER(T2) for ligand, we obtained complete recombination in embryos at various stages using two daily gavage doses of 5 mg tamoxifen. Interestingly, *mll2*F embryos induced at early stages (E4.5 and E5.5) recapitulated the embryonic phenotype of *mll2* null mutants at E 10.5, which further validated the effectiveness of the system. We are currently testing if two oral doses of 5 mg tamoxifen are tolerated by the females of early stages (E0.5 to E11.5) and permit pregnancy to develop to term.

Finally, we have tested induction in neonates by feeding lactating mothers tamoxifen, assuming that the milk would efficiently transmit the ligand. With 5 daily doses of 5 mg tamoxifen to the mother during postnatal period P5 to P9, the recombination was complete in all tissues and 30 to 50% in the brains of pups dissected at P13 to P15.

The superiority of RosaCreER(T2) mice for producing induced recombination is diminished by a serious side effect of CreER(T2) expression. Clearly, we observed a

high rate of illness and lethality in mMll2F/F;Rosa26CreER(T2) mice (74/172). Illness occurred between the 5th and the 15th day after induction, with most cases from day 8 to day 10. In contrast, the tamoxifen caused no side effect on wild type mice (0/28). The first symptoms of illness were reduced mobility and constant weight loss that indicated pronounced dehydration. During progression of the illness, mice sustained severe diarrhea observable at the anus of animals. Dissections of sick mice revealed that the entire intestine was filled with liquid. The gall bladder and stomach were distended and the gastric content of sick mice had on average twice the weight as in wild type mice. Surprisingly, the gastrointestinal phenotype was not caused by mutagenesis of mll2, as it also occurred in control mice of the Rosa26-CreER(T2) line. In fact, the morbidity seemed to originate from activated CreER(T2) protein. This conclusion is substantiated by the observation that the diarrhea occurred in only 16% (13/82) of mice heterozygous for Rosa26-CreER(T2), but in 76% (61/80) of homozygous mice. The 2 different strains that were used, C57BL/6 or 129/ola, did not differ significantly the incidence of this disease. Furthermore, the oil was not the cause of the diarrhea; pups homozygous for Rosa26-CreER(T2) that did not receive oil but were induced by lactating mothers developed an identical phenotype. Finally, as most inductions were performed outside the Specific Pathogen Free (SPF) laboratory, we also induced mice inside the colony under pathogen free conditions and observed a similar rate of illness. This excluded the possibility that the diarrhea was a result of severe infection (i.e. as observed in INF- γ k.o. mice), which could have implied an immunodeficiency triggered by the induction. We assume that the diarrhea is caused by activated ER(T2) and not an effect of cre activity. Several Cre lines including some with ubiquitous expression have proven that constitutive recombinase activity does not produce such a severe phenotype (Schwenk et al., 1995; Schmidt et al., 2000). In contrast, the Rosa26-CreER(T2) is the first line that expresses the triple mutated ER-T2 (G400V/M543A/L544A) in all tissues. Indeed, a tissue specific mouse line that expresses CreER(T2) only in germ cells does not develop the illness (Weber et al., 2002). Therefore, we speculate that the diarrhea of Rosa26-CreER(T2) mice is caused by the effect of activated fusion protein in one specific tissue. Being aware of this tissue would leave the CreER(T2) sequence to be applicable in lines specific for all other tissues. We have not identified the tissue responsible for the phenotype, but we suspect that the gastrointestinal phenotype is caused by a defect in the pancreas, as the pancreas of ill mice often looked brownish compared to healthy mice.

Further, no phenotype was reported from two previous ubiquitous CreER lines (Hayashi et al., 2002; Vooijs et al., 2001). However, the authors apparently did not breed their lines to homozygosity, which could have increased the chances of noticing a possible phenotype. One of these lines, Rosa26-CreER(T), has an identical expression pattern of the fusion protein but a different ER (G521R). This raises the issue as to whether only the ER(T2) has a toxic effect, while other mutated ER versions (e.g. ER-T1 [G400V/L539A/L540A]) produce no side effects and are more valuable for applications in the mouse.

3.3 The Mll2 gene

Analyses of mice lacking Mll2 function have demonstrated that the gene is dispensable in adults but essential during development. Mll2 ^{-/-} embryos failed in gestation between E 8.5 and E11. The growth and differentiation of most tissues until mid-gestation was retarded but not prevented in the absence of Mll2 function. However, completion of embryogenesis is dependent on the activity of the gene. The phenotype is first noticeable at E7.5 by a growth retardation of the mll2 ^{-/-} embryos compared to their wild type and heterozygote littermates. During further development the retardation of mutants increased gradually. Interestingly, the retarded mutant embryos still developed normally until E 9.5 and were morphologically identical to E8.5 wild type embryos. However, from E 9.5 mutants had widespread morphological abnormalities that affected the entire body structure. Despite proper neurulation and closure of the head fold, the neural tube appeared to be kinked, which is often a characteristic of a lack of paraxial mesoderm. Indeed, while somites were visible in mutants at early stages, somite development was clearly lacking at later stages. While the overall number of proliferating cells is normal in mll2^{-/-} embryos, there is a significant increase of apoptosis throughout the whole embryo. In average, 20% of all cells were apoptotic in Mll2 mutants, while less than 1% were apoptotic in wild type embryos. The elevated apoptosis rate could account for the retarded phenotype without specific defects of early mutants. Due to the increased elimination of cells, more proliferation events are necessary to reach a critical cell number that could be required for progression in development. The mechanism by which the absence of Mll2 leads to increased

apoptosis is unclear. Possibly, Mll2 is directly involved as an inhibitor in the regulation of apoptosis. If that was the case, overexpression of Mll2 should theoretically render cells more resistant to apoptotic stimuli i.e. UV radiation, chemical insult, or serum deprivation (possible future experiments). Alternatively, a widespread misregulation of gene expression in cells lacking Mll2 function could initiate the cellular suicide program. Indeed, we detected a misregulation of specific genes during embryogenesis; Hoxb1, mox1 and six3 expression was absent in mll2^{-/-} embryos at E9.5. Moreover, normal expression of wnt1, brachyury, Shh, and otx2 in mutants at E10.5 indicated that the absence of hoxb1, mox1 and six3 was specific and not due to a global failure of transcription as could occur in a dying embryo. Further, expression of hoxb1 and mox1 was normal in mutants of earlier stages (E8.5). Mll2 mutants expressed mox1 from the 1 to 8 somite stage (E7.7 to E8.4), while all mutants at later stages had lost expression. Interestingly, some mutants at the 10 somite stage showed a loss of mox1 expression in anterior somites, while newly formed posterior somites still expressed mox 1. During somitogenesis, a cyclic biological clock leads to formation of a new pair of somites every 2 hours. Consequently, we conclude that the loss of mox 1 expression at the 10 somite stage occurred 20 hours after formation of the first somite pair. Therefore, Mll2 function is not required for initial expression of mox1 but is soon required to maintain it. The role of Mll2 to sustain expression of specific homeotic transcription factors supports the model of epigenetic maintenance. According to this model, the expression of certain genes can be divided in two different phases. First, the *establishment phase* produces the specific expression pattern of a gene, which is in part initiated by the presence of transcription factors and DNA binding proteins. Second, the *maintenance phase* epigenetically “locks” the active state of the gene and preserves the specific gene expression. The maintenance of expression therefore becomes independent of the initiating factors, which are often transiently available. The mechanism of maintenance is not well understood, but probably involves alteration of methyl marks on histone tails, which subsequently recruit activators of transcription and modify chromatin towards an “active state”. Mll2 methylates histones and is probably a major component in a conserved pathway to maintain Hox expression, presumably by counterbalancing the heterochromatic effects of the Pc-G genes.

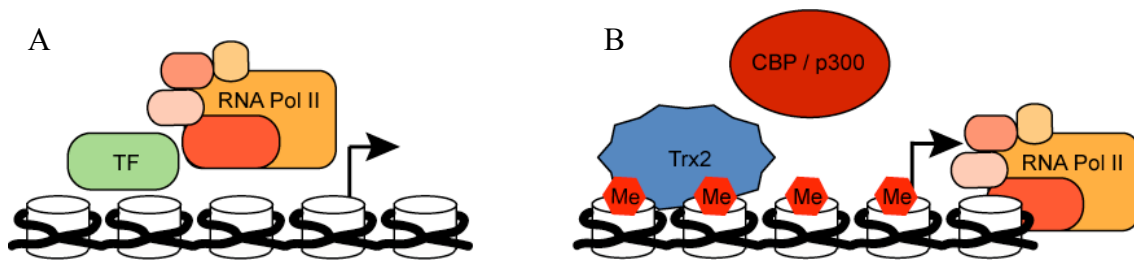


Fig. 54 (A) The “establishment phase” produces the specific expression pattern of a gene, which is in part initiated by the presence of transcription factors and DNA binding proteins at the promoter and recruitment of the basal transcription machinery. (B) The “maintenance phase” is characterized by recruitment of epigenetic regulators like Trx2/Mll2 that subsequently “locks” the active state of the gene. Due to this mechanism, the established expression pattern is preserved even in absence of the initiating factors. The mechanism of maintenance is not well understood, but probably involves alteration of methyl marks on histone tails, and/or recruitment of activators of transcription i.e. the histone acetyltransferases CBP/p300.

During embryogenesis, *Hoxb1* expression starts at E7.5 and is subsequently lost in *Mll2* mutants at E9.5. As this is when morphological abnormalities are first observed, it is likely that they are an effect of the loss of expression of this and several other potential target genes. However, it is not clear whether the embryonic lethality is a consequence of the specific defect in maintenance of homeotic genes. Alternatively, the increased apoptosis could perturb unspecifically and cause a lagging of development, which culminates in lethality. We tested this possibility by induced mutagenesis of *mll2* in conditional embryos. Pregnant females were induced at various stages (E4.5 to E 19) by tamoxifen gavage, which produced recombination efficiencies in embryos of up to 100%. Consequently, we obtained litters where all embryos were mutants (6-12 embryos) as opposed to the conventional approach where intercrosses of heterozygous mice yield 25% mutants per litter (1-3 embryos). We propose that a variation of this approach where induction is performed at fertilization (if possible) could greatly facilitate the analysis of any embryonic lethal phenotype. The earliest time of induction in our analysis was E4.5, which presumably results in full recombination at E5.5 and complete absence of *mll2* protein between E6.5 and E7.5. Induced embryos dissected at E10.5 fully recapitulated the *mll2* null allele phenotype. Consequently, the absence of Mll2 from E6.5 is sufficient to recapitulate the null phenotype and indirectly indicates that the protein is dispensable until gastrulation. Moreover, the delayed removal of *mll2* protein in induced embryos did not change their phenotype compared to null embryos.

Clearly, this excluded a nonspecific, cumulative deficiency and indicated a specific requirement for *mll2* function between E7.5 and E11. As *mll2* is dispensable in adults, we performed further inductions at E7.5, E12.5 and E16.5 and dissected embryos 5 days later. Surprisingly, none of the induced conditional mutants had any morphological abnormalities. The induction at E7.5 presumably leads to absence of the protein between E9.5 to E10.5, therefore the essential Mll2 function could be restricted to the period from E7.5 to E10.5. However, it remains to be investigated if embryos induced at E7.5, which are viable at E11.5, develop to term and are born as healthy pups.

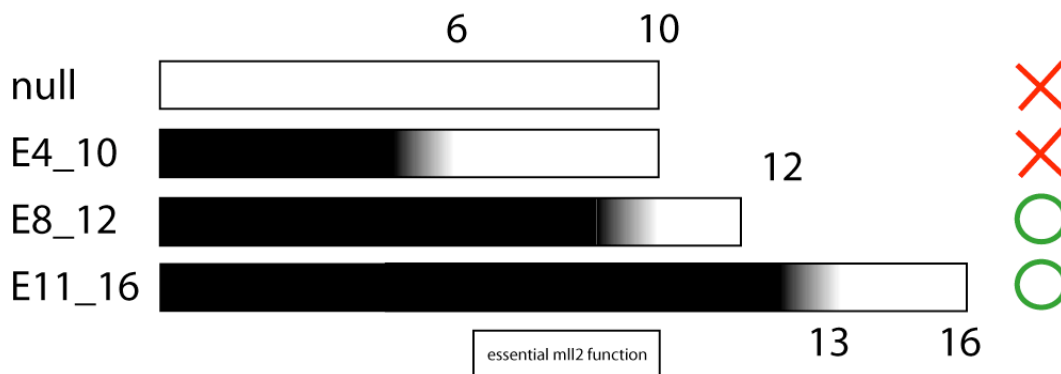


Fig. 55 Presence of *Mll2* protein during embryogenesis of null mutants and induced mutants. E4_10: Tamoxifen gavage of pregnant females at E4 results in absence of *mll2* protein at E6. Dissections at E 10 revealed an identical phenotype as null mutants (red cross). Inductions at E8 and E 11 result in absence of *mll2* protein at E12 and E16, respectively. Dissections of these embryos 5 days after induction revealed no abnormalities compared to control embryos (green cross).

In adults, mutagenesis of *mll2* did not cause any detectable abnormalities during their lifetime. Therefore, Mll2 function is dispensable in most tissues. However, both males and females were sterile after induction. The infertility of males was caused by apoptosis of spermatogonia, which indicated an essential function of Mll2 in this cell type. Other unipotent stem cells located in the gut epithelium, skin and bone marrow were not affected. Circulating WBC were fully recombined and therefore originated from *mll2*^{-/-} haematopoietic stem cells. Furthermore, histological analysis of the gut epithelium revealed no increased apoptosis after induction. The relatively mild phenotype could be a result of functional compensation from other epigenetic regulators or might indicate the presence of different parallel regulatory pathways, which for Mll2 would most likely be the close homologue Mll.

ES cells	MEFs	fetal (until E11)	adult
dispensible	dispensible	essential	dispensible in most tissues essential in spermatogonia
apoptosis	apoptosis?	apoptosis	apoptosis in spermatogonia but no other unipotent stem cells (gut epithelium, skin, bone marrow)
Mll2 ^{-/-} differentiate : neural cells cardiomyocytes		increasing growth retardation from E7.5 no morphological abnormalities until E8.5 morphological abnormalities from E9.0	Infertility
reduced <i>hoxb1</i> expression (50%)	reduced <i>mox1</i> expression ?	specific loss of expression: <i>hoxb1</i> , <i>mox1</i> , <i>six3</i>	Specific loss of expression in spermatogonia not yet identified

Fig. 56 *Mll2* phenotype in ES cells, mouse embryonic fibroblasts (MEF), embryonic development and adult mouse.

4. Methods

4.1 DNA methods

4.1.1 Restriction enzyme digestion

DNA fragments are cleaved with commercially available restriction enzyme. For calculation of the amount of enzyme, the following rule is applied: 1 unit of restriction enzyme cuts 1 µg DNA within 1 hour.

Every enzyme is used with its corresponding buffer in 1x concentration. The optimal temperature and further information about conditions for every digest is gathered from the *New England Biolabs* (NEB) catalogue. Incubation is at least 1 hour.

x µl DNA (1 – 10 µg)
2 µl NEB buffer
1 µl restriction enzyme
add to 20 µl with sterile water

4.1.2 Ligation

DNA ligations were set up by mixing vector and insert DNA (insert in three fold molar excess to vector) in a volume of 10 µl with one unit DNA T4 ligase and the buffer suggested by the supplier. The reaction was incubated at 16°C for 1 hour or o/n. The ligation is ATP dependent, which is supplied in the 10x buffer. 10x buffer was stored at – 20°C and replaced by a fresh vial after 1-2 years.

x µl fragment DNA
y µl vector DNA
add to 8 µl with sterile water
1 µl 10x buffer
1 µl T4 Ligase

4.1.3 Transformation of chemical competent *E.coli* cells

- Thaw competent cells on ice.
- Add about 10ng DNA in 5 µl H₂O.
- Leave 15 min on ice.
- Heat shock 100s at 42°C.
- Leave the tubes for 4 min on ice then add 800µl LB-media
- For Ampicilin: 0 to 30 min at 37°C shaking at 12000 rpm
- For Kanamycin: 60 min at 37° C shaking at 12000 rpm
- Spin down 4000 rpm for 4 min at RT.
- Take off 850µl, resuspend cell pellet in the remaining 150µl and plate on agarose plates containing the appropriate selection marker.

4.1.4 Preparation of chemical competent *E. coli* cells

- Grow cells on agar plate (e.g. XL-1 blue on tet)
- start from single colony
- grow a 5 ml o/n culture
- inoculate 4 ml into 200 ml LB medium [30 µg/ml] Tet
- Grow to OD₆₀₀ = 0.35
- spin 10 min. at 3000 rpm at 4°C (e.g. 4 x 50 ml Falcon tubes)
- resuspend pellet in 40 ml icecold buffer (4 x 10 ml per tube)
- 2nd spin 10 min. at 3000 rpm at 4°C
- resuspend in 20 ml icecold buffer + 800 µl DMSO (4 x 5 ml per tube)
- divide into 200 µl aliquots and snap freeze in liquid N₂

100 ml 2x Zout

12 ml 1M CaCl₂ (147 g/mol)

8 ml 1M KAc (98 g/mol) Potassium acetate

30 g Sucrose

Adjust pH with acidic acid to 5.6 – 5.9 (2 drops of 1M)

Filter sterile and keep at –20°C

Buffer (prepare fresh)

30 ml 2x Zout

5.4 ml 0.5M MnCl₂

0.72 g RbCl (Rubidium chloride)

24.6 ml water

4.1.5 Mini preparation of plasmid DNA

- Transfer 1 ml of o/n culture into an Eppendorf tube.
- Spin 2 min at 16,000 x g at RT, remove supernatant and resuspend the bacterial pellet in 200 µl P1 buffer.
- Add 200 µl P2 buffer, mix by inverting.
- Add 200 µl P3 buffer, mix by inverting.
- Leave 15 min at RT to let the RNase in P1 work, then cool 5 min on ice.
- Spin at 16,000 x g for 3 min.
- Transfer supernatant, containing plasmid DNA, into a 2- ml Eppendorf tube.
- Add 30 µl (5% vol.) P3 for precipitation
- Precipitate DNA to remove residual salt by adding 900 µl isopropanol, invert
- Spin 10 min at 16,000 x g at RT
- Wash pellet with 70% ethanol
- Dry pellet for 5 min
- Resuspend in 50 µl water or TE and use 10 µl for analytic restriction digests.

P1 buffer:

50mM Tris-HCl, pH 8

10mM EDTA

100 µg/ml RNase A

P2 buffer:

200mM NaOH

1% SDS

P3 buffer:

3 M potassium acetate

4.1.6 Maxi preparation of plasmid DNA

The principle of this method is based on alkaline lysis of the bacterial cell, followed by binding of the plasmid DNA to an anion-exchange resin under appropriate low-salt and pH conditions. RNA, proteins and low-molecular-weight-impurities are removed by a medium salt wash. Plasmid DNA is eluted by a high salt buffer, and then concentrated and desalted by isopropanol precipitation.

- Inoculate a starter culture of 200 ml LB medium, containing the appropriate selective antibiotic, and grow o/n at 37°C, shaking 300rpm.
- Harvest the bacterial cells by centrifugation 6,000 x g for 10 min at 4°C (Beckman JLA 16.250 250 ml)
- Resuspend the pellet in 10 ml buffer P1.
- Add 10 ml buffer P2, mix gently by inverting, then incubate at RT for 5 min
- Add 10 ml buffer P3. Mix immediately by inverting, then incubate on ice for 20 min
- Separate aqueous phase from precipitate by pouring through a filter (Falcon) funnel.
- Equilibrate the QIAGEN-tip 500 by applying 10 ml QBT buffer (1/3 of column), and allow the column to empty by gravity flow.
- Apply the supernatant to the column and let it enter by gravity flow
- Wash twice with 30 ml QC buffer (1 column vol.), then elute DNA with 15 ml buffer QF.
- Precipitate DNA by adding 10.5 ml (= 0,7 volumes) isopropanol to the eluted DNA.
- Mix and spin 30 min at 15,000 x g at 4°C (Beckman JS 13.1 30ml Corex glass tubes with adaptor)
- Wash pellet with 70% ethanol, and spin at 10,000 x g for 10 min.
- Dry the pellet and dissolve the DNA in 300 µl TE, adjust to [1 µg/µl]

QBT buffer:

750mM NaCl

50mM MOPS

15% isopropanol

0.15% triton X-100

QC buffer:

1 M NaCl

50mM MOPS

15% isopropanol

QF buffer:

1.25 M	NaCl
50mM	Tris, pH 8.5
15%	isopropanol

4.1.7 Maxi preparation of BAC DNA

For purification of large amounts of BAC (Bacterial artificial chromosomes), a modified version of the protocol described in section 4.1.6 was used. The amount of buffers P1, P2 and P3 were duplicated (20ml instead of 10ml each). The elution buffer QF was heated to 65°C before elution of DNA. For cloning purposes, this method yielded BAC DNA of sufficient quality. However, if BAC DNA is used for ES cell electroporation (targetings and stable lines), a purification by CsCl centrifugation is highly recommended.

4.1.8 DNA precipitation

- Add sodium acetate to a final concentration of 0.3M, mix by inverting.
- Add to a final concentration of 70% ethanol, mix by inverting.
- Spin 15 min at 16,000 x g 4°C
- Decant the supernatant and wash pellet with 70% ethanol.
- Spin 15 min at 16,000 x g at 4°C, decant supernatant.
- Dry the pellet and resuspend in an appropriate volume of H₂O or TE.

4.1.9 Phenol-Chloroform extraction

To remove proteins from your DNA mix, the sample has to be phenol extracted. After adding phenol/chloroform and mixing, proteins will enter the organic phase, while DNA will stay in the aqueous phase.

- Add 1 volume phenol/chloroform/isoamylalcohol (25:24:1) and vortex for 10s.
- Spin 5 min at 16,000 x g at RT
- Transfer upper water-layer into new tube and ethanol-precipitate.

4.1.10 Agarose gel electrophoresis

DNA molecules become orientated in an electric field and migrate through a gel matrix (in this case agarose) at rates that are inversely proportional to the size of the linear fragment. Larger molecules migrate more slowly because of greater frictional drag and because they find their way through the pores of the gel less efficiently than smaller molecules.

The gels used contained 0.4% to 3 % agarose. Low agarose concentrations are suitable for separation of large fragment sizes, while higher concentrations were used for small fragments. Higher agarose concentrations yield sharper bands and are preferable if small size differences have to be resolved.

Linear fragment size	% agarose
30 kb to 15 kb	0.4 %
15 kb to 1 kb	1 %
2.5 kb to 0.1 kb	2 %
< 100 bp	3 %

DNA samples were mixed with 1x DNA loading buffer, gels were run at 100 Volts (5 –10 V/cm). DNA was visualized by 20ng/ml ethidium bromide.

For small gel electrophoresis, 1xTBE (Tris-borate) was used as running buffer. Gel volume was 50 ml and running buffer volume 200 ml.

For large gel electrophoresis, 1xTAE (Tris-acetate) was used as running buffer. Gel volume was 350 ml and running buffer volume 2 liters.

10x DNA loading buffer:

25% Ficoll
100mM EDTA
BFB and XCF

TBE (0.5x):

0.45 M Tris
0.45 M boric acid
1mM EDTA (pH8)

5x TBE:

54 g Tris
27.5 g boric acid
20 ml 0.5M EDTA (pH 8)
add to 1 liter

TAE (1x):

40 mM
1 mM EDTA

50x TAE:

Tris 242 g Tris
57 ml glacial acetic acid
100 ml 0.5M EDTA (pH 8)
add to 1 liter

4.1.11 Polymerase Chain Reaction (PCR)

The PCR reaction is divided into 3 steps:

1. Denaturation of the DNA template
2. Primer annealing
3. Polymerisation

All steps were performed in consecutive cycles in a *Stratagene* Robocycler PCR machine. The PCR product is a double stranded DNA, consisting of the region of the complementary strain between the flanking primers. For establishment of difficult genomic PCR reactions, MgCl concentration where varied and DMSO was added. Used DNA concentrations are crucial, as genomic PCR reactions are inhibited when too much template is used. Moreover, Phenol extraction of DNA prior to PCR improved results.

PCR mix:

5 µl	10x PCR reaction buffer
2.5 µl	1.2 mM dNTP (stock 25mM ; 4x 10 µl [100mM] A/C/T/G in 360 µl water)
(2.5 µl)	(optional 5% DMSO)
0.5 µl	1µM antisense/sense primer (stock [100 pmol/µl])
x µl	10 ng – 200 ng template DNA
0.5 µl	2.5 units Taq polymerase
add to 50 µl with sterile water	

Reaction conditions vary among different experiments, but are usually conformed to the following cyclic pattern: 1 min initial denaturation at 94°C, 35 cycles consisting of 1 min denaturation at 94°C, 1 min annealing at the relevant temperatures (depending on the primer composition) and variable times of extension at 72°C depending on the size of the PCR product. The last cycle was 10 minutes of additional extension at 72°C.

4.1.12 PCR product purification

For extraction PCR products were loaded on an agarose gel and extracted with the agarose gel extraction kit from *QIAGEN*. DNA fragments ranging from 80bp to 10 kb binds to silica-membrane of the columns in the presence of high salt concentrations. Short oligos (most primers), nucleotides, salts and polymerases pass through during washing steps, while the PCR product is eluted from the column with TE or water.

- Excise the band from the gel using a UV plate and a blade. (Protect from UV light with goggles and gloves and minimize time of exposure of DNA)
- Weigh the gel piece and add 3 volumes PB buffer
- Shake 10 min at 55°C
- Apply on column and spin 30 sec at 10,000 x g.
- 2x wash with 750 µl PE buffer, discard flow-through
- Spin once more after removal of 2nd wash
- Place QIAquick into a clean 1.5-ml eppendorf tube, add 50 µl TE, let stand for 5 min and spin 10,000 x g for 30 sec to elute DNA.

4.1.13 Cloning of PCR products and DNA fragments

Purified PCR products or DNA fragments were cloned with the TOPO-TA cloning kit (Invitrogen) using a modified protocol provided by the supplier. The ligation reaction was incubated for 5 min. at room temperature and transformed in *E. coli* cells as described in section 4.1.3. We reduced the volume of used pCR-TOPOII vector from 1 µl to 0.2 µl per ligation reaction.

1 to 4 µl DNA
1 µl salt solution
0.2 µl pCR-TOPOII vector
add to 6 µl with water

- incubate 5 min at RT before transformation

4.1.14 DNA extraction from ES cells

- Remove media from confluent layer of ES cells in 24-well plate. This will yield about 30-40 µg genomic DNA.
- Add 500 µl lysis buffer and incubate o/n at 37°C.
- Take the 500 µl cell lysate and transfer into 1ml-tubes
- Add 500 µl phenol/chlorophorm/isoamylalcohol (25:24:1) and rotate 1 hour on a rotating drum
- Spin for 10 min at 10,000 x g at RT, transfer 500 µl aqueous phase into new tube
- Add 500 µl Chlorophorm and rotate 1 hour on a rotating drum
- Spin for 10 min at 10,000 x g at RT, transfer 500 µl aqueous phase into new tube
- Add 25 µl P3 / 400 µl isopropanol, mix, and take of supernatant (without spin)
- Wash with 70% Ethanol and spin 5 min at 10,000 x g at RT
- Take off supernatant and let pellet dry for not longer than 2-5 min
- Add 100 µl TE and incubate for 2 hrs at 37°C with gentle shaking
- The average DNA concentration should be 0.5-1 µg/µl

Lysis buffer:

50mM Tris-HCl, pH 8

100mM EDTA

100mM NaCl

1% SDS

just before use add 0.5 mg/ml Proteinase K

Proteinase K stock:

dissolve 100 mg Proteinase K in 10 ml water, aliquot at 1 ml and store at -20 °C.

4.1.15 DNA extractions from mouse tails

- Add 400 µl lysis buffer to the mouse-tail and incubate at 55°C o/n
- Add 400 µl phenol/chlorophorm/isoamylalcohol (25:24:1) and incubate in a rotating wheel for one hour.
- Spin 9,300 x g for 10 min at RT.
- Transfer supernatant into new tube, add 400 µl chlorophorm and incubate again for one hour in a rotating wheel.
- Spin 9,300 x g for 10 min at RT.
- Transfer supernatant into new tube and add 3M potassium acetate, pH5.5 to 5%.
- Mix and add isopropanol to 70-80%. Shake hard by hand to precipitate DNA and let the DNA sink to the bottom of the tube.
- Take off supernatant and wash pellet with 70% Ethanol.
- Spin 9,300 x g for 5 min at RT.
- Discard supernatant. Remove excess liquid by pipetting and air-dry for 2-5 min.
- Resuspend DNA pellet in 200 µl TE and incubate for 2 hrs at 37°C with gentle shaking
- The average DNA concentration from 0.5 cm tail cuts should be 50 - 200 ng/µl.

4.1.16 Southern analysis

For southern blot analysis, restriction digested DNA is separated on a standard agarose gel and transferred onto a nylon membrane. The membrane can be hybridised with a radiolabelled probe that binds a specific DNA fragment. Southern blotting was carried out with genomic DNA to verify homologous integration of the *mll2* targeting construct into the genomic *mll2* locus, and to assess cre recombination efficiencies of the conditional *mll2^F* allele. Furthermore, southern blotting of plasmid DNA, cosmid DNA, or BAC DNA was used for restriction digest mapping and verification of cloning procedures.

- Digest 7-10 µg of genomic DNA with the desired restriction enzymes o/n
x µl DNA
6 µl NEB buffer
6 µl restriction enzyme
add to 60 µl with water
- Adding 2 x 3 µl restriction enzyme (morning and evening) improves digest efficiency. Essential for good genomic southern results is the use of ideal restriction enzymes, which are not blocked by CpG methylation. Good enzymes are EcoRI, PstI, KpnI, and NcoI.
- Add 1x gel running buffer and load onto a 0.7% TAE gel
(No EtBr in the agarose, EtBr may be added before loading to the marker)
- Run gel 24 hours at 20 - 40 V in 1x TAE at 4°C
- Take a picture under UV light with a ruler aligned next to the marker
- (Depurinate 20 min in HCl, often decrease quality)
- Denature gel 2x 15 min in 0.4M NaOH
- Neutralize 1x 20 min in 10x SSC
- Label nitrocellulose membrane (0.45 µm), wet in water then 10x SSC
- Blot onto a nitrocellulose membrane in 10x SSC o/n.
- Mark slots with pencil on the membrane, **rinse in 6x SSC** and vacuum dry for 2 hours at 80°C

Depurination solution

37% HCl 10 ml
add water to 1 liter

Denature solution

NaCl 87 g
NaOH pellets 20 g
add to 1 liter

Neutralisation solution

NaCl 87 g
Tris 121 g
37% HCl appr. 50 ml

20x SSC

NaCl 175 g
tri-Sodium citrate dihydrate 88 g

add to 1 liter with water

Radioactive DNA probe:

- Use the random primed DNA labeling kit (*Roche*)
- Use 50-100 µg DNA fragment and add vol. to 11 µl with water
- Denature 10 min at 100°C and subsequent cooling on ice.
- Add 4 µl High prime (enzyme, primer, and nucleotide mix, Roche)
- Add 5 µl [$\alpha^{32}\text{P}$]dCTP (50 µCi)
- Incubate for 60 min at 37°C.
- Spin (5 min) a G-50 sephadex column inserted in a cut 2 ml Eppi in a 12 ml Falcon
- Load 20 µl reaction volume
- Spin 5 min at 16,000 x g at RT.
- Collect flow through from Eppendorf tube and determine volume (50 to 200 µl)
- Measure activity of 1 µl and calculate total activity (usually 1 - 5 x 10⁷ CpM)
- For hybridization, use about 2x10⁷ counts per 10x10 cm membrane

Radioactive RNA probe:

A T3 or T7 polymerase reaction with radioactive labeled dUTP is used to transcribe an RNA-probe from a DNA fragment.

- Digest 5 µg plasmid DNA with the appropriate restriction enzyme
- For antisense probe use a cutting site on the 3' end and the polymerase transcribing from the 5' end of the insert
- Extract DNA with Phenol/Chloroform and check an aliquot on an agarose gel

Transcription-mix: 1µg linearized DNA
 1x transcription buffer (Stratagene)
 1mM rATP, rGTP, rCTP
 60 µCi UTP³²
 5 units RNAsin
 5 units T3 or T7 Polymerase

- Incubate at 37°C for 15 min.
- Add 5 units RQ-DNAse to destroy the template for transcription
- Incubate at 37°C for 15 min
- Measure activity

Hybridisation

- Wet the membrane in 25mM NaHPO₄ and roll it into a glass tube.
- Add 10 ml Hybridisation buffer to the tube and pre-hybridise for 30 min in a turning oven at 72°C for RNA probes, at 64 to 67°C for DNA probes.
- Denature the probe for 5 min. at 95°C and add to the tube
- Hybridize o/n.
- For washing, prewarm wash buffer on heater to 55°C (Thermometer!)
- 1st wash rinse briefly
- 2nd and 3rd wash (usually 30 min.) according to radioactive radiation

- (should be below 5 CpM similar to background count)
- Wrap membrane in saran and expose 24 hours on phosphorimager plates, 2 to 14 days on Kodak MR films in a film cassette at -70°C

1M Hybridization stock (Church)

Sodium hydrogen phosphate (Na_2HPO_4)	71 or 89g
Adjust pH to 7.2 with Phosphoric acid (H_3PO_4)	2-3 ml

1x Hybridisation buffer:

250mM Na_2HPO_4 pH 7.2	50 ml 1M stock
7 % SDS	35 ml 20% stock
water	15 ml
1% BSA	1 g
1mM EDTA	100 μl 0.5M stock

wash buffer:

20mM NaH_2PO_4 pH 7.2	40 ml 1M stock
1% SDS	50 ml 20% stock
1mM EDTA	2 ml 0.5M stock
	add to 1 liter with water

20% SDS:

(Wear a mask for weighting SDS powder)
Dissolve 200 g SDS o/n in 1 liter water

4.1.17 ET cloning

In *E.coli*, the classical homologous recombination pathway involves RecA as a strand invasion protein and the RecBCD complex as the major cellular exonuclease. Since RecBCD also plays a role in recognition and destruction of foreign linear DNA, it is impossible to introduce a linear fragment of DNA for homologous DNA engineering. Hence homologous recombination in *E.coli* has proven to be a difficult process.

The alternative to the recA based pathway is ET/Red recombination developed by Zhang et al. in 1998. Homologous recombination is initiated by either of the two functionally equivalent protein pairs: RecE/RecT from the λ phage and Red α /Red β from the λ phage (Zhang et al., 1998; Muyrers et al., 1999). RecE and Red α are 5' \rightarrow 3' exonucleases, while RecT and Red β are DNA single strand annealing proteins (Muyrers et al., 2000). They serve to circumvent both RecA and RecBCD whereas RecBCD-strains can be used. Alternatively, Rec BCD can be inhibited by expression of the Red γ protein so that use of linearized DNA is possible.

In the fundamental reaction, a linear DNA molecule carrying a selectable marker flanked by 40-60 bp regions of sequence homologous to the desired integration location on a circular DNA molecule. The recombinogenic, linear DNA fragment can be generated by PCR with oligonucleotides containing 3' the PCR primer sequence and 5' the 40-60 bp homology arm.

ET/Red recombination has proven to be successful in cloning of regular plasmids, BACs and the *E. coli* chromosome with a very high efficiency rate. In this thesis ET cloning was applied to modify the knock out cassette for Trx2 and for the creation of the EYFP-Trx2 targeting cassette.

PCR reaction and recipient plasmid DNA preparation

- PCR mix:

10-20 ng	template DNA
1 μ M	5' primer and 3' primer each
1x	PCR reaction buffer (Roche)
0.2mM	dNTP
2.5 units	Taq polymerase (Roche)
fill up with dH ₂ O to 50 μ l final volume	
- Perform PCR in Stratagene robocycler:
- PCR protocol:

3 min 94°C	1 min 94°C	
	40 sec 62°C	
	1 min 72°C	35 cycles
	10 min 72°C	
- Pool PCR products, add 400 U DpnI, 1x NEB-buffer4 and fill up with dH₂O to 150 μ l volume.
- Perform DpnI digest at 37°C for two hours to remove residual template DNA.
- Ethanol-precipitate digestion-mix and resuspend in 10 μ l dH₂O.
- For cotransformation extract recipient plasmid DNA with Phenol/Chlorophorm and resuspend in in dH₂O at 1 μ g/ μ l.

Preparing electro-competent cells

- Prepare 10% glycerol with dH₂O, and cool down for at least three hours before usage.
- Grow 5 ml o/n cultures of DH10B-YZA cells in 5 μ g/ml tetracycline.
- Make a hole in the lid of an eppendorf tube and dilute o.n culture 1:50 in 1.4 ml fresh selective medium.
- Grow for 2 hrs at 30°C with shaking to an OD₆₀₀ of 0.2.
- Add arabinose to a concentration of 0.1-0.2%.
- Transfer to 37°C and continue growing for about one hour until cells reach log phase (OD₆₀₀= 0.35-0.4).
- Spin down the cells at 11,200 x g for 30 sec at 4°C.
- Discard the supernatant, place the tube on ice and resuspend pellet in 1 ml icecold 10% glycerol.
- Spin down the cells at 13,400 x g for 30 sec at 4°C.
- Discard the supernatant, place the tube on ice and resuspend pellet in 1 ml icecold 10% glycerol.
- Spin down the cells at 13,400 x g for 30 sec at 4°C.
- Discard the supernatant, leaving 20-30 μ l to resuspend pellet in the remaining solution.
- Use cells immediately for best transformation efficiency or snap freeze in liquid N and store at -80°C.

Electro-Transformation

- Precool 1-mm-cuvettes on ice for 5 min.
- Thaw electrocompetent and arabinose-induced cells on ice (or use them straight after preparation). Add 1 μ l PCR product (corresponds to 2-3 μ g/0.2-0.3 pmol) and 1 μ l recipient plasmid (corresponds to 1 μ g/0.1-0.2 pmol).
- Co-Electroporate the cells at 1200 V.
- Immediately add 1 ml LB medium and transfer back into eppendorf tube.
- Incubate at 30°C for 70 min shaking at 1200rpm.
- Spin at 5000 rpm for 2 min, aspirate the supernatant, but leave 100 μ l liquid.
- Resuspend the cells in the remaining liquid, plate on appropriate antibiotic and incubate o/n at 37°C.

4.2 RNA methods

4.2.1 Diethylpyrocarbonate (DEPC) – treated water

- Add 1 ml of DEPC to 1 liter of water (0.1% solution), use up opened aliquot (hydrolyzes quickly and can therefore not be stored)
- Let stand for 1 hour at 37°C or o/n at RT and autoclave 15 min at 15 psi on liquid cycle

Glassware and plasticware should be filled with fresh 0.1% DEPC and allowed to stand o/N at RT.

4.2.2 Total RNA extraction from cells

- Grow ES on 10-cm-dish to confluence.
- Wash once with PBS, add 1 ml TRI REAGENT™ and collect cell lysate with a sterile cell scraper. Pass several times through a pipette to form a homogenous lysate.
- Let samples stand for 5 min at RT.
- Add 0.2 ml chlorophorm per ml of TRI REAGENT™
- Shake vigorously for 15 sec and allow to stand for 2-15 min at RT
- Centrifuge 15 min at 12,000 x g for at 4°C. Centrifugation separates the mixture into 3 phases: a organic phase containing protein, an interphase containing DNA, and a colorless upper aqueous phase containing RNA.
- Transfer the aqueous phase to a fresh tube and add 0.5 ml isopropanol per ml of TRI REAGENT™
- Mix and let sample stand for 10 min at 4°C.
- Centrifuge 10 min at 12,000 x g at 4°C.
- Remove the supernatant and wash the RNA pellet by adding 1 ml 75% Ethanol per ml of TRI REAGENT™ used.
- Vortex the sample and centrifuge for 5 min at 12,000 x g at 4°C.
- Samples can be stored in ethanol up to one year at -20°C.
- Air-dry the RNA pellet for 5 min. and resuspend in 50 µl RNase free H₂O and store at -80°C

4.2.3 Total RNA extraction from tissue

- Use 100 mg tissue and cut into little pieces with scissors
- Add 1 ml TRI REAGENT™
- Let samples stand for 5 min at RT.
- Add 0.2 ml chlorophorm
- Shake vigorously for 15 sec and allow to stand for 2-15 min at RT
- Centrifuge 15 min at 12,000 x g for at 4°C
- Transfer the aqueous phase to a fresh tube and add 0.5 ml isopropanol
- Mix and let sample stand for 10 min at 4°C.
- Centrifuge 10 min at 12,000 x g at 4°C.
- Remove the supernatant and wash the RNA pellet with 1 ml 70% Ethanol
- Vortex the sample and centrifuge for 5 min at 12,000 x g at 4°C.

- Air-dry the RNA pellet for 5 min. and resuspend in 50 µl RNase free H₂O and store at -80°C

4.2.4 Northern blotting

- Pour a 1.2% agarose gel:
Use 150 ml water with 2.4 g agarose in a 600 ml beaker
boil 3 – 5 min until dissolved (water vol. will decrease)
add 40 ml 5x formaldehyde running buffer
add 35.5 ml 37% formaldehyde (6 % final)
pour gel under hood
- Use 30µg total RNA per lane:

2 µl 5x
3.5 µl formaldehyde
10 µl formamide
x µl RNA
add to 27 µl with DEPC water
- heat 15 min. at 65°C then put on ice

2 µl RNA loading dye
1 µl EtBr [1 mg/ml] in DEPC
- Run gel in running buffer (1xMOPS) at 120 V for 2.5 hours
Let run until 2nd LD band is 8 cm before end of gel.
Do not use EtBr in lower samples if two combs are used. Alternatively stain gel in 0.5µg/ml Ethidiumbromide for 30 min, take picture and destain in H₂O for 30 min.
- Blot o/n in 300 ml 10x SSC in disposable plastic box on nitrocellulose membrane BiodyneB.
- Rinse membrane in 2x SSC.
- Air-dry on 3mm paper then vacuum bake for 3 hrs at 80°C

Hybridization

DNA probe on DNA: 65° C

DNA probe on RNA: 72° C

as described in section 4.1.13, or alternatively:

- Wet filter in 5x SSC and transfer to hybridization tube
- Prehybridize for 1-3 hrs at 42°C in 15 ml prewarmed Hybridization mix
- Remove and add 15 ml fresh prewarmed Hybridization mix
- Add denatured random primed DNA probe.
- Hybridize o/n at 42°C in a rotating wheel.
- Wash 15 min at RT in wash buffer 1, then 2x 20 min at 65°C in wash buffer 2.
- Expose to X-Ray film.

10x MOPS:

200mM MOPS	20.9 g MOPS
50mM Na-acetate	800 ml Na-acetate (DEPC !)
10mM EDTA	20 ml 0.5M EDTA
adjust pH 7.0 with NaOH	appr. 17 ml 2N NaOH (plastic pipett)

20x SSC:

3M NaCl	175 g NaCl
0.3M sodiumcitrat	88 g tri-Sodium citrate dihydrate
adjust with NaOH 10N to pH 7	add. to 1 liter with water

50x Denhardt:

1% Ficoll type 400
1% BSA fraction 5 in H ₂ O

LB stock:

10% Ficoll type 400
0.1% bromphenolblue in H ₂ O

Hybridization mix:

50% formamid
5x SSC
50mM NaP pH 6.5
8x Denhardt
0.5 mg/ml yeast RNA
1% SDS

RNA sample buffer:

53% formamide
6.7% formaldehyde
1x MOPS
18% L.B. stock

wash buffer1:

2x SSC
1% SDS

wash buffer2:

0.2X SSC
0.1% SDS

4.2.5 Reverse Transcription of RNA (cDNA synthesis)

A typical procedure uses between 1 ng – 1 µg total RNA or 10 pg – 1 µg mRNA.

- Mix in a sterile RNase-free tube:

2 µl Oligo(dT) [≅ 1 µg]
1 µg total RNA
add to 13 µl DEPC water

- Heat 5 min. at 70°C, than cool 5 min. on ice
- Add to the tube:

1 µl RNase out
5 µl 5x M-MLV RT reaction buffer
5 µl 10 mM nucleotide mix (A,C,G,T)
1 µl reverse transcriptase [≅ 200 units]

- Mix gently, spin down, and incubate 1 h at 37° to 40°C
- Stop reaction for 15 min at 70°C
- Add 1 µl RNase H and incubate 20 min at 37°C
- For RT-PCR use 1 µl per reaction

4.2.6 Quantitative RT-PCR with SYBR green

The SYBR green dye detects the absolute increase of DNA concentration during a PCR run. It is therefore essential to establish PCR assays that produce specific products, as unspecific amplification products or “smear” will produce a signal. Primers have to be designed according to the following priorities:

- 1) PCR product between 50 and 250 nucleotides
- 2) Identical annealing temperature (+/- 0.3°) of se and as primer (55-63°C)
- 3) Exclusion of primers with duplex formation above -5 kcal/mol
- 4) Annealing preferably in 3' UTR (efficiently reverse transcribed sequence)
- 5) Annealing in different exons to distinguish genomic DNA contamination

The amplification efficiencies ($1 \geq E$) of individual PCR assays have to be determined by serial dilutions of template covering at least 10-5 magnitudes (1:1 to 1:10000). If the efficiency of an assay is close to 1, than $X_n = X_o (1+E)^n$ can be simplified to $2^{-\Delta\Delta C_t}$ for quantification of results.

PCR reactions where pipetted in triplicates in 20 µl total volume at RT and spun briefly before the PCR run. Calibrators where assays for tubulin, GAPDH or Rpl19. Nontemplate controls (NTC) where used to detect primer duplex products. Rox dye served to normalize for dye degradation.

6 µl se/as primer (150-300 nM)
4 µl cDNA (1:4)
10 µl 2x SYBR green

Primer concentration:	Primer stock [100 pmol/µl]
300 nM	dillute 1:50
300 nmol/l	mix se and as 1:1 [1pmol/µl final]
300 pmol/ml	store at -20°
0.3 pmol/µl = 6 pmol/20 µl	

4.2.7 DIG labeling of RNA probe (cRNA synthesis)

Transcription efficiencies vary between different enzymes; SP6 RNA polymerase usually gives better yield than T7 or T3 RNA polymerases.

- Linearize (o/n) 5 µg of vector containing the probe in the polylinker on the opposite side of the RNA polymerase promoter used to transcribe as probe (3' – 5')
- Add 500 µl water and 500 µl phenol:chloroform and vortex 1 min
- Centrifuge 10 min at 13 g
- Take supernatant and add 500 µl chloroform
- Centrifuge 10 min at 13 g
- Take supernatant and precipitate DNA with 25 µl P3/400µl isopropanol
- Centrifuge 10 min at 13 g
- Wash pellet in 70 % EtOH
- Resuspend in 20 µl TE
- Use 1 µg DNA for *in vitro* transcription:

x µl DNA (1 µg)
4 µl 5x transcription buffer
1 µl RNasin
2 µl 10x DIG mix
Add to 18 µl with DEPC water
2 µl RNA polymerase

- Incubate 2 h at 37° C
- Add 2 µl DNaseI and incubate 15 min at 37° C
- Add 1 µl 0.5 M EDTA
- Precipitate with 5 µl 5M LiCl / 75 µl 100% EtOH at –20° C
- Centrifuge 10 min at 13 g and wash in 70% EtOH
- Resuspend big white pellet in 100 µl DEPC water + 3 µl RNasin
keep at –20°C
(Long term storage in hybridization buffer containing formamid)
- Check aliquot on a gel, usually for *in situ* use 8 µl per 1ml hybridization

4.2.8 Whole mount *in situ* hybridization on mouse embryo

Embryos should be fixed in methanol at least o/n before being used for *in situ* hybridization. All steps before hybridization with the probe should be carried out under RNase – free conditions. The Proteinase K digest is the critical step of the protocol and appropriate digestion times for individual probes have to be established.

- Dissect embryo rapidly in DEPC PBS/0.4 % BSA
- Fix 2 – 4 hours in 4% PFA
- 2x 5 min. PBT
- Store in 100% MeOH
- Transfer 5 min each in decreasing MeOH dillutions
100% > 75% > 50% > 25%
- 2x 5 min PBT
- (optional 1 hour 6% hydroxyn peroxide in PBT)
- 3x 5 min PBT

- Digest in 1:1000 Proteinase K solution (10µg/ml)

E6.5 10sec
E7.5 2 – 3 min
E8.5 5 – 7 min
E9.5 10 – 14 min

- Stop digest by transfer for 10 min in 1:10 glycine (2mg/ml)
- 2x 5min PBT
- Refix 20min PFA/glutaraldehyde (1ml PFA + 8µl GA)
- 3x 5min PBT
- 1x (1:1) Hybmix
- 1 – 3 hours in Hybmix at 65°C
- Heat probe 8 min at 80°C
- Hybridize o/n at 65°C
- 2x 30min sol1 at 65°C
- 1x 10min sol1/sol 2 at 65°C
- 3x 5min sol2 at RT
- 1 hour at 37°C in 1:1000 RNaseA (stock 100mg/ml)
- 1x 5min sol 2
- 1x 5min sol 3
- 3x 5min TBST
- 1 – 1.5 hours in 1% blocking solution/2mM levamisole at 4°C
- o/n in anti-DIG-antibody (1:1000) in 1% blocking solution/2mM levamisole at 4°C
- 3x 5min TBST/2mM levamisole at RT
- 5x 1 hour TBST/2mM levamisole at RT
- 3x 10min NTMT/2mM levamisole at RT
- Develop in dark in 1 ml NTMT/2mM levamisole (+ 3,5 µl NBT / 4.5 µl BCIP) at RT

4% PFA

Heat 200 ml PBS to 60°C

Add 8 g PFA

Add 2 drops 2N NaOH

filter and keep aliquots at –20°C

PBT (0.1% Tween20)

Add 500 µl Tween20 to 500 ml DEPC-PBS

Methanol (50ml)

75% 37.5 ml MeOH in 12.5 ml PBT

50% 25 ml MeOH in 25 ml PBT

25% 12.5 ml MeOH in 37.5 ml PBT

Hydrogen peroxydase (6% in PBT)

10 ml 30% hydrogen peroxydase

40 ml PBT store at 4°C

Proteinase K

Dilute stock [10mg/ml] 1:1000 in PBT

Glycine

Dilute stock [20 mg/ml] 1:10 in PBT

Deionized formamide

Mix formamide with Dowex XG8 mixed bed resin (BioRad AG 501-X8 Resin) and stirr with a magnetic stirrer for 1 hour.

Filter and keep aliquots at -20C

20x SSC

NaCl 175 g

tri-Sodium citrate dihydrate 88 g

add to 1 liter with DEPC water

10% SDS

Dissolve 10g SDS in 100 ml DEPC water

Hybridization buffer

25 ml deionized formamide

12.5 ml 20x SSC

5 ml 10% SDS

500 µl tRNA yeast [stock 100 µg/ml]

500 µl heparine [stock 5 mg/ml]

6.5 ml DEPC water

Solution 1 (50 ml)

25 ml formamide

12.5 20x SSC

5 ml 10% SDS

7.5 ml sterile water

Solution 2 (50 ml)

5 ml 5M NaCl

500 µl 1M TrisHCl pH=7.5

50 µl Tween20

44 ml sterile water

Solution 3 (50 ml)

25 ml formamide

5 ml 20x SSC

20 ml sterile water

TBST (100 ml)

2.8 ml 5M NaCl

250 µl 1M KCl

2.5 ml 1M TrisHCl pH=7.5
100 µl Tween20
93.5 ml sterile water

Blocking solution

Dissolve 1 g blocking reagent (Roche 1 096 176) in 100 ml TBST. Heat to 70°C and mix with a magnetic stirrer, than filter through a paper filter. Add 50 mg [2 mM] levamisole before use.

4.3 Protein methods

4.3.1 Crude protein extracts

- Remove media from ES cell dish and wash once with PBS
- Add icecold PBS and collect cells with a sterile scraper. Wash plate once with icecold PBS and add to the collected cells.
- Spin 5 min 1000 rpm at 4°C, remove supernatant and resuspend cell pellet in 1 ml icecold PBS. Transfer to 2ml-Eppendorff tube.
- Spin 2 min 5,900 x g, remove supernatant, shock-freeze cells in liquid N. Store at -80°C.
- Add about 500 µl ml buffer E to frozen cell pellet (leave cells in liquid N until use) resuspend carefully and combine cell suspensions from same cell identity.
- Transfer solution into plastic vial filled to 70% with 1-mm-glass-beads (sterile), close lid without airbubbles
- Bead-beat for 30 sec at 5000 rpm then cool two min on ice. Repeat six times.
- Leave on ice, spin down at 16,000 x g for one min at 4°C.
- Take out 800 µl supernatant transfer to precooled polycarbonate thick wall ultracentrifuge tubes (6.5 ml /16x64 mm/Beckmann /355647) on ice.
- Add 500 µl cold buffer E, mix, spin again and add 500 µl supernatant to the corresponding ultracentrifuge tube.
- Ultracentrifuge 100,000 x g for 1 hour at 4°C in a MLA80 rotor.

Aliquot at 4°C and immediately shock freeze in liquid N. Store at -80°C. (Use approximately 40 µl protein extract from 10 x 15-m-plates for one small western gel)

Buffer E :

20mM HEPES pH 8.0

350mM NaCl

10% Glycerol

0.1% Tween 20

1% Proteinase inhibitor cocktail (Sigma) add freshly

2mM EDTA add freshly

4.3.2 Nuclear extracts

- Grow ES cell on gelatinized 10 cm plate without feeders.
- Trypsinize or collect cells with a sterile cell scraper and spin down cell pellet at 1000 rpm for 5 min (*Multifuge 3 S-R*, rotor 6445).
- Put cells on ice and resuspend in 1 ml extraction buffer without NP40 per 2-10 x 10⁶ cells. Add same volume NP40 buffer and mix carefully, leave on ice.
- Leave on ice for 20 min. (Clean nuclei are smooth and refract light. If nuclei are not released from cells try (i) douncing (loose fitting pestle) and/or (ii) pipetting up/down repeatedly through a small bore pipette)
- Spin down nuclei 1500 rpm for 5 min at 4°C.
- Remove supernatant and store nuclei pellet at -80°C.

Nuclei extracion buffer:

15 mM Tris-HCl pH 7.5

60 mM KCl

15 mM NaCl

5 mM MgCl₂

0.5 mM EGTA

300 mM Sucrose

1% NP40

add 0.5mM β -mercaptoethanol fresh before use

add 1% proteinase inhibitor cocktail fresh before use

add to 100 ml with water

4.3.3 Polyacrylamide gel electrophoresis (PAGE)

- Prepare stacking and running gel.
- Mix desired amount of protein extract with 3X PLB.
- Boil for 4-5 min at 99°C.
- Spin shortly and leave at RT until loading.
- Load protein samples onto prepared protein gel assembly with a Hamilton pipette and run gel at 80-150V for one to three hours depending on the protein size you wish to detect.

Stacking gel:

5% Acrylamide

125mM Tris pH 6.8

0.1% SDS

0.1% APS

0.1% TEMED

Running gel:

5-15% Acrylamide

375mM Tris pH 8.8

0.1% SDS

0.1% APS

0.04% TEMED

3X protein loading buffer:

250mM Tris

25% Glycerol

5% SDS

0.25% Bromphenolblue

4.3.4 Coomassie staining of protein gels

- Disassemble protein gel assembly and transfer protein gel to a box filled with staining solution. Incubate for five hours at RT or o/n at 4°C on a rocking platform.
- Remove staining solution wash once with H₂O and add destaining solution. Incubate for five hours at RT or o/n at 4°C on a rocking platform with

occasional renewal of destaining solution, until the gel has reached the desired staining intensity.

Staining solution:

45% methanol
10% glacial acetic acid
1 g/L Coomassie R250
in H₂O

Destain solution:

30% methanol
10% glacial acetic acid
in H₂O

4.3.5 Western analysis

For detection of standard protein-antibody detections without requirement for extraordinary sensitivity, this basic western protocol was used. Here polyclonal antibodies against K4-dimethylated histone H3 were bound by a secondary antibody anti-rabbit peroxidase. The ECL mix used after the second antibody binding reacts with the peroxidase group and produces chemiluminescence, which can be detected on a normal Kodak film.

- If nuclei extract is the desired starting material, use nuclei pellet from one 10-cm-dish. Add – NP40 buffer to a concentration of 10⁵ cells/μl. Use about 5x 10⁵ cells for loading.
- If protein extract is the desired starting material, use desired protein amounts for loading.
- Add 3x protein loading buffer and load on a large Polyacrylamid gel.
- Run o/n 80V at 4°C (or 4 hours 175V) until the blue front is just leaving the gel.
- Blot for 45 min, 15V in a semi-dry blotter.
- Incubate in blocking buffer for two hours at RT (or o/n at 4°C).
- Add primary antibody (K4H3 1:1000, Actin 1:2000) in blocking buffer and incubate for one hour at RT.
- Wash three times five min in PBS/0.1% Tween
- Add secondary antibody (anti rabbit 1: 2000) in blocking buffer and incubate for one hour at RT.
- Wash once with PBS/Tween for 10 min, then three times 5 min.
- Mix ECL solutions (Amersham) 1:1 and add to cover the membrane completely.
- Incubate for 5 min, drain on a piece of tissue and expose to X-ray film for 1-20 min.

Blocking buffer :

5% milkpowder
0.1% Tween in PBS

PBS/Tween :

0.1% Tween in PBS

4.4 Cell culture

4.4.1 Preparing Mouse Embryonic Fibroblast cells (MEFs, feeders)

All ES cell experiments were performed in feeder dependent 129 cell lines. To maintain their pluripotency in long-term culture, these ES cell lines should be grown on monolayers of mitotically inactivated fibroblast cells (Thomas and Capecchi, 1987; Leighton et al., 1995). Feeder cells are derived from mouse embryonic fibroblast tissue, expanded up to maximally 15 cell divisions and then inactivated by mitomycin treatment to prevent further cell divisions. Feeder cells are obtained from dissections of E 13.5 embryo

For cultivation feeder cells are thawed onto 0.1% gelatin coated Falcon plates and incubated at 37 °C, 5% CO₂. Cells were passaged one day after they reached 100% confluency (roughly every three days) by trypsinization. The original vial purchased by *Mediocre* was expanded to in total 21 15-cm-dishes before a 2-2.5 hour treatment with 10 µg/ml mitomycin. Those mitomycin treated feeder cells were frozen and upon need plated in 100% confluency (about 10⁶ cells) one day before seeding the ES cells.

Feeder -media:

10% Fetal Calf Serum
100 µg/ml penicillin/streptomycin
2mM L-glutamine
in DMEM high glucose

4.4.2 Expanding MEF cells

- Thaw original feeder vial onto gelatin coated 10-cm-dish. After one day, the plate should be 100% confluent. Change media and leave one more day in the incubator.
- Remove media and rinse plates with 1x PBS.
- Add 1x trypsin/EDTA (2 ml on a 10-cm-dish, 7 ml on a 15-cm-dish) and leave the plate at 37°C for 2 min. Immediately add feeder media to inactivate the trypsin.
- Pipet the suspension up and down to remove cell clumps.
- Transfer the suspension into a 15-ml-falcon tube containing media and spin 1000 rpm for 5 min at RT (*Multifuge 3 S-R*, rotor 6445).
- Aspirate supernatant and resuspend cells in media. Then split 1/3 and plate on new gelatin coated dishes.
- Repeat this procedure until you reach 21 times confluent 15-cm-dishes.

4.4.3 Freezing MEF cells

- Trypsinize cells from a confluent 15-cm-dish as described.
- After spinning down in media, resuspend cells from one plate in 0.5 ml media and cool down on ice for 5 min.
- Add 0.5 ml 2x freezing media and transfer to 1-ml freezing vials then freeze at -80°C.

- Transfer to liquidN the next day. This vial contains enough feeder cells to cover five 10-cm-dishes.

<u>2x freezing media:</u>		<u>1ml</u>	<u>4ml</u>
25%	Fetal Calf Serum	250 µl	1 ml
10%	DMSO	100 µl	400 µl
	in DMEM high glucose	650 µl	2.6 ml

4.4.4 Culturing mouse ES cells

Mouse embryonic stem (ES) cells are totipotent cells derived from the inner cell mass of 3.5 day blastocysts. They can be modified and reintroduced into blastocysts, giving rise to manipulated chimeric animals. (Thompson et al. 1989)

If they are held under certain growth conditions, they can also differentiate to various cell types. To avoid this, LIF serum is added to the ES medium. It suppresses differentiation, so that the silencing of genomic regions during the differentiation process is prevented.

For cultivation ES cells were thawed onto feeder coated 10-cm Falcon plates and incubated at 37 °C, 5% CO₂. After ES cells are thawed it is recommended to passage them every second day by trypsinization. Reseeding should be calculated in a way that the cells reach 100% confluency after 48 hours in culture.

For long-term storage ES cells are kept in liquid nitrogen in a cell density of 5×10^6 cells in freezing medium containing DMSO as a cryoprotectant. Since DMSO is harmful to cells it should contact ES cells as short as possible before and after freezing.

ES cell media:

15%	Fetal Calf Serum
100 u:µl/ ml	penicillin/streptomycin
100µM	non-essential amino acids
1mM	sodium acetate
1µM	β-mercaptoethanol
2mM	L-glutamine
600 U/ml	LIF “ESGRO”
	in DMEM high glucose

4.4.5 Harvesting ES cells

- Remove media and rinse plates with 1x PBS.
- Add 1x trypsin/EDTA (2 ml on a 10-cm-dish) and leave the plate at 37°C for 5 min.
- Pipet the suspension up and down to remove cell clumps.
- Transfer the suspension into a 15-ml-falcon tube containing ES media and spin 1000 rpm for 5 min at RT (*Multifuge 3 S-R*, rotor 6445).
- Aspirate supernatant and resuspend cells in 3-8 ml of ES media. Then plate out an appropriate fraction on a new dish. A rough estimate is that a confluent 10cm dish should yield $1-4 \times 10^7$ cells and approximately $1-5 \times 10^6$ cells should be seeded on a 10cm dish in 10 ml media.

4.4.6 Freezing ES cells

- Trypsinize cells from a confluent 10-cm-dish as described.
- After spinning down in media, resuspend cells from one plate in 2 ml ES media and cool down on ice for 5 min.
- Add 2 ml 2x freezing media and separate into 1-ml freezing vials then freeze immediately at 80°C.
- Transfer to liquidN the next day.

2x freezing media:

50% Fetal Calf Serum
20% DMSO
in DMEM high glucose

4.4.7 Preplating

For all western experiments it was desirable to harvest a pure colony of targeted ES cells without contamination of wt feeder cells. In order to obtain this purity, ES cells cultured on feeders were preplated. This preplating event removes feeder cells to about 90%.

- For 10cm-dish add 3 ml trypsin/EDTA remove and add 3 ml again.
- Leave plate in the incubator for 15 min.
- Add 7 ml ES media and strongly pipet up and down to disrupt cell colonies.
- Spin 5 min at 1000rpm and remove supernatant.
- Resuspend in 10 ml ES media and transfer the cells onto a gelatine uncoated tissue culture dish.
- Leave in the incubator for 20-30 min
- Carefully pipet off the supernatant and transfer ES cells (90% feeder-free) onto a new 0.1% gelatinized dish.

4.4.8 Electroporation

To transform DNA constructs into ES cells the electroporation method was applied. For electroporation it is best to use cells that are passaged twice after thawing.

- Trypsinize cells from a 10-cm-dish and make sure that it is really a single cell suspension!
- After spinning in media for 5 min, aspirate the media, and resuspend the cell pellet in 5 ml PBS. Take an aliquot for counting and spin 1000 rpm at RT for 5 min.
- During the centrifugation step, count the number of cells on a haemocytometer
- Aspirate the supernatant and resuspend cell pellet in an appropriate volume of PBS, so that the final volume of 800µl for the electro execution contains 10^7 cells.
- Use 40 µg linearized targeting plasmid in 50 µl PBS. Pipet linearized DNA into the gene pulser cuvette (0.4 cm electrode gap) and add 800µl cell suspension.
- Set Bio-Rad electroporator at 240V, 500µF and pulse the cells (the pulse time should be between 5 and 6s, time constant should be 5 to 6).

- Transfer the electroporated cells to 60-80 ml media and distribute cell suspension onto 6-8 gelatinized 10-cm-dishes.

4.4.9 Transformation

Stable transformation

- Thaw ES cell clone onto a feeder coated cell culture dish.
- After two passages perform electro-transformation as described.
- Plate transformed cells on six 10-cm feeder-coated dishes.
- Selection: After 24 to 40 hrs change media and add selection medium
Selection markers are ordered by stringency

Puro	1 µg/ml
Hygromycin	200 µg/ml
G418 (neomycin)	250 µg/ml

- Incubate for 8-10 days with occasional change of selection media.
- Pick about 96 undifferentiated colonies into feeder containing 48-well-dishes.
- After two days, trypsinize and transfer onto new feeder containing 48-well-dishes.
- After another two days, split each clone in two: One third stays in the 48-well-dish. Cool 5 min on ice then add 2x freezing media and freeze at -80°C. Transfer the remaining two thirds trypsinized cell suspension into gelatinized 24-well-dishes containing 800 µl ES selection media. After 3-5 days these wells will be confluent and cells can be used for DNA extraction.

Transient transformation

Transient transformation in this thesis was applied to introduce the Cre recombination plasmid pMC-Cre into mll2F/F ES cells.

- Thaw ES cells and passage twice before collecting 10^6 cells for electroporation.
- Use 40 µg unlinearized McCre plasmid resuspended in 50 µl 1x PBS and perform electrotransfection as described.
- After electroporation seed $5-50 \times 10^3$ cells per feeder coated plate and incubate for 7-9 days with occasional media change (no selection!).
- Pick about 96 undifferentiated colonies into feeder containing 48-well-dishes.
- After two days, trypsinize and transfer onto new feeder containing 48-well-dishes.
- After another two days, split each clone in three: One third stays in the 48-well-dish. Cool 5 min on ice then add 2x freezing media and freeze at -80°C. One third is transferred into G418 containing media to check for Cre mediated deletion of the neomycin selection marker. Transfer the remaining one third trypsinized cell suspension into gelatinized 24-well-dishes containing 800 µl ES media. After 3-5 days these wells will be confluent and cells can be used for DNA extraction.

4.4.10 Apoptosis assay

Cleavage of genomic DNA during apoptosis may yield double-stranded, low molecular weight DNA fragments as well as single strand breaks (“nicks”) in high molecular weight DNA. Those DNA strand breaks can be identified by labeling free 3’OH termini with modified nucleotides in an enzymatic reaction. The Kit performs in three consecutive steps:

1. Labeling of DNA strand breaks, by Terminal deoxynucleotidyltransferase (TdT), which catalyzes polymerization of labeled nucleotides to free 3’-OH DNA ends in a template-independent manner (TUNEL reaction).
 2. Detection of incorporated fluorescein by anti-fluorescein antibody Fab fragments from sheep. Analysis under fluorescence microscope.
- Grow ES cells in 24-well-plate on coverslips.
 - Wash with PBS.
 - Fix air-dried samples with freshly prepared fixation solution for one hour at RT.
 - Wash with PBS.
 - Incubate in permeabilisation solution for two min on ice.
 - For positive control incubate fixed and permeabilized cells with DNaseI in digestion buffer for 10 min at RT to induce DNA strand breaks, prior to labeling procedures.
 - Prepare TUNEL reaction mixture by adding 50 µl enzyme solution to 450 µl label solution. Mix well to equilibrate components.
 - Rinse slides twice with PBS.
 - Take coverslips out of the well, dry by touching a paper towel and place upside down onto a drop of 50 µl TUNEL reaction mixture.
 - For negative control incubate fixed and permeabilized cells in 50 µl label solution (without TdT) instead of TUNEL reaction mixture.
 - Incubate for one hour at 37 °C in a humidified atmosphere in the dark.
 - Dip coverslips 3x in PBS
 - Samples can be analyzed in a drop of PBS under a fluorescence microscope at this state. Use an excitation wavelength in the range of 450-500 nm and detection in the range of 515-565 nm (green).

Fixation solution:

4% paraformaldehyde in PBS

Permeabilisation solution:

0.1% Triton X-100

0.1% sodium citrate in H₂O

Digestion buffer:

3U/ml DNaseI

50mM Tris-HCl, pH 7.5

10mM MgCl₂

1 mg/ml BSA

Label solution:

nucleotide mixture in reaction buffer (content of “*In Situ* Cell Death Detection Kit”)

Enzyme solution:

Td from calf thymus in storage buffer (10x) (content of “*In Situ* Cell Death Detection Kit”)

4.5. Histology

4.5.1 Perfusion of mouse

- Use a 27G3/4 **0.4 x 19** syringe with tubing and peristaltic pump, adjust pump every time. Mark 5mm with edding and bend syringe
- Anesthetize mouse with 0.2 ml / 10 g body weight i.p. injection. If bulb appears appears on skin, injection is subcutan. Mouse is anesthetized after 1 min for approx. 40 min. Check by pinching limb
- Dissect mouse, insert syringe in heart until 5mm mark , fix tubing
- Cut right ventricle with right hand immediately switch on the pump with left hand
- Rinse mouse with PBS until liver and testis are colorless (usually 5 min.)
- Pause pump and change to PFA, rinse with 30 ml PFA (usually 30 min.)
- Check perfusion quality (liver and tail should be hard)

4.5.2 Paraffin sections of testis

- Dissect testis
- Fix 6 hours in Bouins solution, cut testis in half after 2 hours
- 70% EtOH 2 x 2h
- 95% EtOH 2 x 2h
- 100% EtOH 3 x 2h (o/N)
- EtOH:Xylene [1:1] 30min at RT
- Xylene 2 x 2h at RT
- Xylene:wax 30min at 60°C
- Wax 2 x 2h at 60°C
- Embed testis in wax form.
- Cut 5 mm sections float on DEPC-treated, distilled water
- Keep at 37°C for 24h

Bouins solution (Sigma HT10-1-32)

85% saturated aqueous picric acid,
10%Formaldehyde [40%W/v],
1% glacial acetic acid

Xylenes (FLUKA 95690 1liter)

instead of Xylene you can use Histolene/Histosol:

Histolene (Fronine Pty Ltd., Riverstone NSW) or Histosol (non-toxic citrus extract)
Harris Haematoxylin (Sigma)

Haematoxylin stain

Xylene	2 x 5min
100% EtOH	2 x 5min
95% EtOH	2 x 5min
70% EtOH	2 x 5min
running tap water	5 min
distilled water	5 min

Haematoxylin	5sec
Wash in tap water	
70%	5min
95%	5min
100% twice	5min
Xylene	2 x 5min

Mount in DPX under coverslips

Following *in situ* counterstain and mount with glycerol vinyl alcohol (GVA)
Histomount (Australian Laboratory Services, North Melbourne, AUS)

4.5.3 Paraffin sections of embryos

- Dissect embryos
- Fix 1-2 hours in formalin at 4°C
- 70% EtOH 4 x 15 min
- 95% EtOH 4 x 15 min
- 100% EtOH 4 x 15 min
- EtOH:Xylene [1:1] 5 min at RT (embryo should sink to bottom of tube)
- Xylene 2 x 10 min at RT (embryo should sink to bottom of tube)
- Xylene:wax 30 min at 60°C
- Wax 2 x 1h at 60°C
- Embed embryo in wax form.
- Cut 5 mm sections float on DEPC-treated, distilled water
- Keep at 37°C for 24h

4.5.4 Immunohistochemistry on paraffin sections

- Deparaffinise sections and rehydrate to distilled water:

Xylene	2 x 5min
100% EtOH	2 x 5min
95% EtOH	2 x 5min
70% EtOH	2 x 5min
running tap water	5 min
distilled water	5 min

- Optional: place 10 min in 0.5% hydrogen peroxide/methanol to block endogenous peroxidases. Wash sections in tap water.
- High temperature antigen unmasking: place slides 20 min in a microwave at 700W in 1800 ml 10 mM citrate buffer pH 6.0 (buffer will boil)

- Incubate 10 min at RT in blocking serum
- Incubate 1 h at RT in primary antibody diluted in blocking serum
- Wash 5 min in PBS
- Incubate 10 min at RT in biotinylated secondary antibody
- Wash 5 min in PBS
- Incubate 10 min in streptavidin/peroxidase complex
- Wash 5 min in PBS
- Prepare peroxidase substrate solution (Liquid DAB substrate kit)
 - To 5 ml dist. water: Add **2 drops** of buffer stock solution and mix well
 - Add **4 drops** of DAB stock solution and mix well
 - Add **2 drops** of hydrogen peroxide sol. and mix well
 - If a black stain is required, add 2 drops of nickel sol.
- Incubate tissue section 2 to 10 min with the substrate solution at RT
- Wash 5 min in water
- Counterstain and mount slides

10 mM citrate buffer (ph 6.0)

Citric acid 3.84 g

Add 1800 ml distilled water

Adjust ph 6.0 with NaOH

Add to 2000 ml with distilled water

4.5.5 TUNEL staining on paraffin sections

- Use the *In situ* Cell Death Detection Kit (Roche) : Cat. 1 684 809
- Rehydrate the section
 - 2x 5min Xylene
 - 2x 5min 100% EtOH
 - 2x 5min 70% EtOH
 - 2x 5min water
- **20 min at 37°C** in 10 ml [10 mM Tris with 10µg/ml Proteinase K].
 - 10 ml water
 - 100 µl 1M Tris (ph 7.4)
 - 10 µl Proteinase K from Stock (10mg/ml)
- wash 3x with PBS
- Prepare the Tunel reaction mixture [1:10] from vial1:vial2
For each slide you need 25 µl , (use 2,5 µl vial1 with 22.5 µl vial 2)
- Incubate **1h at 37 C** in a humidified atmosphere in the dark.
- Wash 3x in PBS
- Incubate **30min at 37°C** with 50 µl converter-AP in a humidified atmosphere in the dark.
- Wash 3x in PBS
- Incubate **10min at RT** in 50 – 100 µl substrate solution
- Rinse 3x in PBS
- Mount under glass coverslip.

Haematoxylin / Eosin stainings are much stronger due to the Proteinase K digestion
Proper Haematoxylin dilutions and incubation times need to be established.

4.5.6 Cryosection

- Fix sample in 4% PFA (1hour – o/n)
- Wash 4x 25min in PBS
- Transfer to sucrose gradient (8% / 15% / 30%) until the tissue sinks to the bottom
- embed in tissue tek and freeze on dry ice
- cut 6 – 10 μ m sections on a cryostat. Usually the blade should be cooled to -22°C and the sample to -20°C , but temperatures have to be determined for every session. Keep sections at -20°C .

4.5.7 Immunohistochemistry on cryosection

- Permeabilize and block the sections in blocking buffer
- Incubate with 1st antibody in blocking solution o/n at 4°C in a humidified chamber
- Wash 6x 15min in TBS/Tween
- Incubate with 2nd antibody 1 hour at RT
- Wash 6x 15min, incubate 10min with DAPI [1:3000], wash again
- Mount slides

Blocking buffer

TBS

0.3 % Triton

50 mM Glycin

10% FCS

4.5.8 Whole mount LacZ staining of embryos

- Dissect embryos at RT in transport solution. Fix embryos in 4% PFA on ice for 30 min to 1 hour (depending on developmental stage of the embryo).
- Transfer into a 10-cm-dish containing cold PBS to wash.
- Transfer embryos into a 5-cm-dish containing freshly prepared staining solution.
- Incubate at 37°C o/n. To avoid evaporation and drying out of the embryos place dishes into a box layed out with wet tissue.
- To take pictures wash embryos in PBS twice.
- If it is intended to make sections of the embryos, cryopreseve them in sucrose solution o/n at 4°C .

Fixing solution:

4% Paraformaldehyde

Transport solution:

PBS/ 0.4% BSA

Staining solution:

0.01% Sodium-Deoxycholate
0.02% NP40
2 mM MgCl₂
8 mg Spermidin-trihydrochloride
fill to 30 ml with PBS. Stable at 4°C for several weeks.
10 mM Ferrocyanide add just before use
10mM Ferricyanide add just before use
2 mM Xgal add just before use

Sucrose solution:

30 % sucrose in PBS

4.5.9 Whole mount Fast-red staining of primordial germ cells (PGC)

- Dissect embryos (E 7.5 to E 9.5) in cold PBS.
- Fix for 1-2 h at 4° C in 4% PFA.
- Wash 3x 2min in PBS.
- Dehydrate in 70 % EtOH for 1-2 h at 4° C.
- Wash 3x 5min in distilled water.
- Stain in fresh naphthylphosphate / fast red TR solution for 15 – 20 min. at RT
- Wash in PBS.
- Transfer to 70% glycerol to clear and count PGC's under a microscope
- For older embryos (E 9.0 – 9.5), the hindgut was isolated and transferred to 70% glycerol.

1M Tris-maleate (ph 9.0)

use a large volume of 1M Tris
adjust ph 9.0 by adding 1M Tris-maleate

Fast red solution

25 mM Tris-maleate (ph 9.0)	Tris-maleate	(Sigma T-3128)
1 mg/ml Fast red TR	Fast-Red TR salt	(Aldrich 20,155-3)
0.4 mg/ml naphthyl phosphate	α-naphthylphosphate	(Sigma N-7255)
8 mM MgCl		

4.6. Transgenic mice

4.6.1 Genotyping

Pups were weaned at three weeks of age. A 1cm tail cut was used for genotyping. Tail-DNA extraction was performed according to the protocol in section 4.1.12. Genotyping was based on a PCR strategy (for further details please refer to the results section)

4.6.2 Tamoxifen gavage of mouse

- 100 mg Tamoxifen-free base (Sigma, T5648) was suspended in 100 µl Ethanol and solved in 900 µl peanut oil (Sigma). This 10 mg/100 µl tamoxifen solution was shaken rigorously at 55°C (Tamoxifen precipitates at RT) and divided in aliquots of 50 µl (1 daily dose = 5mg). Store at -20°C.
- Heat to 37°C before administration. Verify that tamoxifen is properly dissolved.
- Feed orally to mice with a feeding needle. Fix the mice at their neck and ridge so that the belly is directed to the floor. Hold the mouse tightly so that it can not move the head, but not too tight to avoid choking. Carefully introduce the feeding needle in the mouth behind the tongue (max. 1 cm). It is helpful to mark 1 cm on the needle with an edding pen in order to see how deep you have inserted the needle.
- Introduce slowly 50 µl of the Tamoxifen solution with the syringe. Make sure that they swallow (can be seen).
- Repeat this procedure for 5 days once a day.

Gavage needles from Heiland, Germany
'Knopfkanülen', 1,2x4mm, Nr. 370-129
Phone +341-9976990,
Fax 0800-6666699

5. Material

5.1 Chemicals

Acrylamide	Sigma
Agarose	Gibco
Ampicillin	Sigma
APS	Sigma
Bacto-Agar	Difco
Beta-mercaptoethylamine	Sigma
Bisacrylamide	Sigma
Bromphenolblue	Merck
BSA	Sigma
CaCl ₂	Merck
Chloramphenicol	Sigma
Chromiumpotassiumsulfate	Sigma
Coomassie	Merck
Cyclohexemide	Sigma
DTT	Biomol
EGTA	Sigma
Ethidiumbromide	Sigma
Ferricyanide	Sigma
Ferrocyanide	Sigma
Ficoll	Sigma
G418	Gibco
Gelatine	Merck
Glycine	Merck
HCl	Merck
Hepes	Biomol
Hygromycin B	Roche
IPTG	Sigma
KAc	Merck
Kanamycin sulfate	Sigma
KCl	Merck
KH ₂ PO ₄	Merck
KH ₄ Ac	Merck
L-Arabinose	Sigma
L-Cystein	Sigma
Methyl green	Sigma
Methylene blue	Sigma
MgCl ₂	Sigma
Milkpowder	Hairler
Mitomycin	Sigma
MnCl ₂	Sigma
MOPS	Sigma
Na ₂ HPO ₄	Merck
Na-Citrate	Merck
NaCl	Merck

NaOAc	Merck
NaOH	Merck
N-lauroylsarcosine	Sigma
OCT (tissuetek)	Sacura
Paraformaldehyde	Sigma
PI	Sigma
RbCl ₂	Sigma
Retinoic acid	Sigma
SDS	Bio-Rad
Sodiumdeoxycholate	Sigma
Spermidintrihydrochloride	Sigma
Sucrose	Sigma
Tetracycline	Sigma
Titriplex (EDTA)	Merck
Trizma	Merck
Urea	Merck
XCFF	Merck
X-Gal	Biomol
ZnSO ₄	Sigma

5.2 Solutions

Acrylamide-Bisacrylamide mix (30%)	Severn Biotech LTD
Beta-mercaptoethanol	Sigma
BioRad protein assay	Bio-Rad
DMEM (Glutamax)	Gibco
DMSO	Sigma
ECL solutions	Amersham-
Pharmacia	
EN ³ HANCE	NEN
Eosine	Sigma
Ethanol	Merck
Eukitt	Fluka
FCS	Gibco
Formamid	Sigma
Glacial acetic acid	Merck
Gluteraldehyde	Sigma
Glycerol	Merck
Isopropanol	Merck
L-Glutamine	Gibco
LIF-ESGRO	Chemicon
Methanol	Merck
Non essential amino acids	Biochrom
NP40	Roche
Penicillin/Streptomycin	Gibco
Phenol/Chlorophorm/Isoamylalkohol	Sigma
Sodium Pyruvate	Gibco
TEMED	Sigma
TRI Reagent	Sigma

Triton-X100	Sigma
Trypsin/EDTA	Gibco
Tween 20	Sigma

5.3 Buffer

<u>LB (Luria Bertoni media)</u>	1%	bacto tryptone
	0.5%	bacto yeast
	1%	NaCl
<u>PBS</u>	171mM	NaCl
	3.4mM	KCl
	10mM	Na ₂ HPO ₄
	1.9mM	KH ₂ PO ₄
<u>TE (pH 8.0)</u>	10mM	Tris
	1mM	EDTA (pH 8.0)

5.4 Other reagents

5.4.1 Enzymes, marker and nucleotides

1kb ladder	Gibco
DNAse I	Sigma
dNTP mix	Amersham-
Pharmacia	
Klenow large fragment	NEB
Prestained protein marker, broad range	NEB
Proteinase inhibitor cocktail	Sigma
Proteinase K	Merck
Restriction enzymes	NEB
RNA polymerase T3/T7	NEB
RNAse A	Sigma
rNTP mix	Amersham-
Pharmacia	
T4 DNA ligase	NEB
Taq and PCR buffer	Roche

5.4.2 Kits

Adsvantage-GC cDNA PCR Kit	Clontech
In situ cell death detection Kit, AP	Roche
Plasmid Maxi preparation Kit	Qiagen
Qiaquick PCR purification Kit	Qiagen
Random primed DNA labeling Kit	Roche
Western Star protein detection Kit (AP conjugate)	Tropix

5.4.3 Antibodies

Anti-beta Actin (monoclonal)

Sigma

Anti-dimethylH3/K4 (polyclonal)

Abcam

Anti-mouse Ig, horseradish peroxidase, from sheep

Amersham-Pharmacia

Anti-rabbit Ig, horseradish peroxidase, from donkey

Amersham-Pharmacia

6. References

- Acampora, D., Avantaggiato, V., Tuorto, F., Briata, P., Corte, G. and Simeone, A. (1998) Visceral endoderm-restricted translation of Otx1 mediates recovery of Otx2 requirements for specification of anterior neural plate and normal gastrulation. *Development*, **125**, 5091-5104.
- Ahmad, K. and Henikoff, S. (2002) The histone variant H3.3 marks active chromatin by replication-independent nucleosome assembly. *Mol Cell*, **9**, 1191-1200.
- Ando, H., Haruna, Y., Miyazaki, J., Okabe, M. and Nakanishi, Y. (2000) Spermatocyte-specific gene excision by targeted expression of Cre recombinase. *Biochem Biophys Res Commun*, **272**, 125-128.
- Ang, S.L., Conlon, R.A., Jin, O. and Rossant, J. (1994) Positive and negative signals from mesoderm regulate the expression of mouse Otx2 in ectoderm explants. *Development*, **120**, 2979-2989.
- Ang, S.L., Jin, O., Rhinn, M., Daigle, N., Stevenson, L. and Rossant, J. (1996) A targeted mouse Otx2 mutation leads to severe defects in gastrulation and formation of axial mesoderm and to deletion of rostral brain. *Development*, **122**, 243-252.
- Atchison, F.W. and Means, A.R. (2003) Spermatogonial depletion in adult Pin1-deficient mice. *Biol Reprod*, **69**, 1989-1997.
- Baker, T.G. (1963) A Quantitative and Cytological Study of Germ Cells in Human Ovaries. *Proc R Soc Lond B Biol Sci*, **158**, 417-433.
- Bannister, A.J., Zegerman, P., Partridge, J.F., Miska, E.A., Thomas, J.O., Allshire, R.C. and Kouzarides, T. (2001) Selective recognition of methylated lysine 9 on histone H3 by the HP1 chromo domain. *Nature*, **410**, 120-124.
- Bedell, M.A., Jenkins, N.A. and Copeland, N.G. (1997a) Mouse models of human disease. Part I: techniques and resources for genetic analysis in mice. *Genes Dev*, **11**, 1-10.
- Bedell, M.A., Largaespada, D.A., Jenkins, N.A. and Copeland, N.G. (1997b) Mouse models of human disease. Part II: recent progress and future directions. *Genes Dev*, **11**, 11-43.
- Bornslaeger, E.A., Mattei, P. and Schultz, R.M. (1986a) Involvement of cAMP-dependent protein kinase and protein phosphorylation in regulation of mouse oocyte maturation. *Dev Biol*, **114**, 453-462.

- Bornslaeger, E.A., Poueymirou, W.T., Mattei, P. and Schultz, R.M. (1986b) Effects of protein kinase C activators on germinal vesicle breakdown and polar body emission of mouse oocytes. *Exp Cell Res*, **165**, 507-517.
- Braunstein, M., Sobel, R.E., Allis, C.D., Turner, B.M. and Broach, J.R. (1996) Efficient transcriptional silencing in *Saccharomyces cerevisiae* requires a heterochromatin histone acetylation pattern. *Mol Cell Biol*, **16**, 4349-4356.
- Brownell, J.E., Zhou, J., Ranalli, T., Kobayashi, R., Edmondson, D.G., Roth, S.Y. and Allis, C.D. (1996) Tetrahymena histone acetyltransferase A: a homolog to yeast Gcn5p linking histone acetylation to gene activation. *Cell*, **84**, 843-851.
- Chabot, B., Stephenson, D.A., Chapman, V.M., Besmer, P. and Bernstein, A. (1988) The proto-oncogene c-kit encoding a transmembrane tyrosine kinase receptor maps to the mouse W locus. *Nature*, **335**, 88-89.
- Chung, S.S., Cuzin, F., Rassoulzadegan, M. and Wolgemuth, D.J. (2004) Primary spermatocyte-specific Cre recombinase activity in transgenic mice. *Transgenic Res*, **13**, 289-294.
- Cooke, H.J. and Saunders, P.T. (2002) Mouse models of male infertility. *Nat Rev Genet*, **3**, 790-801.
- Danielian, P.S., Muccino, D., Rowitch, D.H., Michael, S.K. and McMahon, A.P. (1998) Modification of gene activity in mouse embryos in utero by a tamoxifen-inducible form of Cre recombinase. *Curr Biol*, **8**, 1323-1326.
- de Rooij, D.G. (2001) Proliferation and differentiation of spermatogonial stem cells. *Reproduction*, **121**, 347-354.
- Dhalluin, C., Carlson, J.E., Zeng, L., He, C., Aggarwal, A.K. and Zhou, M.M. (1999) Structure and ligand of a histone acetyltransferase bromodomain. *Nature*, **399**, 491-496.
- Ekwall, K., Olsson, T., Turner, B.M., Cranston, G. and Allshire, R.C. (1997) Transient inhibition of histone deacetylation alters the structural and functional imprint at fission yeast centromeres. *Cell*, **91**, 1021-1032.
- Feil, R., Wagner, J., Metzger, D. and Chambon, P. (1997) Regulation of Cre recombinase activity by mutated estrogen receptor ligand-binding domains. *Biochem Biophys Res Commun*, **237**, 752-757.
- Flanagan, J.G., Chan, D.C. and Leder, P. (1991) Transmembrane form of the kit ligand growth factor is determined by alternative splicing and is missing in the Sld mutant. *Cell*, **64**, 1025-1035.

- Geissler, E.N., Ryan, M.A. and Housman, D.E. (1988) The dominant-white spotting (W) locus of the mouse encodes the c-kit proto-oncogene. *Cell*, **55**, 185-192.
- Ginsburg, M., Snow, M.H. and McLaren, A. (1990) Primordial germ cells in the mouse embryo during gastrulation. *Development*, **110**, 521-528.
- Gomperts, M., Wylie, C. and Heasman, J. (1994) Primordial germ cell migration. *Ciba Found Symp*, **182**, 121-134; discussion 134-129.
- Gossen, M., Freundlieb, S., Bender, G., Muller, G., Hillen, W. and Bujard, H. (1995) Transcriptional activation by tetracyclines in mammalian cells. *Science*, **268**, 1766-1769.
- Grant, P.A. (2001) A tale of histone modifications. *Genome Biol*, **2**, REVIEWS0003.
- Hayashi, S. and McMahon, A.P. (2002) Efficient recombination in diverse tissues by a tamoxifen-inducible form of Cre: a tool for temporally regulated gene activation/inactivation in the mouse. *Dev Biol*, **244**, 305-318.
- Hirshfield, A.N. (1989a) Granulosa cell proliferation in very small follicles of cycling rats studied by long-term continuous tritiated-thymidine infusion. *Biol Reprod*, **41**, 309-316.
- Hirshfield, A.N. (1989b) Rescue of atretic follicles in vitro and in vivo. *Biol Reprod*, **40**, 181-190.
- Hsueh, A.J., Billig, H. and Tsafiriri, A. (1994) Ovarian follicle atresia: a hormonally controlled apoptotic process. *Endocr Rev*, **15**, 707-724.
- Hughes, C.M., Rozenblatt-Rosen, O., Milne, T.A., Copeland, T.D., Levine, S.S., Lee, J.C., Hayes, D.N., Shanmugam, K.S., Bhattacharjee, A., Biondi, C.A., Kay, G.F., Hayward, N.K., Hess, J.L. and Meyerson, M. (2004) Menin associates with a trithorax family histone methyltransferase complex and with the *hoxc8* locus. *Mol Cell*, **13**, 587-597.
- Iizuka, M. and Smith, M.M. (2003) Functional consequences of histone modifications. *Curr Opin Genet Dev*, **13**, 154-160.
- Imai, S., Armstrong, C.M., Kaeberlein, M. and Guarente, L. (2000) Transcriptional silencing and longevity protein Sir2 is an NAD-dependent histone deacetylase. *Nature*, **403**, 795-800.
- Jacobs, S.A. and Khorasanizadeh, S. (2002) Structure of HP1 chromodomain bound to a lysine 9-methylated histone H3 tail. *Science*, **295**, 2080-2083.

- Johnson, J., Canning, J., Kaneko, T., Pru, J.K. and Tilly, J.L. (2004) Germline stem cells and follicular renewal in the postnatal mammalian ovary.
Nature, **428**, 145-150.
- Jordan, V.C. and Murphy, C.S. (1990) Endocrine pharmacology of antiestrogens as antitumor agents.
Endocr Rev, **11**, 578-610.
- Kilby, N.J., Snaith, M.R. and Murray, J.A. (1993) Site-specific recombinases: tools for genome engineering.
Trends Genet, **9**, 413-421.
- Kolodner, R., Hall, S.D. and Luisi-DeLuca, C. (1994) Homologous pairing proteins encoded by the Escherichia coli recE and recT genes.
Mol Microbiol, **11**, 23-30.
- Kouzarides, T. (2002) Histone methylation in transcriptional control.
Curr Opin Genet Dev, **12**, 198-209.
- Kuhbandner, S., Brummer, S., Metzger, D., Chambon, P., Hofmann, F. and Feil, R. (2000) Temporally controlled somatic mutagenesis in smooth muscle.
Genesis, **28**, 15-22.
- Lachner, M. and Jenuwein, T. (2002) The many faces of histone lysine methylation.
Curr Opin Cell Biol, **14**, 286-298.
- Lachner, M., O'Carroll, D., Rea, S., Mechtler, K. and Jenuwein, T. (2001) Methylation of histone H3 lysine 9 creates a binding site for HP1 proteins.
Nature, **410**, 116-120.
- Lallemand, Y., Luria, V., Haffner-Krausz, R. and Lonai, P. (1998) Maternally expressed PGK-Cre transgene as a tool for early and uniform activation of the Cre site-specific recombinase.
Transgenic Res, **7**, 105-112.
- Landry, J., Sutton, A., Tafrov, S.T., Heller, R.C., Stebbins, J., Pillus, L. and Sternglanz, R. (2000) The silencing protein SIR2 and its homologs are NAD-dependent protein deacetylases.
Proc Natl Acad Sci U S A, **97**, 5807-5811.
- Lecureuil, C., Fontaine, I., Crepieux, P. and Guillou, F. (2002) Sertoli and granulosa cell-specific Cre recombinase activity in transgenic mice.
Genesis, **33**, 114-118.
- Logie, C. and Stewart, A.F. (1995) Ligand-regulated site-specific recombination.
Proc Natl Acad Sci U S A, **92**, 5940-5944
- .

- Luger, K., Mader, A.W., Richmond, R.K., Sargent, D.F. and Richmond, T.J. (1997) Crystal structure of the nucleosome core particle at 2.8 Å resolution. *Nature*, **389**, 251-260.
- McLaren, A. (2000) Germ and somatic cell lineages in the developing gonad. *Mol Cell Endocrinol*, **163**, 3-9.
- Metzger, D., Clifford, J., Chiba, H. and Chambon, P. (1995) Conditional site-specific recombination in mammalian cells using a ligand-dependent chimeric Cre recombinase. *Proc Natl Acad Sci U S A*, **92**, 6991-6995.
- Milne, T.A., Hughes, C.M., Lloyd, R., Yang, Z., Rozenblatt-Rosen, O., Dou, Y., Schnepp, R.W., Krankel, C., Livolsi, V.A., Gibbs, D., Hua, X., Roeder, R.G., Meyerson, M. and Hess, J.L. (2005) Menin and MLL cooperatively regulate expression of cyclin-dependent kinase inhibitors. *Proc Natl Acad Sci U S A*, **102**, 749-754.
- Muyrers, J.P., Zhang, Y. and Stewart, A.F. (2001) Techniques: Recombinogenic engineering--new options for cloning and manipulating DNA. *Trends Biochem Sci*, **26**, 325-331.
- Muyrers, J.P., Zhang, Y., Testa, G. and Stewart, A.F. (1999) Rapid modification of bacterial artificial chromosomes by ET-recombination. *Nucleic Acids Res*, **27**, 1555-1557.
- O'Gorman, S., Dagenais, N.A., Qian, M. and Marchuk, Y. (1997) Protamine-Cre recombinase transgenes efficiently recombine target sequences in the male germ line of mice, but not in embryonic stem cells. *Proc Natl Acad Sci U S A*, **94**, 14602-14607.
- Ogawa, T., Dobrinski, I., Avarbock, M.R. and Brinster, R.L. (2000) Transplantation of male germ line stem cells restores fertility in infertile mice. *Nat Med*, **6**, 29-34.
- Oliver, G., Mailhos, A., Wehr, R., Copeland, N.G., Jenkins, N.A. and Gruss, P. (1995) Six3, a murine homologue of the sine oculis gene, demarcates the most anterior border of the developing neural plate and is expressed during eye development. *Development*, **121**, 4045-4055.
- Peterson, C.L. and Laniel, M.A. (2004) Histones and histone modifications. *Curr Biol*, **14**, R546-551.
- Rea, S., Eisenhaber, F., O'Carroll, D., Strahl, B.D., Sun, Z.W., Schmid, M., Opravil, S., Mechtler, K., Ponting, C.P., Allis, C.D. and Jenuwein, T. (2000) Regulation of chromatin structure by site-specific histone H3 methyltransferases. *Nature*, **406**, 593-599.

- Rhinn, M., Dierich, A., Shawlot, W., Behringer, R.R., Le Meur, M. and Ang, S.L. (1998) Sequential roles for Otx2 in visceral endoderm and neuroectoderm for forebrain and midbrain induction and specification. *Development*, **125**, 845-856.
- Richards, J.S., Jonassen, J.A. and Kersey, K. (1980) Evidence that changes in tonic luteinizing hormone secretion determine the growth of preovulatory follicles in the rat. *Endocrinology*, **107**, 641-648.
- Richards, J.S., Sharma, S.C., Falender, A.E. and Lo, Y.H. (2002) Expression of FKHR, FKHL1, and AFX genes in the rodent ovary: evidence for regulation by IGF-I, estrogen, and the gonadotropins. *Mol Endocrinol*, **16**, 580-599.
- Roguev, A., Schaft, D., Shevchenko, A., Pijnappel, W.W., Wilm, M., Aasland, R. and Stewart, A.F. (2001) The *Saccharomyces cerevisiae* Set1 complex includes an Ash2 homologue and methylates histone 3 lysine 4. *Embo J*, **20**, 7137-7148.
- Rossant, J. and Nagy, A. (1995) Genome engineering: the new mouse genetics. *Nat Med*, **1**, 592-594.
- Russell, E.S., Neufeld, E.F. and Higgins, C.T. (1951) Comparison of normal blood picture of young adults from 18 inbred strains of mice. *Proc Soc Exp Biol Med*, **78**, 761-766.
- Santisteban, M.S., Kalashnikova, T. and Smith, M.M. (2000) Histone H2A.Z regulates transcription and is partially redundant with nucleosome remodeling complexes. *Cell*, **103**, 411-422.
- Schmahl, J., Eicher, E.M., Washburn, L.L. and Capel, B. (2000) Sry induces cell proliferation in the mouse gonad. *Development*, **127**, 65-73.
- Schmidt, E.E., Taylor, D.S., Prigge, J.R., Barnett, S. and Capecchi, M.R. (2000) Illegitimate Cre-dependent chromosome rearrangements in transgenic mouse spermatids. *Proc Natl Acad Sci U S A*, **97**, 13702-13707.
- Schneider, R., Bannister, A.J. and Kouzarides, T. (2002) Unsafe SETs: histone lysine methyltransferases and cancer. *trends Biochem Sci*, **27**, 396-402.
- Schwenk, F., Baron, U. and Rajewsky, K. (1995) A cre-transgenic mouse strain for the ubiquitous deletion of loxP-flanked gene segments including deletion in germ cells. *Nucleic Acids Res*, **23**, 5080-5081.
- Seibler, J., Zevnik, B., Kuter-Luks, B., Andreas, S., Kern, H., Hennek, T., Rode, A., Heimann, C., Faust, N., Kauselmann, G., Schoor, M., Jaenisch, R., Rajewsky, K., Kuhn, R. and Schwenk, F. (2003) Rapid generation of inducible mouse mutants. *Nucleic Acids Res*, **31**, e12.

- Shimshek, D.R., Kim, J., Hubner, M.R., Spergel, D.J., Buchholz, F., Casanova, E., Stewart, A.F., Seeburg, P.H. and Sprengel, R. (2002) Codon-improved Cre recombinase (iCre) expression in the mouse.
Genesis, **32**, 19-26.
- Smith, J.S., Brachmann, C.B., Celic, I., Kenna, M.A., Muhammad, S., Starai, V.J., Avalos, J.L., Escalante-Semerena, J.C., Grubmeyer, C., Wolberger, C. and Boeke, J.D. (2000) A phylogenetically conserved NAD⁺-dependent protein deacetylase activity in the Sir2 protein family.
Proc Natl Acad Sci U S A, **97**, 6658-6663.
- Smith, M.M. (2002) Centromeres and variant histones: what, where, when and why?
Curr Opin Cell Biol, **14**, 279-285.
- Sorrentino, V., Giorgi, M., Geremia, R., Besmer, P. and Rossi, P. (1991) Expression of the c-kit proto-oncogene in the murine male germ cells.
Oncogene, **6**, 149-151.
- Strahl, B.D., Grant, P.A., Briggs, S.D., Sun, Z.W., Bone, J.R., Caldwell, J.A., Mollah, S., Cook, R.G., Shabanowitz, J., Hunt, D.F. and Allis, C.D. (2002) Set2 is a nucleosomal histone H3-selective methyltransferase that mediates transcriptional repression.
Mol Cell Biol, **22**, 1298-1306.
- Turner, B.M., Birley, A.J. and Lavender, J. (1992) Histone H4 isoforms acetylated at specific lysine residues define individual chromosomes and chromatin domains in *Drosophila* polytene nuclei.
Cell, **69**, 375-384.
- Vandel, L. and Trouche, D. (2001) Physical association between the histone acetyl transferase CBP and a histone methyl transferase.
EMBO Rep, **2**, 21-26.
- Vidal, F., Sage, J., Cuzin, F. and Rassoulzadegan, M. (1998) Cre expression in primary spermatocytes: a tool for genetic engineering of the germ line.
Mol Reprod Dev, **51**, 274-280.
- Weber, P., Schuler, M., Gerard, C., Mark, M., Metzger, D. and Chambon, P. (2003) Temporally controlled site-specific mutagenesis in the germ cell lineage of the mouse testis.
Biol Reprod, **68**, 553-559.
- Wilkinson, D.G. and Krumlauf, R. (1990) Molecular approaches to the segmentation of the hindbrain.
Trends Neurosci, **13**, 335-339.
- Wu, J. and Grunstein, M. (2000) 25 years after the nucleosome model: chromatin modifications.
Trends Biochem Sci, **25**, 619-623.

- Wysocka, J., Myers, M.P., Laherty, C.D., Eisenman, R.N. and Herr, W. (2003) Human Sin3 deacetylase and trithorax-related Set1/Ash2 histone H3-K4 methyltransferase are tethered together selectively by the cell-proliferation factor HCF-1.
Genes Dev, **17**, 896-911.
- Yokoyama, A., Wang, Z., Wysocka, J., Sanyal, M., Aufiero, D.J., Kitabayashi, I., Herr, W. and Cleary, M.L. (2004) Leukemia proto-oncoprotein MLL forms a SET1-like histone methyltransferase complex with menin to regulate Hox gene expression.
Mol Cell Biol, **24**, 5639-5649.
- Zhang, Y., Buchholz, F., Muirers, J.P. and Stewart, A.F. (1998) A new logic for DNA engineering using recombination in *Escherichia coli*.
Nat Genet, **20**, 123-128.

Acknowledgements

I wish to thank Francis Stewart who gave me the opportunity to participate in his excellent research. I am truly grateful for his support during my epic journey.

I am grateful to Konstantinos Anastassiadis for his supervision in lab matters and beyond.

Taking a leaf from his book, I have made progress and I will always remember that.

I would like to thank the members of my PhD committee Frank Buchholz and Michele Solimena for helpful discussions and Aria Baniahmad for reviewing my thesis.

I wish to thank Frank van der Hoeven who generated the Mll2 mouse line.

Thanks to Julia Schaft for her ambitious efforts, the Mll2^{-/-} ES cells and the Mll2 antibody.

Thanks to Sandra Lubitz who identified Mll2 target genes in ES cells, and to Daniela Röllig who has made an excellent diploma thesis.

Thanks to Giuseppe Testa for many elucidations and the unique entertainment, and to Yu min Zang and Joep Muylers for their advice on Red/ET recombination.

Thanks to Michelle Meredyth Stewart for critical reading of the manuscript.

Thanks to the wonderful people from the Stewart lab for being good company.

I hope we meet again and I wish you all the best for your futures.

I am grateful to my parents and my sister Maion for their support and their affection.

Last but not least,

I wish to express my gratitude to Jennifer Volz for her patience and her caring attention.

You are always the first and the last thing on my mind.

Eidesstattliche Erklärung

Hiermit erkläre ich an Eidesstatt, dass ich die vorliegende Arbeit selbstständig verfaßt, und keine unzulässigen oder nicht angegebenen Hilfsmittel benutzt habe.

Die Arbeit hat weder in dieser, noch in ähnlicher Form, bereits einer anderen Prüfungsbehörde vorgelegen.

Dresden, den 26. April 2005

Stefan Glaser